Notes on graphene*

Chuan Liu[1]

(CLQCD Collaboration)

[1] *School of Physics and Center for High Energy Physics, Peking University, Beijing 100871, P. R. China*

(Dated: December 6, 2016)

Some basics related to the graphene project is reviewed. Things covered include: lattice structures, electron band theory, second quantization, path integral representations, numerical simulations, etc. On the elementary side, I will *not* touch basics on equilibrium statistical physics and quantum mechanics. For these subjects, please consult your textbooks or lecture notes. On the more advanced topics, I will also not touch group theory and quantum field theory, though path integrals for the coherent states are briefly discussed.

PACS numbers: 12.38.Gc,11.15.Ha
Keywords: Solid state physics, second quantization and path integral, Monte Carlo simulations

CONTENTS

I. Basics in lattice structures 2
A. Lattice structures 2
B. Reciprocal lattices 3
C. Periodic boundary conditions 5
D. Symmetry of the lattice 6

II. Energy bands in solids 6
A. Bloch theorem 6
B. The tight binding model 7
C. The tight binding model: second quantized version 8

III. Tight-binding model for graphene 9
A. Hybridized orbitals and tight-binding Hamiltonian for graphene 9
B. Diagonalization of the Hamiltonian 11

IV. Some statistical physics for many-body systems [1] 12
A. The density operator for ensembles [2] 12
B. Partition functions for ideal quantum gases 13
C. Electronic properties of solids 14
D. Beyond the independent electron approximation 14

V. Path integral representation for the partition function [3] 15
A. Coherent states 16
B. Path integral representation for the Hubbard model 17
C. Evaluation of fermionic trace 20
D. The sign problem 22
E. A simple example: independent electron system 23

VI. Monte Carlo simulation of Hubbard model 25
A. Markov process and Monte Carlo simulation 26
B. The hybrid Monte Carlo algorithm 26
C. Some detailed issues concerning the hybrid Monte Carlo algorithm 28

VII. Green's functions and physical observables[4] 30
A. Two-point functions 30
B. Two-point functions in path-integral 32
C. More complicated physical quantities: Wick's theorem 33

VIII. Half-filled Hubbard model on graphene 34
A. An improved formula for the path integral 36
B. Possible acceleration of the program 37
C. Spin correlation functions 39

IX. The perturbative calculation at small $\hat{U}$ 40
A. The free electron propagator 40
B. Effective action to first order 41
C. The gap equation 42
D. Effective action to second order 43
E. The electron self-energy 44

References 46

I. BASICS IN LATTICE STRUCTURES

In this section, basics on solid state physics such as lattice structure, reciprocal lattices are briefly reviewed. For more sophisticated discussions, please refer to the solid state books. For English books, please refer to Ref [1] and Ref. [2]. For the Chinese books on solid state physics, please refer to Ref. [3] and Ref. [**?**].

A. Lattice structures

Lattices are collections of points (or atoms, physically speaking) which form a structure that has discrete translational and rotational symmetries.

A lattice can be constructed by the translation of a minimal building block along linearly independent directions. This minimal building block is called the primitive cell for the lattice.

In d space dimensions, one can pick d linearly independent vectors: $\{\mathbf{a}_i : i = 1, \cdots, d\}$, which forms a d-dimensional parallelogram. If we translate a parallelogram by $\mathbf{R} = \sum_{i=1}^{d} n_i \mathbf{a}_i$ with n_i being integers and this process can cover the whole d-dimensional space, the minimal choice then forms a primitive cell and the set of $\{\mathbf{a}_i\}$ is called a basis for the lattice and $\mathbf{R}$ is called a lattice vector. In three-dimensions, the volume of the primitive cell formed by the basis vectors $\mathbf{a}_1$, $\mathbf{a}_2$ and $\mathbf{a}_3$ is given by: $\Omega = |\mathbf{a}_1 \cdot (\mathbf{a}_2 \times \mathbf{a}_3)|$. The choice of basis vectors are not unique. However, the volume of the primitive cell must be identical if the basis indeed forms a primitive cell (minimal unit).

Averagely speaking, a primitive cell can contain only one atom, in which case we call it a Bravais lattice, or more than one atom which is known as non-Bravais lattice (also called complex crystal lattice). On a Bravais lattice, each point is equivalent to any other lattice points. In other words, every lattice point can be obtained by translating from any other lattice point by a suitable lattice vector $\mathbf{R}$. In non-Bravais lattice, however, inequivalent points exist in each primitive cell.

Example I.1 *Three-dimensional simple cubic (SC) lattice is the set of points:* $\{n_1\mathbf{e}_1 + n_2\mathbf{e}_2 + n_3\mathbf{e}_3 : n_1, n_2, n_2 \in \mathbb{Z}\}$ *with* $\mathbf{e}_1$, $\mathbf{e}_2$, $\mathbf{e}_3$ *being unit vector in* x, y *and* z *directions respectively.* $\{\mathbf{e}_1, \mathbf{e}_2, \mathbf{e}_3\}$ *also forms a basis for the simple cubic lattice. A primitive cell is formed by the cube formed by these three unit vectors.*

Example I.2 *Given a SC lattice, if we add a new lattice point at the center of each primitive cell cube, we obtain a body-centered cubic (BCC) lattice. BCC is also a Bravais lattice whose basis may be chosen as:*

$$\mathbf{a}_1 = (1, 0, 0), \mathbf{a}_2 = (0, 1, 0), \mathbf{a}_3 = (1/2, 1/2, 1/2) \ . \quad (1)$$

It is easy to see that the parallelogram formed by these three vectors, when translated by $\{n_1\mathbf{a}_1 + n_2\mathbf{a}_2 + n_3\mathbf{a}_3 : \mathbf{n} \in \mathbb{Z}^3\}$ *indeed fill the whole three-dimensional space.*

Example I.3 *Given a SC lattice, if we add a new lattice point at the center of the square for each cubic cell, we obtain a face-centered cubic (FCC) lattice. FCC is also a Bravais lattice whose basis may be chosen as:*

$$\mathbf{a}_1 = (1/2, 1/2, 0), \mathbf{a}_2 = (1/2, 0, 1/2), \mathbf{a}_3 = (0, 1/2, 1/2) \ . \quad (2)$$

It is easy to see that the parallelogram formed by these three vectors, when translated by $\{n_1\mathbf{a}_1 + n_2\mathbf{a}_2 + n_3\mathbf{a}_3 : \mathbf{n} \in \mathbb{Z}^3\}$ *indeed fill the whole three-dimensional space.*

Example I.4 *The above examples are all Bravais lattices. A common example for non-Bravais lattice in three-dimensions is the diamond lattice. To get a diamond structure, take a cube with FCC arrangement. Draw* 4 *cubic diagonals and add four points at four diagonals so that the four added points form tetrahedrons with the points at the corner and the face-centers. Taking the basis vectors as the conventional FCC lattice, it is found that each primitive cell in fact contains two lattice points.* [5]

The above examples are all three-dimensional. In fact, for our purposes, we only need two-dimensional lattice. Closely related to our project are the triangular lattice and honeycomb lattice.

Example I.5 *For a two-dimensional triangular lattice with lattice spacing* a*, we can take the basis vectors as:*

$$\mathbf{a}_1 = a(+1/2, \sqrt{3}/2) \ , \mathbf{a}_2 = a(-1/2, \sqrt{3}/2) \ . \quad (3)$$

With this choice, all lattice points can be parameterized as: $\mathbf{R} = n_1\mathbf{a}_1 + n_2\mathbf{a}_2$*, with* n_1 *and* n_2 *being integers. Obviously each point is equivalent and two-dimensional triangular lattice is a Bravais lattice.*

---

[5] Okay, it is not so easy to visualize this. But if you draw very good pictures you can persuade yourself. Pictures can also be found by google "diamond lattice structure", for example.

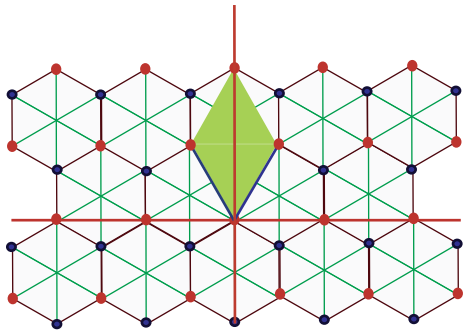

FIG. 1. Illustration of graphene lattice. It is obtained from two sets of triangular lattices, called A (red points) and B (blue points), respectively.

Example I.6 *A honeycomb lattice (see Fig. 1) is a non-Bravais lattice derived from the triangular lattice (a Bravais lattice). In fact, it can be viewed as two sets of interpenetrating triangular lattices, as indicated by the red lattice points and blue lattice points in Fig. 1. The primitive cell is obtained by taking the primitive cell of one of the two sets of triangular lattices (shown in the figure by the green shaded region). Suppose the lattice spacing of the honeycomb is a (i.e. the distance between a blue point and its neighboring red point), we can take the basis vectors for the primitive cell as:*

$$\mathbf{a}_1 = a(+\sqrt{3}/2, 3/2)\ , \mathbf{a}_2 = a(-\sqrt{3}/2, 3/2)\ . \tag{4}$$

Starting from the origin and translate with lattice vector: $\mathbf{R} = n_1\mathbf{a}_1 + n_2\mathbf{a}_2$, with n_1 and n_2 being integers, we obtain one set of triangular lattices (indicated by the red points in Fig. 1). The area for the primitive cell is verified to be $3\sqrt{3}a^2$ (which is the same as the area of a hexagon in the honeycomb lattice).

The primitive cell for the triangular lattice consists of two equilateral triangles, one up-sided, one down-sided. We can now add one lattice point to each down-sided triangles. [6] *These newly added points also form a triangular lattice (the blue points in Fig. 1). The two sets of triangular lattices altogether form a honeycomb lattice. Therefore, in each primitive cell, there are two lattice points. We call one set A (red points), the other set B (blue points). The points in set A and set B are mutually nearest neighbors.*

Take a lattice point in set A, say the origin, then its nearest neighbors can be parameterized by three vectors:

$$\boldsymbol{\delta}_1 = a(0,1), \boldsymbol{\delta}_2 = a(+\sqrt{3}/2, -1/2), \boldsymbol{\delta}_3 = a(-\sqrt{3}/2, -1/2). \tag{5}$$

¶ The choice for the basis vectors and the primitive cell is *not* unique. One particular choice is the following: On a given lattice, if we take an arbitrary point as the origin and draw lattice vectors: $\mathbf{R} = l_1\mathbf{a}_1 + l_2\mathbf{a}_2 + l_3\mathbf{a}_3$ with different integers l_i's. Draw perpendicular planes which passes the midpoint of these vectors. These planes are called Bragg planes associated with each lattice vector. These Bragg planes then partition the whole space into different regions. It can be shown that the simply connected region containing the origin in fact forms a primitive cell for the lattice. That is to say, if we translate this region by arbitrary lattice vectors $\mathbf{R}$, we could cover the whole space. This choice of primitive cell is called a Wigner-Seitz primitive cell.

B. Reciprocal lattices

Due to translational symmetry, physical quantities are also periodic under lattice translations. To characterize such a property, it is convenient to introduce three new vectors: [7]

$$\begin{cases} \mathbf{b}_1 = (2\pi)\dfrac{\mathbf{a}_2 \times \mathbf{a}_3}{\mathbf{a}_1 \cdot (\mathbf{a}_2 \times \mathbf{a}_3)}, \\ \mathbf{b}_2 = (2\pi)\dfrac{\mathbf{a}_3 \times \mathbf{a}_1}{\mathbf{a}_2 \cdot (\mathbf{a}_3 \times \mathbf{a}_1)}, \\ \mathbf{b}_3 = (2\pi)\dfrac{\mathbf{a}_1 \times \mathbf{a}_2}{\mathbf{a}_3 \cdot (\mathbf{a}_1 \times \mathbf{a}_2)}, \end{cases} \tag{6}$$

The vectors defined above are called reciprocal basis vectors. Note that the quantities in the denominator in the above equations are in fact identical and is nothing but the volume of the primitive cell. The reciprocal vectors satisfy the unique property:

$$\mathbf{a}_i \cdot \mathbf{b}_j = (2\pi)\delta_{ij}\ . \tag{7}$$

That is to say, although $\mathbf{a}_i$'s are not necessarily orthogonal, they are mutually orthogonal with the $\mathbf{b}_i$'s. With the reciprocal vectors $\mathbf{b}_i$'s as basis vectors, we can construct a new lattice structure whose points are given by

$$\mathbf{K} = h_1\mathbf{b}_1 + h_2\mathbf{b}_2 + h_3\mathbf{b}_3\ , \tag{8}$$

[6] Adding to the up-sided ones is equivalent. But adding points to both will yield a finer triangular lattice, not the honeycomb lattice.

[7] Our definition here differs from that in some solid state physics books by a factor of (2π). This convention makes it easier to write plane waves on the lattice.

with h_1, h_2, h_3 being integers. This lattice is known as the reciprocal lattice of the original lattice generated by the $\mathbf{a}_i$'s and the vector $\mathbf{K}$ given above is called a reciprocal lattice vector. It is easy to verify from the definition (6) that the volume of the primitive cell for the reciprocal lattice is given by $\Omega^* = \mathbf{b}_1 \cdot (\mathbf{b}_2 \times \mathbf{b}_3) = (2\pi)^3/\Omega$ with $\Omega = \mathbf{a}_1 \cdot (\mathbf{a}_2 \times \mathbf{a}_3)$ being the volume of the primitive cell for the original lattice. In fact, these two lattices are mutually reciprocal to each other. In other words, if we were to form "the reciprocal lattice of the reciprocal lattice" we would have obtained the original lattice back again (apart from factors of 2π).

The reciprocal vectors are useful in many aspects. For example, given an arbitrary vector $\mathbf{x}$, let us decompose it into superposition of basis vectors $\mathbf{a}_i$'s: $\mathbf{x} = \xi_1\mathbf{a}_1 + \xi_2\mathbf{a}_2 + \xi_3\mathbf{a}_3$ (ξ_i's are usually non-integers). Then the "coordinates" ξ_i can be obtained via: $\xi_i = \mathbf{x}\cdot\mathbf{b}_i/(2\pi)$.

Another more commonly used area is the following. Due to translational symmetry of the lattice, some physical quantities (e.g. the lattice potential energy experienced by a electron) are periodic in the coordinate $\mathbf{x}$ when translated by a lattice vector:

$$F(\mathbf{x}) = F(\mathbf{x} + \mathbf{R}) \ , \tag{9}$$

with $\mathbf{R} = l_1\mathbf{a}_1 + l_2\mathbf{a}_2 + l_3\mathbf{a}_3$ being an arbitrary lattice vector (i.e. l_i's being integers). Writing the above periodic condition in terms of the coordinates ξ_i's we find:

$$F(\xi_1, \xi_2, \xi_3) = F(\xi_1 + l_1, \xi_2 + l_2, \xi_3 + l_3) \ . \tag{10}$$

That is to say, when viewed as a function of the ξ_i's, the function is periodic in each of the ξ_i's with period 1. Thus, the function can be expanded into Fourier series:

$$F(\xi_1, \xi_2, \xi_3) = \sum_{h_1,h_2,h_3} \tilde{F}_{h_1h_2h_3} e^{2\pi i(h_1\xi_1 + h_2\xi_2 + h_3\xi_3)} \ , \tag{11}$$

where the Fourier coefficient $\tilde{F}_{h_1h_2h_3}$ may be obtained via:

$$\tilde{F}_{h_1h_2h_3} = \int d^3\xi F(\xi_1, \xi_2, \xi_3) e^{-2\pi i(h_1\xi_1 + h_2\xi_2 + h_3\xi_3)} \ , \tag{12}$$

where the integration range for each ξ_i is from 0 to 1 (i.e. over its period). Another more convenient way of writing the above equations is:

$$\begin{cases} F(\mathbf{x}) = \sum_{\mathbf{K}} \tilde{F}_{\mathbf{K}} e^{i\mathbf{K}\cdot\mathbf{x}} \ , \\ \tilde{F}_{\mathbf{K}} = \frac{1}{\Omega} \int_\Omega d^3\mathbf{x} F(\mathbf{x}) e^{-i\mathbf{K}\cdot\mathbf{x}} \ , \end{cases} \tag{13}$$

where we have used $\mathbf{K} = h_1\mathbf{b}_1 + h_2\mathbf{b}_2 + h_3\mathbf{b}_3$ as the label in the reciprocal (Fourier) space while the three-dimensional integral is over a primitive cell of the original lattice.

On the reciprocal space lattice, take any lattice point as the origin and form a Wigner-Seitz primitive cell around it. This Wigner-Seitz cell in reciprocal lattice is called the first Brillouin zone (FBZ) of the reciprocal lattice. First Brillouin zone can also be defined as those points which can be reached by going from the origin along a path that passes no Bragg planes. Similarly, second Brillouin zone consists of those points which can be reached from the origin along a path that passes through only one Bragg plane. Higher Brillouin zones are defined analogously.

Here comes the examples of reciprocal lattices.

Example I.7 *For simple cubic (SC) lattice of lattice spacing a, the basis vectors are:*

$$\mathbf{a}_1 = (a, 0, 0), \mathbf{a}_2 = (0, a, 0), \mathbf{a}_3 = (0, 0, a) \ ,$$

and the volume of the primitive cell is simply $\Omega = a^3$. The reciprocal vectors are:

$$\mathbf{b}_1 = (2\pi/a, 0, 0), \mathbf{b}_2 = (0, 2\pi/a, 0), \mathbf{b}_3 = (0, 0, 2\pi/a) \ ,$$

and the reciprocal lattice is also a SC lattice with lattice spacing $(2\pi)/a$ and primitive cell volume of $(2\pi)^3/a^3$.

Example I.8 *Take the body-centered cubic (BCC) lattice as in Example I.2. The basis vectors for the BCC lattice are:*

$$\mathbf{a}_1 = a(1, 0, 0), \mathbf{a}_2 = a(0, 1, 0), \mathbf{a}_3 = a(1/2, 1/2, 1/2) \ .$$

The volume of the primitive cell is $\Omega = a^3/2$ and the reciprocal basis vectors are:

$$\mathbf{b}_1 = \frac{2\pi}{a}(1, 0, -1), \mathbf{b}_2 = \frac{2\pi}{a}(0, 1, -1), \mathbf{b}_3 = \frac{2\pi}{a}(0, 0, 2) \ . \tag{14}$$

It might not be so easy to realize that, in reciprocal space this is a face-centered cubic (FCC) lattice with the size of the cube given by $4\pi/a$. One way of seeing this is to define a new reciprocal vector: $\mathbf{b}'_3 = \mathbf{b}_1 + \mathbf{b}_2 + \mathbf{b}_3 = (2\pi/a)(1, 1, 0)$. Then it is easily seen that $\mathbf{b}_1$, $\mathbf{b}_2$ and $\mathbf{b}'_3$ are indeed equivalent to those basis vectors of a FCC lattice as shown in Example I.3. The volume for the primitive cell in the reciprocal space is $\Omega^* = 2(2\pi)^3/a^3$ as it should. Therefore, FCC and BCC lattices are mutually reciprocal to each other.

For the purpose of our project, we only need two-dimensional cases. In this case, things are somewhat simplified. Only two basis vectors $\mathbf{a}_1$ and $\mathbf{a}_2$ are needed for a two-dimensional lattice. We may take $\mathbf{a}_3 = \mathbf{e}_3$ to be the unit vector in the z direction and the reciprocal vectors are:

$$\mathbf{b}_1 = (2\pi)\frac{\mathbf{a}_2 \times \mathbf{e}_3}{|\mathbf{a}_1 \times \mathbf{a}_2|} , \mathbf{b}_2 = (2\pi)\frac{\mathbf{e}_3 \times \mathbf{a}_1}{|\mathbf{a}_1 \times \mathbf{a}_2|} . \tag{15}$$

Therefore, the direction of $\mathbf{b}_1$ is obtained by rotating $\mathbf{a}_2$ clockwise by $\pi/2$ while the direction of $\mathbf{b}_2$ is obtained by rotating $\mathbf{a}_1$ counterclockwise by $\pi/2$.

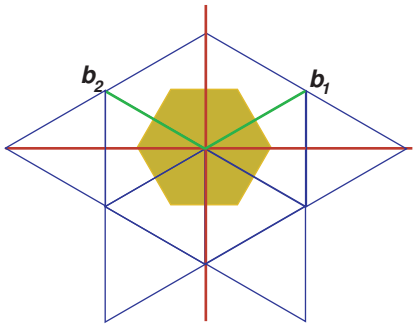

FIG. 2. Illustration of the first Brillouin zone (FBZ) for the triangular lattice. The reciprocal lattice is also a triangular lattice with basis vectors given by $\mathbf{b}_1$ and $\mathbf{b}_2$ (marked green in the figure). The FBZ is the hexagon shaped shaded area (the Wigner-Seitz primitive cell) around the origin of reciprocal lattice. Since the Bravais lattice for the honeycomb is also a triangular lattice, the FBZ for honeycomb is the same as the triangular lattice shown in this figure.

Example I.9 *Take the triangular lattice as shown in Example I.5. The reciprocal vectors are given by:*

$$\mathbf{b}_1 = \frac{2\pi}{a}(+1, 1/\sqrt{3}), \mathbf{b}_2 = \frac{2\pi}{a}(-1, 1/\sqrt{3}) .$$

The reciprocal lattice is also a triangular lattice with the volume of the primitive cell being $\Omega^* = 2/(\sqrt{3}a^2)$.

Example I.10 *For the honeycomb lattice (non-Bravais lattice) discussed in Example I.6, we only have to consider the Bravais lattice associated with it which is still the triangular lattice. Assuming the lattice spacing for the honeycomb to be* a*, the reciprocal vectors are:*

$$\mathbf{b}_1 = \frac{2\pi}{a}(+1/\sqrt{3}, 1/3), \mathbf{b}_2 = \frac{2\pi}{a}(-1/\sqrt{3}, 1/3) . \tag{16}$$

This forms a triangular lattice in reciprocal space. It is easy to check that FBZ for the lattice is a hexagon shaped area centered at the origin on the reciprocal lattice (see Fig. 2).

C. Periodic boundary conditions

So far our discussion only concerns infinite lattices. For practical reasons, it is also useful to consider lattices with finite number of points (finite lattices). In theoretical investigations, finite lattices with open boundaries are usually more complicated since one has to specify the boundary conditions. Therefore, in theoretical investigations (in particular, numerical investigations) we prefer large but finite systems without boundaries. This can be realized by the so-called periodic boundary conditions, also know as the Born-von Karmen conditions.

We assume that, instead of having infinite of primitive cells, we have only finite number of them. In particular, we identify the points: $\mathbf{x}$ with $\mathbf{x} + N_i\mathbf{a}_i$ with N_i $i = 1, \cdots, d$ being some (large) positive integers and $\mathbf{a}_i$ being the i-th basis vector for the primitive cell. Geometrically speaking, this forms a d-dimensional torus. In other words, we partition the whole three-dimensional Euclidean space by $\mod(\mathbf{x}, N_i\mathbf{a}_i), i = 1, \cdots, d$. To put it more explicitly, we have only N_i units of primitive cell along $\mathbf{a}_i$ direction.

Under periodic boundary conditions, any function $\psi(\mathbf{x})$ becomes periodic in $N_i\mathbf{a}_i$:

$$\psi(\mathbf{x}) = \psi(\mathbf{x}+\mathbf{T}) , \mathbf{T} = l_1N_1\mathbf{a}_1 + l_2N_2\mathbf{a}_2 + l_3N_3\mathbf{a}_3 , \tag{17}$$

with l_i's being integers. Therefore, we could perform Fourier expansion on the function:

$$\begin{cases} \psi(\mathbf{x}) = \sum_{\mathbf{k}} \tilde{F}_{\mathbf{k}} e^{i\mathbf{k}\cdot\mathbf{x}} , \\ \tilde{F}_{\mathbf{k}} = \frac{1}{V}\int_V d^3\mathbf{x}\psi(\mathbf{x})e^{-i\mathbf{k}\cdot\mathbf{x}} , \end{cases} \tag{18}$$

where $\mathbf{k}$ is given by:

$$\mathbf{k} = \frac{h_1}{N_1}\mathbf{b}_1 + \frac{h_2}{N_2}\mathbf{b}_2 + \frac{h_3}{N_3}\mathbf{b}_3 , \tag{19}$$

with h_i's being integers. Such a representation for $\mathbf{k}$ automatically satisfy:

$$e^{i\mathbf{k}\cdot\mathbf{T}} = 1 , \tag{20}$$

with $\mathbf{T} = l_1N_1\mathbf{a}_1 + l_2N_2\mathbf{a}_2 + l_3N_3\mathbf{a}_3$.

One important case is when the function $\phi(\mathbf{R})$ is *only defined* on lattice vector points $\mathbf{R}$. We then have:

$$\begin{cases} \phi(\mathbf{R}) = \frac{1}{\sqrt{N_1N_2N_3}}\sum_{\mathbf{k}} \tilde{\phi}_{\mathbf{k}} e^{i\mathbf{k}\cdot\mathbf{R}} , \\ \tilde{\phi}_{\mathbf{k}} = \frac{1}{\sqrt{N_1N_2N_3}}\sum_{\mathbf{R}} \phi(\mathbf{R})e^{-i\mathbf{k}\cdot\mathbf{R}} , \end{cases} \tag{21}$$

In this case, since $\mathbf{R}$ is the lattice vector, adding the above $\mathbf{k}$ by multiples of $\mathbf{b}_i$ (or equivalently speaking, adding the corresponding h_i by multiples of N_i) will not change physics and therefore is viewed as completely identical situation. Thus, the number of different $\mathbf{k}$ is simply $N_1 \times N_2 \times N_3$ and each integer h_i is defined mod (N_i). Usually, people like to take more symmetric choice: $h_i = (-N_i/2, -N_i/2+1, \cdots, N_i/2]$ such that in reciprocal space the range of $\mathbf{k}$ is symmetric around the origin. The natural choice is to take $\mathbf{k}$ in the first Brillouin zone (FBZ) of the reciprocal lattice defined before.

D. Symmetry of the lattice

Symmetries of various lattice in three or two dimensions are systematically described by their corresponding symmetry groups. These groups are non-empty sets that contain all the symmetry operations of the lattice, including rotations, reflections and lattice translations. Rotations and reflections are with respect to a symmetry center and they form what is called a point groups. When combined with lattice translations point groups are enlarged to space groups. [8] Since the details of this subject involves group theory and its representations, I will not cover it here, just to make things simpler. Interested reader can consult related books on point groups and space groups.

II. ENERGY BANDS IN SOLIDS

Crystalline solids are quite complicated systems. It is a quantum-mechanical many-body system with interactions. Roughly speaking, we can think of them as being made up of electrons and atom cores which form a specific lattice structure. The Hamiltonian of the system consists of three major parts: 1) kinetic energies for the electrons; 2) interactions of the electrons with the lattice (the atoms) via a periodic potential $V(\mathbf{x})$; 3) interactions (Coulomb or others) among the electrons. The third interaction complicates the treatment since it involves pairwise interactions of electrons and the system becomes a genuine many-body system (also known as strong correlated electron systems).

To make things easier, within the so-called independent electron approximation electron-electron interaction is omitted. Then we are left with a system of independent electrons, with each electron interacts with the lattice but they do not interact with each other. The systems then becomes a quantum mechanical system involving one electron interacts with a periodic potential $V(\mathbf{x}) \equiv V(\mathbf{x}+\mathbf{R})$, with $\mathbf{R}$ an arbitrary lattice vector. This is the setup of electron band theory. [9] Band theory in solids are discussed in all solid state textbooks, see relevant chapters in Ref. [1**?** –3].

A. Bloch theorem

As said above, within framework of independent electron approximation, one has to solve Schrödinger equation of a single electron interacting with the lattice via a periodic potential:

$$\hat{H}\psi(\mathbf{x}) \equiv \left(-\frac{\hbar^2}{2m}\nabla^2 + V(\mathbf{x})\right)\psi(\mathbf{x}) = E\psi(\mathbf{x}) \ , \qquad (22)$$

where $\hat{H}$ is the Hamiltonian of the single electron within the independent electron approximation. The key point is that the lattice potential $V(\mathbf{x})$ is periodic when translated by a lattice vector $V(\mathbf{x}) = V(\mathbf{x}+\mathbf{R})$ where $\mathbf{R} = l_1\mathbf{a}_1 + l_2\mathbf{a}_2 + l_3\mathbf{a}_3$ is an arbitrary lattice vector. This implies that the translational operator $\hat{T}_{\mathbf{R}}$, which implements the unitary change in Hilbert space when a lattice translation $\mathbf{R}$ is performed, must commute with the Hamiltonian: $[\hat{T}_{\mathbf{R}}, \hat{H}] = 0$. Thus, the eigenfunctions $\psi(\mathbf{x})$ can be chosen as common eigenfunctions for both the Hamiltonian and the translational operator $\hat{T}_{\mathbf{R}}$. Now, take the finite lattice with $N_1 \times N_2 \times N_3$ primitive cells with periodic boundary conditions applied. It then follows that the eigenfunction can be written as:

$$\psi(\mathbf{x}) = e^{i\mathbf{k}\cdot\mathbf{x}}u_{\mathbf{k}}(\mathbf{x}) \ , \quad u_{\mathbf{k}}(\mathbf{x}+\mathbf{R}) = u_{\mathbf{k}}(\mathbf{x}) \ , \qquad (23)$$

where $\mathbf{k}$ is vector taken in the first Brillouin zone (FBZ) of the reciprocal lattice: $\mathbf{k} = \frac{h_1}{N_1}\mathbf{b}_1 + \frac{h_2}{N_2}\mathbf{b}_2 + \frac{h_3}{N_3}\mathbf{b}_3$, with l_i being integers in the range of $(-N_i/2, N_i/2]$. This result is also known as the Bloch theorem in solid state physics.

[8] In mathematics, this is accomplished by the so-called semi-direct product of the two groups.

[9] If we were to omit all interactions, then we are left with a free electron gas theory which is the ideal fermi gas treated in standard statistical mechanics.

B. The tight binding model

For a single electron in latticized solids, if it is close to an atom at $\mathbf{R}$, the electron will interact most strongly with that particular atom. Therefore, ignoring the effects of other atoms, the quantum-mechanical motion of the electron is characterized by atomic eigenfunctions $\phi_\alpha(\mathbf{x}-\mathbf{R})$ satisfying:

$$\left[-\frac{\hbar^2}{2m}\nabla^2 + U(\mathbf{x}-\mathbf{R})\right]\phi_\alpha(\mathbf{x}-\mathbf{R}) = E_\alpha\phi_\alpha(\mathbf{x}-\mathbf{R}) \ . \tag{24}$$

Here $U(\mathbf{x}-\mathbf{R})$ is the atomic potential energy of the electron around the atom at $\mathbf{R}$, α designates an atomic orbital (eigenstate) with energy E_α and eigenfunction $\phi_\alpha(\mathbf{x}-\mathbf{R})$.

The tight-binding model amounts to express the wavefunction of the lattice electron in terms of linear superposition of these orbitals. So we write:

$$\psi(\mathbf{x}) = \sum_{\mathbf{R}} a_{\mathbf{R}}\phi_\alpha(\mathbf{x}-\mathbf{R}) \ . \tag{25}$$

When this is substituted into the Schrödinger equation of the lattice electron, we get

$$\sum_{\mathbf{R}} a_{\mathbf{R}}\left[(E_\alpha - E) + (V(\mathbf{x}) - U(\mathbf{x}-\mathbf{R}))\right]\phi_\alpha(\mathbf{x}-\mathbf{R}) = 0 \ . \tag{26}$$

Assuming that the atomic orbitals are "tight" such that we have:

$$\int d^3\mathbf{x}\phi^*_\alpha(\mathbf{x}-\mathbf{R}')\phi_\alpha(\mathbf{x}-\mathbf{R}) = \delta_{\mathbf{R}\mathbf{R}'} \ . \tag{27}$$

Therefore, we get the set of equations for coefficients $a_{\mathbf{R}}$ as

$$\begin{cases} (E_\alpha - E)a_{\mathbf{R}} - \sum_{\mathbf{R}} J(\mathbf{R}-\mathbf{R}')a'_{\mathbf{R}} = 0 \ , \\ J(\mathbf{R}-\mathbf{R}') = \int d^3\mathbf{r}\phi^*_\alpha(\mathbf{r}-(\mathbf{R}-\mathbf{R}'))[U(\mathbf{r}) - V(\mathbf{r})]\phi_\alpha(\mathbf{r}) \ . \end{cases} \tag{28}$$

This set of equations is solved by:

$$a_{\mathbf{R}} = \frac{1}{\sqrt{N}}e^{i\mathbf{k}\cdot\mathbf{R}} \ . \tag{29}$$

with $N = N_1N_2N_3$ and $\mathbf{k}$ being a vector in the FBZ of the reciprocal lattice. Substitute this into the equation we finally get:

$$\begin{cases} \psi^{(\alpha)}_{\mathbf{k}}(\mathbf{x}) = \frac{1}{\sqrt{N}}\sum_{\mathbf{R}} e^{i\mathbf{k}\cdot\mathbf{R}}\phi_\alpha(\mathbf{x}-\mathbf{R}) \ , \\ E(\mathbf{k}) = E_\alpha - \sum_{\mathbf{R}} J(\mathbf{R})e^{-i\mathbf{k}\cdot\mathbf{R}} \ , \\ J(\mathbf{R}) = \int d^3\mathbf{r}\phi^*_\alpha(\mathbf{r}-\mathbf{R})[U(\mathbf{r}) - V(\mathbf{r})]\phi_\alpha(\mathbf{r}) \ . \end{cases} \tag{30}$$

Normally, since the atomic orbitals are centered at the lattice points, the function $J(\mathbf{R})$ decays exponentially when $|\mathbf{R}|$ is increased. In most applications, taking only the nearest neighbors on the lattice suffices. It is also noted that, adding the wave vector $\mathbf{k}$ by multiples of reciprocal basis vectors will not change the expression (so restricting the values $\mathbf{k}$ inside the FBZ is enough). In fact, the above wavefunction $\psi^{(\alpha)}_{\mathbf{k}}(\mathbf{x})$ satisfies the Bloch theorem discussed in the previous subsection:

$$\psi^{(\alpha)}_{\mathbf{k}}(\mathbf{x}) = e^{i\mathbf{k}\cdot\mathbf{x}}\left[\frac{1}{\sqrt{N}}\sum_{\mathbf{R}} e^{i\mathbf{k}\cdot(\mathbf{R}-\mathbf{x})}\phi_\alpha(\mathbf{x}-\mathbf{R})\right], \tag{31}$$

and the function in the square bracket is easily verifed to be a periodic function (the function $u_{\mathbf{k}}(\mathbf{x})$ in Bloch theorem) when translated by an arbitrary lattice vector $\mathbf{R}'$.

Example II.1 *Consider the band theory of electrons on three-dimensional simple cubic (SC) lattices. The first Brillouin zone is a cube at the center of reciprocal lattice with size $2\pi/a$. If we take only the s-wave orbital, there is only one overlap integral between nearest neighbors:*

$$J_s(\mathbf{R}) = \int d^3\mathbf{r}\phi^*_s(\mathbf{r}-\mathbf{R})[U(\mathbf{r}) - V(\mathbf{r})]\phi_s(\mathbf{r}) \ . \tag{32}$$

where $\mathbf{R} = (1,0,0)a$ plus five other possible nearest neighbors. Since the s-orbital wavefunction is isotropic, the integral in fact does not depend on the direction of $\mathbf{R}$. In other words, all six nearest neighbors give rise to the same integral. If we denote this integral simply by J_s and call it the s-orbital hopping parameter. If we ignore other neighbors, the energy eigenvalues are given by:

$$E(\mathbf{k}) = E_s - 2J_s\left(\cos(k_1a) + \cos(k_2a) + \cos(k_3a)\right) \ . \tag{33}$$

Within the FBZ, the argument of each of the cos*-functions runs from $-\pi$ to $+\pi$ and the energy is therefore between $E_s - 6J_s$ to $E_s + 6J_s$. Therefore, the energy eigenvalue for the electron forms an energy band of width $12J_s$ centered around E_s. The energy of the electron cannot take values outside the band. For an infinite lattice, the energy levels inside the band is continuous. For a large but finite lattice, the energy values inside the band is quasi-continuous. This is why such a theory is called energy band theory for electrons.*

C. The tight binding model: second quantized version

The tight-binding model introduced in the previous subsection can also be treated within the framework of second quantization. We will first briefly review the basics on second quantization [4] and then re-express the tight-binding model in second-quantized form which is the form commonly used in the literature.

Second quantization is a name due to historical reasons. Within non-relativistic quantum mechanics, it is nothing but changing to a particular representation, namely the occupation number representation of the theory. First recall a quantum mechanical harmonic oscillator whose Hamiltonian is given by: $\hat{H} = (1/2)p^2 + (1/2)x^2$. It is known that, by introducing the annihilation and creation operators: $a = (x - ip)/\sqrt{2}$ and $a^\dagger = (x + ip)/\sqrt{2}$, the Hamiltonian is brought into canonical form: $H = a^\dagger a + 1/2$. Since it is trivial to verify that the creation and annihilation operators satisfy: $[a, a^\dagger] = 1$, it follows that the eigenvalues for the number operator $N \equiv a^\dagger a$ must be non-negative integers with each integer n corresponds to a eigenstate of the Hamiltonian.

Now consider a *multi-particle quantum-mechanical system*. The total Hamiltonian of the system is written as a summation of single-particle contributions $H_a^{(1)}$ (like the kinetic energy), two-particle contributions $H_{ab}^{(2)}$ (like the pairwise interaction energy), etc. So we may write:

$$H = \sum_a H_a^{(1)} + \sum_{a>b} H_{ab}^{(2)} + \cdots \ . \tag{34}$$

Like in the harmonic oscillator case, it is convenient to use the occupation number representation for multi-particle quantum systems. We will use $\{\phi_i(\mathbf{x})\}$ to designates the set of eigenfunctions for a single-particle quantum state labeled by i. For a system of N identical particles, each particle can occupy any of these single-particle quantum states. We can now use occupation numbers to designates the multi-particle quantum states: $|N_1, \cdots, N_i, \cdots\rangle$ where each N_i represents the number of particles on that particular state i. Such eigenstates in occupation numbers are also called Fock states of the multi-particle system. The full wavefunction of the system $\Psi(\xi_1, \cdots, \xi_N) = \langle \xi_1, \cdots, \xi_N | N_1, \cdots, N_i, \cdots, \rangle$ can be obtained by direct products of single-particle wavefunctions and properly symmetrized or anti-symmetrized in accordance with Bose or Fermi statistics. Annihilation operators a_i and creation operators $a_i^\dagger$ are defined via:

$$\begin{cases} a_i|\cdots, N_i, \cdots\rangle = \sqrt{N_i}|\cdots, N_i - 1, \cdots\rangle \ , \\ a_i^\dagger|\cdots, N_i, \cdots\rangle = \sqrt{N_i + 1}|\cdots, N_i + 1, \cdots\rangle \ . \end{cases} \tag{35}$$

Another way of writing the same equation is to give the only non-vanishing matrix element of a_i and $a_i^\dagger$ as:

$$\langle N_i - 1|a_i|N_i\rangle = \sqrt{N_i} \ , \langle N_i|a_i^\dagger|N_i - 1\rangle = \sqrt{N_i} \ . \tag{36}$$

It is easy to verify that:

$$[a_i, a_j^\dagger] = \delta_{ij} \ , \quad [a_i^\dagger, a_j^\dagger] = [a_i, a_j] = 0 \ , \tag{37}$$

and the number operator on state i is given by:

$$N_i = a_i^\dagger a_i \ . \tag{38}$$

If we compute the matrix element of a single-particle operator $H_a^{(1)}$ between two wavefunctions, the matrix element is non-zero only when the occupation number of two states are different by one unit for a pair ij:

$$\langle N_i, N_j - 1|H^{(1)}|N_i - 1, N_j\rangle = H_{ij}^{(1)}\sqrt{N_i N_j} \ . \tag{39}$$

This is so because for the single-particle Hamiltonian and single-particle wavefunction, particle number is conserved (basically single-particle wavefunction satisfies Schrödinger equation which preserves probability). We therefore find that, single-particle contributions may be written in terms of creation and annihilation operators:

$$H^{(1)} = \sum_{i,j} H_{ij}^{(1)} a_i^\dagger a_j \ . \tag{40}$$

This is the so-called second-quantized version for the single-particle Hamiltonian.

Example II.2 *Consider again the electrons in a simple cubic (SC) lattice within tight-binding model as discussed in Example II.1. The Hamiltonian of the electrons has exactly the form as given by Eq. (34). Here the single-particle contribution $H_a^{(1)} = T_a + V(\mathbf{x}_a)$ with T_a being the kinetic energy of the particle a and $V(\mathbf{x}_a)$ is the potential energy of the particle with the lattice. The two-particle contribution: $H_{ab}^{(2)} = e^2/|\mathbf{x}_a - \mathbf{x}_b|$ represents the two-particle Coulomb interaction. Other pairwise interactions (e.g. spin-spin interaction, etc.) can also be added if necessary. Within the independent electron approximation, only $H_a^{(1)}$ is considered and $H_{ab}^{(2)}$ and other interactions involving more than one particles are neglected.*

Let us consider only the s-orbital and only nearest neighbor couplings for $J_s(\mathbf{R})$. Since the wavefunctions $\phi_s(\mathbf{x}-\mathbf{R})$

are approximately orthonormal for different $\mathbf{R}$*, they can be viewed as the set of functions* $\{\phi_i(\mathbf{x})\}$ *in the second quantization procedure. In the second quantized version, an annihilation (creation) operator* $a_{\mathbf{R}}$ *(*$a^\dagger_{\mathbf{R}}$*) is defined and the Hamiltonian is expressed as:*

$$H = -t\sum_{\mathbf{R},\mu}(a^\dagger_{\mathbf{R}+\hat{\mu}}a_{\mathbf{R}} + h.c.)\ , \tag{41}$$

where $\mathbf{R}$ *runs over all lattice points and* $\mathbf{R}+\hat{\mu}$ *represents the nearest neighbor point of* $\mathbf{R}$ *in the positive* μ *direction,* $\mu = 1, 2, 3$*. The hopping parameter* $t = J_s(\mathbf{R} = a(1, 0, 0))$ *is the overlapping integral for nearest neighbors for the* s*-orbital as given by Eq. (32).*

¶ The second quantization procedure briefly introduced above deals with only Bosonic degrees of freedom. The creation and annihilation operators for a particular state i satisfy the canonical commutation relation $[a_i, a_j^\dagger] = \delta_{ij}$ which implies that the number operator $N_i = a_i^\dagger a_i$ takes non-negative integral eigenvalues. However, we know that in Nature, there are particles that are fermionic. For these particles, Pauli's exclusion principle applies. That is to say, the number operator N_i for fermions can take only two possible eigenvalues: 0 or 1. This is realized in the second-quantized version by requiring fermionic creation and annihilation operators $c_i^\dagger$ and c_i to satisfy the anti-commutation relation:

$$\{c_i, c_j^\dagger\} \equiv c_i c_j^\dagger + c_j^\dagger c_i = \delta_{ij}\ , \tag{42}$$

together with $\{c_i, c_j\} = \{c_i^\dagger, c_j^\dagger\} = 0$. This set of anti-commutation relations automatically ensure Pauli's principle, for if we were to create two fermions on any single quantum state $|\Psi\rangle$: $c_i^\dagger c_i^\dagger|\Psi\rangle = -c_i^\dagger c_i^\dagger|\Psi\rangle = 0$, we automatically get a null result.

With this in mind (and the fact that electrons are fermions instead of bosons), the tight-binding Hamiltonian in the second quantization formalism are still given as before, with the modification that the creation and annihilation operators are in fact fermionic operators that satisfy anti-commutation relations. For example, Eq. (41) is still valid but the creation and annihilation operators (i.e. $a^\dagger_{\mathbf{R}+\hat{\mu}}$ and $a_{\mathbf{R}}$) satisfy anti-commutation relations: $\{a_{\mathbf{R}}, a^\dagger_{\mathbf{R}'}\} = \delta_{\mathbf{R}\mathbf{R}'}$, $\{a^\dagger_{\mathbf{R}}, a^\dagger_{\mathbf{R}'}\} = \{a_{\mathbf{R}}, a_{\mathbf{R}'}\} = 0$. Another issue to be mentioned about electrons is that each electron also has an inner degree of freedom, called "spin". An electron has spin $s = 1/2$ such that it has two possible spin states: spin up and spin down. This is reflected by adding a new spin index σ to the creation and annihilation operators of the electrons. For example, we would use $a^\dagger_{\mathbf{R}\sigma}$ to designate the creation operator which creates an electron with spin σ at site $\mathbf{R}$, where $\sigma = +, -$ indicates spin up and spin down states, respectively.

III. TIGHT-BINDING MODEL FOR GRAPHENE

A. Hybridized orbitals and tight-binding Hamiltonian for graphene

Let us now move to the case of graphene, i.e. a honeycomb lattice in two dimensions. As we know from previous discussions (Example I.6 and Example I.10), honeycomb lattice is a non-Bravais lattice with an underlying triangular lattice structure. What is behind this structure is the the so-called sp^2-hybridization for the carbon atoms that form graphene structure. A single carbon atom has the atomic structure $2s^2 2p^2$, i.e. two electrons in s-orbital and two in $2p$-orbital. When carbon atoms are close to each other, however, depending on the specific conditions, different atomic orbitals can mix with each other, forming new hybrid orbitals. This process is also known as orbital hybridization. For the case of graphene, the $2s$-orbital hybridizes with two $2p$-orbitals (say p_x and p_y-orbital), forming three sp^2-hybridized orbitals. These three hybridized orbitals lie in the xy-plane with 120° angle between one another. The un-hybridized p_z orbital is perpendicular to the xy-plane. When forming graphene lattices, three sp^2-hybridized orbitals forms the so-called σ-bond with other neighboring carbon atoms. This sets up the honeycomb lattice structure. The remaining un-hybridized p_z-orbitals of the carbon atoms forms the so-called π-bond. Similar hybridization also shows up in molecules of benzene. The σ-bonds between neighboring carbon atoms are vert tight and therefore can be thought as part of the atomic core in the tight-binding model. Only the π electrons can "propagate" (or "hop") from one atomic core to its neighboring positions. We also point out that, if the full hybridization is realized, i.e. the s-orbital mixes with all three p-orbitals forming four sp^3-hybridized orbitals, the carbon atoms then from a diamond structure lattice in three-dimensions.

With the above explanation, we can write out the tight-binding Hamiltonian for graphene as

$$H = -t\sum_{\mathbf{R}\in\Lambda_A,i,\sigma}\left[a^\dagger_{\mathbf{R},\sigma}b_{\mathbf{R}+\boldsymbol{\delta}_i,\sigma} + b^\dagger_{\mathbf{R}+\boldsymbol{\delta}_i,\sigma}a_{\mathbf{R},\sigma}\right]\ . \tag{43}$$

The form of this Hamiltonian close follow that of Eq. (41) with $a^\dagger_{\mathbf{R},\sigma}$ being the (fermionic) creation operator for spin

σ at site $\mathbf{R}$ which is a lattice site on sublattice A (a triangular lattice), $b_{\mathbf{R}+\boldsymbol{\delta}_i,\sigma}$ being the annihilation operator for spin σ at a nearest neighboring site $\mathbf{R}+\boldsymbol{\delta}_i$ with $i = 1, 2, 3$ indicating three nearest neighbors on the lattice. Here the lattice site $\mathbf{R} \in \Lambda_A$ runs over all sublattice points of triangular lattice A, (hence $(\mathbf{R} + \boldsymbol{\delta}_i) \in \Lambda_B$ belongs to sublattice B). The summation over i runs from 1 to 3 and the vectors $\boldsymbol{\delta}_i$ are defined as in Example I.6, Eq. (5). The summation over spin index σ runs over $+$ and $-$. The parameter t is called the hopping parameter and is related to the corresponding overlapping integral for the orbitals.

We can now introduce a more compact notation by combining the operators on two sublattices into one set of operators:

$$\psi_{\mathbf{R},\sigma} = \begin{pmatrix} a_{\mathbf{R},\sigma} \\ b_{\mathbf{R}+\boldsymbol{\delta}_1,\sigma} \end{pmatrix} . \tag{44}$$

Note this $\psi_{\mathbf{R},\sigma}$ is in fact a four-component operator: [10] its upper two components correspond to annihilation operators (with two different spins respectively) on sublattice A and its lower two components correspond to annihilation operators on sublattice B. For later convenience, I will call this index the chiral index borrowing terminologies in particle physics. So the operator can be denoted as: $\psi_{\mathbf{R},\alpha,\sigma}$ with $\alpha = 1$ for the upper two components and $\alpha = 2$ for the lower two components. Similarly, we can define $\psi^\dagger_{\mathbf{R},\alpha,\sigma}$. In terms of these operators, the canonical anti-commutation relations are: $\{\psi_{\mathbf{R}\alpha\sigma}, \psi^\dagger_{\mathbf{R}'\beta\rho}\} = \delta_{\mathbf{R}\mathbf{R}'}\delta_{\alpha\beta}\delta_{\sigma\rho}$, with all others vanish. If we want, we can also obtain the original operators (those $a_{\mathbf{R}}$'s and $b_{\mathbf{R}}$'s) with the help of projection operators:

$$\begin{cases} P_{L/R} = \dfrac{1 \pm \sigma_3}{2} , \\ \psi^L_{\mathbf{R}} \equiv P_L\psi_{\mathbf{R}} = \begin{pmatrix} a_{\mathbf{R}} \\ 0 \end{pmatrix} , \\ \psi^R_{\mathbf{R}} \equiv P_R\psi_{\mathbf{R}} = \begin{pmatrix} 0 \\ b_{\mathbf{R}+\boldsymbol{\delta}_1} \end{pmatrix} , \end{cases} \tag{45}$$

Borrowing "names" from particle physics, we shall call $a_{\mathbf{R}}$ and $b_{\mathbf{R}}$ the left-handed and right-handed component of the field operator $\psi_{\mathbf{R}}$.

Then, the Hamiltonian of the tight-binding model may be re-written as

$$H = -t \sum_{\mathbf{R},\mathbf{R}',\sigma,\alpha,\beta} \psi^\dagger_{\mathbf{R},\sigma,\alpha}\mathcal{M}_{\mathbf{R},\alpha;\mathbf{R}',\beta}\psi_{\mathbf{R}',\sigma,\beta} . \tag{46}$$

where the matrix $\mathcal{M}_{\mathbf{R},\mathbf{R}'}$ is trivial (i.e. an unit matrix) in spin indices but non-trivial in chiral indices. It is given by (omitting the chiral indices and write out in matrix form)

$$\mathcal{M}_{\mathbf{R},\mathbf{R}'} = \left(\delta_{\mathbf{R},\mathbf{R}'} + \sum_{i=1}^{2} \left[\left(\frac{1+\sigma_3}{2} \right) \delta_{\mathbf{R},\mathbf{R}'+\mathbf{a}_i} + \left(\frac{1-\sigma_3}{2} \right) \delta_{\mathbf{R},\mathbf{R}'-\mathbf{a}_i} \right] \right) \sigma_1 , \tag{47}$$

with σ_1, σ_2 and σ_3 are conventional Pauli matrices in chiral space (i.e. they are matrices carrying chiral indices).

It is then seen that the tight-binding Hamiltonian is a quadratic form in $\psi_{\mathbf{R},\sigma}$, with the matrix $\mathcal{M}$ being Hermitian. Another way of writing the same matrix is:

$$\mathcal{M}_{\mathbf{R},\mathbf{R}'} = \left(\delta_{\mathbf{R},\mathbf{R}'} + \frac{1}{2} \sum_{i=1}^{2} [\delta_{\mathbf{R}+\mathbf{a}_i,\mathbf{R}'} + \delta_{\mathbf{R}-\mathbf{a}_i,\mathbf{R}'}] \right) \sigma_1 - \frac{i}{2}\sigma_2 \sum_{i=1}^{2} [\delta_{\mathbf{R}+\mathbf{a}_i,\mathbf{R}'} - \delta_{\mathbf{R}-\mathbf{a}_i,\mathbf{R}'}] \tag{48}$$

It is worthwhile to point out that in two dimensions, the Pauli matrices are the corresponding γ-matrices: $\gamma_1 = \sigma_1$, $\gamma_2 = \sigma_2$ while the chiral matrix is $\gamma_3 = \sigma_3$.

[10] Okay, this type of thing is also known as spinors, but, it's just a name. Don't bother too much why.

B. Diagonalization of the Hamiltonian

Using translational invariance, it is easy to diagonalize the Hamiltonian (46). In fact, note that the field operators $\psi_{\mathbf{R}}$ are defined only on triangular lattice points $\mathbf{R}$, therefore we may use the Fourier expansion introduced in subsection I C (basically Eq. (21)):

$$\begin{cases} \psi_{\mathbf{R}} = \dfrac{1}{\sqrt{N_1 N_2}} \sum\limits_{\mathbf{k}} \psi_{\mathbf{k}} e^{i\mathbf{k}\cdot\mathbf{R}} \ , \\ \psi^{\dagger}_{\mathbf{R}} = \dfrac{1}{\sqrt{N_1 N_2}} \sum\limits_{\mathbf{k}} \psi^{\dagger}_{\mathbf{k}} e^{-i\mathbf{k}\cdot\mathbf{R}} \ , \end{cases} \tag{49}$$

with $\mathbf{k}$ taking values in the FBZ as shown in Fig. 2. Such a transformation is unitary in the sense that the new operators in reciprocal space, i.e. $\psi_{\mathbf{k}}$'s satisfy the same canonical anti-commutation relations as the $\psi_{\mathbf{R}}$'s do. In terms of these the Hamiltonian is partly diagonalized:

$$H = -t \sum_{\mathbf{k}} \psi^{\dagger}_{\mathbf{k}} \left[f_1(\mathbf{k})\sigma_1 + f_2(\mathbf{k})\sigma_2 \right] \psi_{\mathbf{k}} \ , \tag{50}$$

with the functions $f_1(\mathbf{k})$ and $f_2(\mathbf{k})$ given explicitly by

$$\begin{cases} f_1(\mathbf{k}) = 1 + \cos(\mathbf{k}\cdot\mathbf{a}_1) + \cos(\mathbf{k}\cdot\mathbf{a}_2) \ , \\ f_2(\mathbf{k}) = \sin(\mathbf{k}\cdot\mathbf{a}_1) + \sin(\mathbf{k}\cdot\mathbf{a}_2) \ . \end{cases} \tag{51}$$

The Hamiltonian in Eq. (50) is already diagonal in $\mathbf{k}$-space. It remains to be diagonalized in chiral space. The matrix to be diagonalized is a 2×2 matrix of the form

$$\begin{pmatrix} 0 & -t[f_1(\mathbf{k}) - i f_2(\mathbf{k})] \\ -t[f_1(\mathbf{k}) + i f_2(\mathbf{k})] & 0 \end{pmatrix} \ . \tag{52}$$

The eigenvalues are easily found to be:

$$E_{\pm}(\mathbf{k}) = \pm t \sqrt{f_1^2(\mathbf{k}) + f_2^2(\mathbf{k})} \ , \tag{53}$$

with the wave-vector $\mathbf{k}$ in the FBZ. The 2×2 unitary matrix V which diagonalize the matrix in Eq. (52) is found to be:

$$V = \frac{1}{\sqrt{2}} \begin{pmatrix} 1 & 1 \\ e^{i\phi_f} & -e^{i\phi_f} \end{pmatrix} \ , \quad e^{i\phi_f} \equiv -\frac{f_1 + i f_2}{\sqrt{f_1^2 + f_2^2}} \ . \tag{54}$$

Using this matrix, we can define:

$$\psi_{\mathbf{k}} = V \cdot \chi_{\mathbf{k}} \ , \psi^{\dagger}_{\mathbf{k}} = \chi^{\dagger}_{\mathbf{k}} \cdot V^{\dagger} \ , \tag{55}$$

and the Hamiltonian (50) reduces to a completely diagonal form

$$H = \sum_{\mathbf{k},\sigma} \left[E_+\mathbf{k} \chi^{\dagger}_{\mathbf{k},1,\sigma} \chi_{\mathbf{k},1,\sigma} + E_-\mathbf{k} \chi^{\dagger}_{\mathbf{k},2,\sigma} \chi_{\mathbf{k},2,\sigma} \right] \ , \tag{56}$$

where we have restored the spin index σ on the operators. If we denote the chiral index $\alpha = 1, 2$ by $\alpha = +, -$, respectively, we may write this expression in a more compact form:

$$H = \sum_{\mathbf{k},\alpha,\sigma} E_{\alpha} \chi^{\dagger}_{\mathbf{k},\alpha,\sigma} \chi_{\mathbf{k},\alpha,\sigma} \ . \tag{57}$$

where the summation over the chiral index $\alpha = +, -$ is understood with $E_{\alpha}(\mathbf{k}) = E_+(\mathbf{k}), E_-(\mathbf{k})$ respectively. Since the transformations from $\psi_{\mathbf{R}}$'s to $\psi_{\mathbf{k}}$'s (i.e. Eq. (49)) and from $\psi_{\mathbf{k}}$'s to $\chi_{\mathbf{k}}$'s (i.e. Eq. (55)) are all unitary, the fermionic operators $\chi_{\mathbf{k},\alpha,\sigma}$ satisfy the canonical anti-commutation relations. This implies that the eigenvalues of the Hamiltonian (57) are simple summations of multiples (well, in fact only zero or one unit due to Pauli's principle) of $E_{\pm}(\mathbf{k})$.

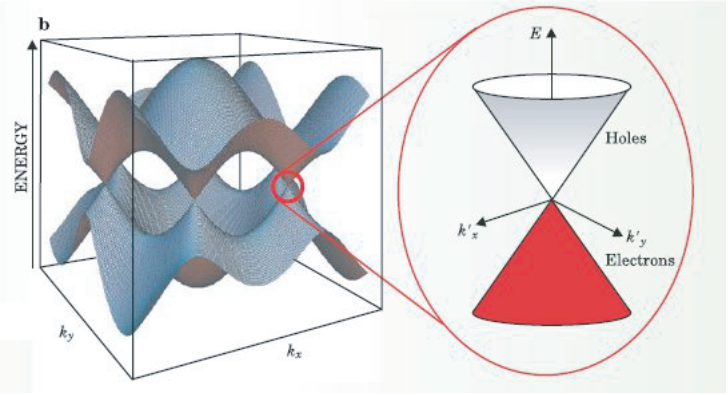

FIG. 3. Illustration of the spectrum $E_{\pm}(\mathbf{k})$ for the tight-binding Hamiltonian for graphene. The neighborhood of a Dirac point is also visualized.

The spectrum $E_{\pm}(\mathbf{k})$ has two branches for values of $\mathbf{k}$ in the FBZ of the reciprocal lattice. This corresponds to the fact that honeycomb lattice contains two lattice points within each primitive cell. The two branches is completely symmetric with respect to $E = 0$. This is shown in Fig. 3. It is interesting to note that, at special points in the FBZ, we have $E_+(\mathbf{k}) = E_-(\mathbf{k}) = 0$. These special points need extra consideration. It is easy to verify that these points are exactly the six corners of the hexagon for the FBZ (see Fig. 2). These points are called Dirac points since, as we will show shortly, around these points the electron behaves like a two-dimensional Dirac fermion with relativistic-like dispersion relation. One thing to be reminded is that, although there are six corners for the FBZ, there are only *two* distinct Dirac points really. This is because each corner is shared by

three neighboring hexagons in reciprocal space, thus we have: $6 \times (1/3) = 2$.

To be more specific, we pick the two Dirac points as follows. The Dirac point $D1$ is the corner on the positive x axis which has the coordinate: $\mathbf{k}_{D1} = (2\pi/a)(2/(3\sqrt{3}), 0)$ and the Dirac point $D2$ is the neighboring corner with coordinate: $\mathbf{k}_{D2} = (2\pi/a)(1/(3\sqrt{3}), 1/3)$. The other four corners can be obtained from $\mathbf{k}_{D1}$ or $\mathbf{k}_{D2}$ by adding reciprocal lattice vectors $\mathbf{b}_1$ or $\mathbf{b}_2$ (or linear combinations of them). We easily verify:

$$\begin{cases} \mathbf{k}_{D1} \cdot \mathbf{a}_1 = \dfrac{2\pi}{3}, \mathbf{k}_{D1} \cdot \mathbf{a}_2 = -\dfrac{2\pi}{3}, \\ \mathbf{k}_{D2} \cdot \mathbf{a}_1 = -\dfrac{2\pi}{3}, \mathbf{k}_{D2} \cdot \mathbf{a}_2 = \dfrac{2\pi}{3}, \end{cases} \tag{58}$$

It is then easy to see that $E_\pm(\mathbf{k}_{D1}) = E_\pm(\mathbf{k}_{D2}) = 0$. Close to the neighborhood of these two points, we have $\mathbf{k} \simeq \mathbf{k}_D + \delta\mathbf{k}$, we may expand the function $E_\pm(\mathbf{k})$ and obtain:

$$E_\pm(\mathbf{k}_D + \delta\mathbf{k}) \simeq \pm\frac{3}{2}ta|\delta\mathbf{k}| \ . \tag{59}$$

As promised, this dispersion relation (i.e. the relation between energy $E(\mathbf{k})$ and momentum $\mathbf{k}$) resembles that for a relativistic massless particle: $E(\mathbf{k}_D + \delta\mathbf{k}) \propto |\delta\mathbf{k}|$. The only difference is that the proportionality coefficient is not the speed of light, but $(3/2)at$ which is much less than the speed of light.

It is also interesting to count number of states in reciprocal space. As we remarked, the value of $\mathbf{k}$ takes values in the FBZ. Therefore, if we have $N = N_1 \times N_2$ lattice points on triangular sublattice A, $\mathbf{k}$ can also take N different values. However, the honeycomb lattice is a non-Bravais lattice with two lattice points per primitive cell. Therefore, there are in fact $2 \times N = 2N$ states and this is reflected by the fact that for each $\mathbf{k}$ we have two branches of $E(\mathbf{k})$: $E_+(\mathbf{k})$ and $E_-(\mathbf{k})$. This has not taken into account the inner spin degree of freedom. Counting the spin in, we have altogether $4N$ single-particle states for N lattice points on sublattice A (hence $2N$ lattice points on the whole honeycomb lattice). If each carbon atom offers one π-orbital electron, we have thus altogether $2N$ Bloch electrons which is exactly the so-called half-filled case(i.e. half of the total number of states $4N$). This means that, at zero temperature, all the electron states below $E = 0$ are filled while those above $E = 0$ are unoccupied. Of course, doping can change the situation.

IV. SOME STATISTICAL PHYSICS FOR MANY-BODY SYSTEMS [11]

In this section, we will briefly review the basics in quantum statistical physics for multi-particle systems. For simplicity, we normally take systems that are made up of almost independent subsystems. For such systems, the total energy of the system is a summation of energies for individual subsystems. The statistical physics for such quantum systems is well-known. It belongs to the ideal Bose gas or Fermi gas systems depending of the nature of its constituent particles. In undergraduate statistical physics, this is treated within the energy representation, i.e. in a representation where the Hamiltonian operator is diagonal. Here, we would like to study the system within a more general framework of statistical physics. We will introduce the so-called density matrix or density operator ρ to characterize the quantum system. This general framework is needed if we were to study interacting quantum systems of many particles.

A. The density operator for ensembles [13]

Quantum systems can be divided into two categories: systems whose dynamics are purely determined by the equations of quantum dynamics (Schrödinger equation) or statistical ensembles (also known as mixed systems) whose properties are characterized by both quantum dynamics and a probability distribution. For ensembles, a further probabilistic description is needed due to lack of further information.

For ensembles we define the density operator ρ as follows:

$$\rho = \sum_\alpha p_\alpha |\alpha\rangle\langle\alpha| \ . \tag{60}$$

In this definition, $\{|\alpha\rangle\}$ with $\alpha = 1, 2, \cdots$ denotes a collection of complete, ortho-normal quantum states which characterize the quantum system. It could be eigenstates of the Hamiltonian or some other states which forms a complete basis in the Hilbert space. $\{p_\alpha\}$ denotes the

[12] Here I assume that the reader already knows equilibrium statistical physics at the undergraduate level. See, for example, my lecture notes [5] and references therein.

[14] Density operator is discussed in more details in most quantum statistical physics courses or quantum mechanics courses. See, for example, Refs. [6, 7].

corresponding probability that the system is in the quantum state $|\alpha\rangle$. If we take the representation where $|\alpha\rangle$ are eigenstates, the density operator is also diagonal with diagonal matrix elements p_α. Of course, to normalize the probability, we have:

$$Tr(\rho) = \sum_\alpha p_\alpha = 1 \ . \tag{61}$$

If $p_\alpha = 1$ for a particular α and zero for other states, we then have a pure state described by $|\alpha\rangle$. Generally speaking, we have a statistical description of a collection of states. It is easy to show that for pure state, we have $\rho^2 = \rho$ which becomes invalid for ensembles.

One easily obtains the time evolution of the density operator as:

$$i\frac{\partial \rho}{\partial t} = -[\rho, H] \ . \tag{62}$$

This looks very much like the time evolution of an operator in the Heisenberg picture except that the sign is the opposite. However, one should keep in mind that the density operator ρ is defined via Schrödinger picture states.

The ensemble average of any quantum operator A can be obtained by taking the trace of the product of A with the density operator:

$$\langle A\rangle = Tr(\rho A) = \sum_\alpha p_\alpha \langle\alpha|A|\alpha\rangle \ . \tag{63}$$

In particular, the entropy of the quantum ensemble can be defined via:

$$S = -k_B Tr(\rho \ln \rho) \ . \tag{64}$$

Two ensembles are particularly useful. One is the canonical ensemble whose density operator and partition function are given by

$$\rho = \frac{e^{-\beta H}}{Z} \ , Z = Tr(e^{-\beta H}) \ , \tag{65}$$

with H being the Hamiltonian of the system and $\beta = 1/(k_B T)$. The other interesting ensemble is the grand canonical ensemble whose density operator and partition function are

$$\rho = \frac{e^{-\beta(H-\mu N)}}{Z} \ , Z = Tr(e^{-\beta(H-\mu N)}) \ , \tag{66}$$

where N being the particle number operator for the system and μ is the chemical potential for the particles. It is easy to verify that if we take the basis of energy eigenstates, all the above formulae reduce to the familiar forms you have seen in equilibrium statistical physics course. For example, taking the energy eigenstates $|s\rangle$ as basis (with energy eigenvalue given by E_s), the density operator is completely diagonal with eigenvalues:

$$\rho_s = \frac{1}{Z} e^{-\beta E_s} \ , Z = \sum_s e^{-\beta E_s} \ . \tag{67}$$

This is exactly the formula in statistical physics course. For the grand canonical ensemble, for non-relativistic systems, particle number is conserved and this means that the number operator commutes with Hamiltonian: $[\hat{H}, \hat{N}] = 0$. [15] Hence, it is possible to pick common eigenstate for both of them: $|S_N\rangle$, an energy eigenstate with N particles, i.e. $\hat{H}|S_N\rangle = E_{S,N}|S_N\rangle$ and $\hat{N}|S_N\rangle = N|S_N\rangle$. With this basis, the density operator is again diagonal:

$$\rho_{S,N} = \frac{1}{Z} e^{-\beta(E_{S,N}-\mu N)} \ , Z = \sum_{S,N} e^{-\beta(E_{S,N}-\mu N)} \ , \tag{68}$$

This is again the familiar formula. However, with the general density operator formalism, we could study the quantum system in other basis as well since the trace is invariant under basis transformations.

B. Partition functions for ideal quantum gases

In statistical physics, if the total energy of a system is a sum of its individual subsystems, i.e. $E = \sum_i \varepsilon_i$, we call it a system with *almost independent subsystems*, or ideal gas systems. In this sense, the system of Bloch electrons in solids is exactly the same as the the free electron gas (ideal Fermi gas). The only difference between the two is the energy for one particular subsystem, ε_i. For pure non-relativistic ideal fermion gas, i denotes different individual electrons with $\varepsilon_i = \hbar^2 \mathbf{k}_i^2/2m$. For the Bloch electrons in a solid, however, $i \to \mathbf{k}$ denotes a Bloch wavefunction with wave vector $\mathbf{k}$ in the FBZ of the lattice and $\varepsilon_{\mathbf{k}} = E(\mathbf{k})$ is the energy in band theory(for example, from a tight-binding model calculation or from some other more sophisticated methods). When the interactions of the electrons with the lattice are neglected, we recover the ideal electron gas model.

---

[15] Here we add a hat on operators just to distinguish an operator with its eigenvalue which is without a hat.

For the purpose of statistical physics, the two systems mentioned above are treated in the same manner, the only difference being the explicit expression for $\varepsilon_{\mathbf{k}}$. For example, the grand partition function is given by:

$$Z = \prod_s \left(1 \pm e^{-\beta(\varepsilon_s - \mu)}\right)^{\pm 1} . \tag{69}$$

Here s is a general index to designate single-particle states and ε_s is the energy eigenvalue for that state; μ is the chemical potential of the system. The $\pm$ sign in the above equation corresponds to the fermion or boson systems, respectively. For the Bloch electrons, $s = (\mathbf{k}, \sigma)$ and ε_s is the band energy (e.g. $E_\alpha(\mathbf{k})$ as in Eq. (53) for the graphene tight binding model).

The expectation value of the particle number on a particular single particle state s is

$$\bar{N}_s = \frac{1}{e^{\beta(\varepsilon_s - \mu)} \pm 1} , \tag{70}$$

where $\pm$ sign corresponds to fermion(boson) systems, respectively. This is the famous Fermi-Dirac (Bose-Einstein) distribution. We will call these two systems ideal Fermi gas or ideal Bose gas.

¶ We are particularly interested in the case of systems made up of identical fermions since electrons are fermions. At zero temperature, $T = 0$, the Fermi distribution is a step function in the energy ε_s, i.e. if $\varepsilon_s > \mu$, $\bar{N}_s = 0$ while for $\varepsilon_s < \mu$, $\bar{N}_s = 1$. Recall that for fermion systems we have Pauli's exclusion principle. This means that, at $T = 0$, all single particle states whose energy is below the chemical potential μ are fully occupied (i.e. $\bar{N}_s = 1$) while states whose energy is above the chemical potential μ are empty (i.e. $\bar{N}_s = 0$). So the chemical potential μ of the fermion system is determined implicitly by

$$N = \sum_{s, \varepsilon_s < \mu} 1 , \tag{71}$$

where N is the total number of fermions of the system being considered. In band theory of solids, single particle energies are functions of the wave vector $\mathbf{k}$ in FBZ: $\varepsilon_s = E(\mathbf{k})$. We may plot the energy $E(\mathbf{k})$ as a function of $\mathbf{k}$ which is within the FBZ. For the graphene within tight binding model, this is exactly what is shown in Fig. 3. Chemical potential μ, also known as the Fermi surface (denoted by ε_F) of the fermion system is the boundary equi-energy surface which separates the states that are occupied from the states that are empty. In other words, at $T = 0$, states below the Fermi surface are all occupied while the states above are all empty.

Example IV.1 *Take the graphene within the tight binding model discussed in Sec. III as an example. We assume that there are $N = N_1 \times N_2$ carbon atoms on lattice A and equal number of carbon atoms on lattice B. From the result of the band energy $E_\pm(\mathbf{k})$, we have altogether $4N$ quantum states, half of which above zero, the other half below zero. Consider only the electrons that form the π bonds (each carbon atom provides one electron). We thus have $2N$ electrons. Therefore, at $T = 0$, these $2N$ electrons will exactly fill all states below zero, i.e. states with $E_-(\mathbf{k})$ with $\mathbf{k}$ in the FBZ (N possible values) and each energy state can hold two electrons of opposite spin $\sigma = +, -$. All states with $E_+(\mathbf{k})$ are empty. Therefore, the Fermi surface (or the chemical potential μ) for the system exactly lies at $\mu = 0$.*

¶ At non-zero temperature, as long as the temperature is not high such that $\mu/(k_B T) \gg 1$, the qualitative feature of the system is more or less the same except that the boundary between the occupied and empty states are not sharp. In fact, the statistical properties of the system can be computed by a series expansion (also known as the Sommerfeld expansion) in terms of $k_B T/\mu_0$.

C. Electronic properties of solids

Having briefly described the band theory of solids, we know review the relation of band theory with the electronic properties of solids. It turns out that many physical properties of latticized solids can be explained fairly well by band theory.

¶ Conductors, insulators and semi-conductors: The basic conclusion here is that empty or completely filled energy bands cannot contribute to conductance of the solid. In other words, for a solid whose band structure is such that all energy bands are either completely empty or completely filled, then the solid must be an insulator. Conductors must corresponds to partially filled energy bands, according to band theory.

D. Beyond the independent electron approximation

So far, we have not touched the question of mutual interactions among the electrons. Physically we know that these interactions exist due to Coulomb repulsion. Not only that, a rough estimate for the order of magnitude of this Coulomb interaction among electrons in a typical

solid is huge. It is of the order of eV while other energies (say the hopping energy between neighboring sites) are even less than this! This seems to pose a serious doubt on the so-called *independent electron approximation*. On the other hand, band theory of electrons, which is based on the independent electron approximation, seems to predict very reasonable results. It can incorporate many physical properties of the latticized solids. So the question boils down to: why the band theory works so well despite the fact electron-electron interaction is huge?

The answer to this question is very complicated. Historically, it is not completely understood until Landau spelled out his Fermi liquid theory. The story is like this: although numerically the electron-electron interaction is huge, most part of this interaction goes into the modification of some physical parameters of the band electrons (its effective mass, etc.). Or using fancier words, most part of the electron-electron interaction only "renormalize" the single electron parameters. So the band electrons behave very much like independent electrons except that its parameters (mass, charge, etc.) are modified (or renormalized) away from its values for free electrons. Of course, not all the effects of electron-electron interaction are included in this manner, but this is the basic picture of Fermi liquid theory. If the interactions among electrons cannot be treated within independent electron approximation for an electron system, we call it a strongly correlated electron system.

Physical properties of a strongly correlated electron system can be dramatically different from those of an independent electron system. Theoretical treatment of strongly correlated systems are also more involved. The general setup of density operators in statistical physics and second quantization is suitable for this study. As an example, let us first look at the famous Hubbard model.

Example IV.2 *Consider the s-orbital tight binding model on a three-dimensional simple cubic lattice as discussed in Example II.2. Within the independent electron approximation, the second-quantized Hamiltonian is basically given by Eq. (41) except that we still have to take into account the spin degree of freedom. So the Hamiltonian within the independent electron approximation is*

$$H_0 = -t \sum_{\mathbf{R},\mu} \left(a^\dagger_{\mathbf{R}+\hat{\mu}\sigma} a_{\mathbf{R}\sigma} + h.c. \right) , \tag{72}$$

where the summation over the repeated spin index σ is understood. Performing a Fourier expansion as in Eq. (49) one can bring the above Hamiltonian into a canonical form: $H_0 = \sum_{\mathbf{k}} E(\mathbf{k}) a^\dagger_{\mathbf{k}\sigma} a_{\mathbf{k}\sigma}$ with the band energy $E(\mathbf{k})$ given by

$$E(\mathbf{k}) = -2t \left(\cos(k_1 a) + \cos(k_2 a) + \cos(k_3 a) \right) . \tag{73}$$

This is the same as Eq. (33) in Example II.1 apart from an irrelevant constant.

To go beyond independent electron approximation, one adds an on-site Coulumb repulsion energy of the form: $U n_{\mathbf{R}+} n_{\mathbf{R}-}$ with $n_{\mathbf{R}\pm} = a^\dagger_{\mathbf{R}\pm} a_{\mathbf{R}\pm}$ being the number operator of a particular spin on site $\mathbf{R}$. Due to Pauli's exclusion principle, $n_{\mathbf{R}\pm}$ can take values of either 0 or 1. Thus, the term $U n_{\mathbf{R}+} n_{\mathbf{R}-} = U$ only when both $n_{\mathbf{R}+}$ and $n_{\mathbf{R}-}$ is 1 and $U n_{\mathbf{R}+} n_{\mathbf{R}-} = 0$ otherwise. Therefore, this term is a reflection of the on-site Coulumb repulsion when a site is occupied by two electrons (with spin up and down each). In the second-quantized version, the Hamiltonian then becomes

$$H = -t \sum_{\mathbf{R},\mu} \left(a^\dagger_{\mathbf{R}+\hat{\mu}\sigma} a_{\mathbf{R}\sigma} + h.c. \right) + U \sum_{\mathbf{R}} n_{\mathbf{R}+} n_{\mathbf{R}-} . \tag{74}$$

This is the Hamiltonian for the famous Hubbard model, a model being extensively studied within strongly correlated electron systems.

Despite its simple appearance, solving the Hubbard model is not an easy task at all. In fact, no exact solution exists so far except for the one-dimensional case which can be solved by Bethe ansatz. Here the word "solve" means to compute the grand partition function of the system:

$$Z = Tr(e^{-\beta H'}) , \tag{75}$$

with $H' \equiv H - \mu N = H - \mu \sum_{\mathbf{R}} (n_{\mathbf{R}+} + n_{\mathbf{R}-})$. Although not exactly solvable, several analytic approximation methods can be applied if the Coulomb interaction parameter U is very large or very small. For general set of parameters, the model could be studied by numerical methods. For example, at half-filling (i.e. $\mu = 0$), the model can be studied using Monte Carlo simulations. Away from half-filling, however, the system suffers from the infamous "sign problem" and Monte Carlo methods cannot be applied directly. This makes the numerical study quite complicated.

V. PATH INTEGRAL REPRESENTATION FOR THE PARTITION FUNCTION [16]

[17] A good reference book on the applications of coherent state path

A. Coherent states

¶ Given a pair of creation and annihilation operators: $a^\dagger$ and a together with a unique vacuum state $|0\rangle$, one can define a state:

$$|\lambda\rangle = e^{\lambda a^\dagger}|0\rangle \ , \tag{76}$$

with $\lambda \in \mathbb{C}$ being a complex number. It is easy to verify that the state defined above is an eigenstate of the annihilation operator with eigenvalue λ:

$$a|\lambda\rangle = \lambda|\lambda\rangle \ . \tag{77}$$

The state given in Eq. (76) is not normalized. Instead, we have:

$$\langle 0|e^{\lambda_1^* a}e^{\lambda_2 a^\dagger}|0\rangle = e^{\lambda_1^*\lambda_2} \ .$$

Therefore, if we define

$$|\lambda\rangle = \exp\left(-\frac{|\lambda|^2}{2}\right)\cdot e^{\lambda a^\dagger}|0\rangle \ , \tag{78}$$

the state is normalized according to: $\langle\lambda|\lambda\rangle = 1$. Such a state is called a coherent state. Taking the conjugate of Eq. (78) we have: $\langle\lambda|a^\dagger = \langle\lambda|\lambda^*$. Therefore, if our quantum operators are normally ordered by moving all annihilation operators to the right and creation operators to the left, such normally ordered operators have simple matrix element when sandwiched between two coherent states. We can simply replace the corresponding operators a and $a^\dagger$ by its eigenvalues λ and λ^* respectively. For example:

$$\langle\lambda_1|(a^\dagger)^2a^3|\lambda_2\rangle = (\lambda_1^*)^2(\lambda_2)^3\langle\lambda_1|\lambda_2\rangle \ .$$

Note that the coherent states are not orthogonal:

$$\langle\lambda_1|\lambda_2\rangle = e^{-(|\lambda_1|^2+|\lambda_2|^2-2\lambda_1^*\lambda_2)} \ . \tag{79}$$

However, they are over-complete:

$$\int (d\lambda^* d\lambda)\,|\lambda\rangle\langle\lambda| = \mathbb{1} \ , \ (d\lambda^* d\lambda) \equiv \frac{d[Re(\lambda)]d[Im(\lambda)]}{\pi} \tag{80}$$

This completeness relation allows us to insert coherent states in between products of operators.

integral methods in many-body physics is Ref. [8], which describes quantum field theories used in many-body systems. Here we will only use a small portion of the material in that book.

¶ Coherent states can also be defined for fermionic systems. Since the creation and annihilation operators anti-commute (apart from contact terms), we need numbers that are anti-commuting in nature. Normal number certainly cannot play this role. We need the so-called Grassmann numbers. The set of Grassman nubmers, denoted by $\mathbb{G}$ satisfy the unique property:

$$\eta_i\eta_j + \eta_j\eta_i = 0 \ , \ \forall\eta_i,\eta_j \in \mathbb{G} \ . \tag{81}$$

For a multi-fermion system with M possible states, we have a pair of (fermionic) creation and annihilation operators: a_i and $a_i^\dagger$, $i = 1,\cdots,M$. We then define the following fermionic coherent state:

$$|\eta_1\cdots,\eta_M\rangle \equiv \sum_{J=0}^{\infty}\frac{(-)^{J(J-1)/2}}{J!}(\eta_i a_i^\dagger)^J|0\rangle \ , \tag{82}$$

where $\eta_1,\cdots,\eta_M$ are a set of Grassmann variables and a summation over i is understood in $(\eta_i a_i^\dagger)$ (repeated indices are summed over, according to Einstein's convention). Formally the summation in this definition extends to infinity but it is really not exceeding $J = M$ due to Pauli's exclusion principle. So the convergence of the summation is not a problem. For brevity, we sometimes denote such a fermionic coherent state by $|\eta\rangle$. The conjugate of definition 82 is given by:

$$\langle\bar\eta_1\cdots,\bar\eta_M| \equiv \langle 0|\sum_{J=0}^{\infty}\frac{(-)^{J(J-1)/2}}{J!}(\bar\eta_i a_i)^J \ , \tag{83}$$

with $\bar\eta_1,\cdots,\bar\eta_M$ being *another* set of Grassmann variables. For brevity, we denote such a fermionic coherent bra-state by $\langle\bar\eta|$. With these definitions, it is easy to verify that they are eigenstates of the fermionic creation and annihilation operators respectively:

$$a_i|\eta\rangle = |\eta\rangle\eta_i \ , \ \ \langle\bar\eta|a_i^\dagger = \bar\eta_i\langle\bar\eta| \ . \tag{84}$$

Please pay attention to the position where the eigenvalues appear. Since Grassmann numbers are anti-commuting in nature, if you want to move the eigenvalue to the left or right of the state itself, possible minus signs might appear.

The fermionic coherent states defined above are not orthogonal (like its bosonic counterpart). They satisfy

$$\langle\bar\eta|\eta\rangle = \exp(\bar\eta_i\eta_i) \ , \tag{85}$$

where in the exponent summation over repeated index i is understood.

One can also define derivative and integrations of Grassmann variables. These are defined to be Grassmann variables and being linear in its operand. For a particular Grassmann variable ξ, since $\xi^2 = 0$ identically, one only has to define:

$$\int d\xi = 0 \, , \int d\xi \xi = 1 \, . \tag{86}$$

Together with the linear property of the integral, the above equation defines the integral for a Grassmann integration unambiguously. Integration of multi-variables are defined accordingly. With this definition, it is easy to verify the completeness relation for the fermionic coherent state:

$$\int \left(\prod_i [d\bar{\eta}_i d\eta_i] \right) e^{-\bar{\eta}\cdot\eta} |\eta\rangle\langle\bar{\eta}| = \mathbb{1} \, , \tag{87}$$

where $\bar{\eta}\cdot\eta = \sum_i \bar{\eta}_i \eta_i$. Note that this form of completeness relation implies the following formula for the trace of an arbitrary operator:

$$Tr(A) = \int \left(\prod_i [d\bar{\eta}_i d\eta_i] \right) e^{-\bar{\eta}\cdot\eta} \langle -\bar{\eta}|A|\eta\rangle \, . \tag{88}$$

A useful property of the Grassmann integral is the Gaussian-like integral given below:

$$\int \left(\prod_i [d\bar{\eta}_i d\eta_i] \right) e^{\bar{\eta}_i \mathcal{M}_{ij} \eta_j} = \det \mathcal{M} \, . \tag{89}$$

This formula will be used extensively later on. It is to be compared with the analogous Gaussian integral for normal complex numbers:

$$\int \left(\prod_i [d\bar{\phi}_i d\phi_i] \right) e^{-\bar{\phi}_i \mathcal{M}_{ij} \phi_j} = [\det \mathcal{M}]^{-1} \, , \tag{90}$$

where $\bar{\phi}_i \equiv \phi_i^*$ and ϕ_i are normal complex numbers. [18] Another path-integral involving fermionic coherent states is the following:

$$\int \left(\prod_i [d\bar{\eta}_i d\eta_i] \right) (\eta_i \bar{\eta}_j) e^{\bar{\eta}_i \mathcal{M}_{ij} \eta_j} = \left[\mathcal{M}^{-1}\right]_{ij} \det \mathcal{M} \, . \tag{91}$$

Another commonly used formula for the matrix element of quadratic Hamiltonian between coherent states is the following:

$$\left\langle \bar{\eta} \left| \exp\left(a_i^\dagger A_{ij} a_j \right) \right| \eta \right\rangle = \exp\left[\bar{\eta}_i \left(e^A \right)_{ij} \eta_j \right] \, . \tag{92}$$

To prove this formula, one has to substitute $A \to tA$ and shows that both the left and right-handed side of the formula satisfy the same first-order ordinary differential equation (ODE) in the variable t. Then following the uniqueness of the first-order ODE, the formula then follows by setting $t = 1$.

B. Path integral representation for the Hubbard model

Consider the strongly correlated electron system like the Hubbard model discussed in subsection IV D. We would like to compute the grand partition function of the system:

$$Z = Tr\left[\exp\left(\beta t \sum_{\mathbf{R},\mu} \left(a^\dagger_{\mathbf{R}+\hat{\mu}\sigma} a_{\mathbf{R}\sigma} + h.c. \right) + \beta\mu \sum_{\mathbf{R}} a^\dagger_{\mathbf{R}\sigma} a_{\mathbf{R}\sigma} - \beta U \sum_{\mathbf{R}} n_{\mathbf{R}+} n_{\mathbf{R}-} \right) \right] \, , \tag{93}$$

with t, mu, U being the hopping energy, chemical potential and the on-site interaction energy, respectively. Since the hopping term and the Coulomb repulsion term in the Hamiltonian do not commute with each other, the partition function cannot be computed easily. However, if we chop the whole β interval into N_t slices: $\beta \equiv N_t a_t$, with $N_t \gg 1$ such that a_t being infinitesimally small, then we have:

[18] Here we have to assume that the matrix $\mathcal{M}$ satisfies certain conditions (e.g. Hermitean and positive definite) in order for the integral to be convergent. Furthermore, the integration measure has to be normalized properly.

$$e^{\hat{t}\sum_{\mathbf{R},\mu}\left(a^\dagger_{\mathbf{R}+\hat{\mu}\sigma}a_{\mathbf{R}\sigma}+h.c.\right)+\hat{\mu}\sum_{\mathbf{R}}a^\dagger_{\mathbf{R}\sigma}a_{\mathbf{R}\sigma}-\hat{U}\sum_{\mathbf{R}}n_{\mathbf{R}+}n_{\mathbf{R}-}}\simeq e^{\hat{t}\sum_{\mathbf{R},\mu}\left(a^\dagger_{\mathbf{R}+\hat{\mu}\sigma}a_{\mathbf{R}\sigma}+h.c.\right)+\hat{\mu}\sum_{\mathbf{R}}a^\dagger_{\mathbf{R}\sigma}a_{\mathbf{R}\sigma}}e^{-\hat{U}\sum_{\mathbf{R}}n_{\mathbf{R}+}n_{\mathbf{R}-}}+\cdots\ , \quad (94)$$

where $\hat{t}=a_t t$, $\hat{\mu}=a_t\mu$, $\hat{U}=a_t U$ and the omitted terms are of $\mathcal{O}(a_t^3)$. Assuming that both X and Y are small quantities (however non-commutative quantities) of $\mathcal{O}(a_t)$. It then follows that: $e^{X+Y}\simeq e^{Y/2}e^X e^{Y/2}\times e^A$ with $\mathcal{A}\sim([X,[X,Y]]$ or $[Y,[X,Y]])\sim\mathcal{O}(a_t^3)$. With this operation, the original partition function is factorized into N_t factors, each containing two exponential factors as given in the r.h.s of the above equation. We will label these N_t factors by a discrete variable τ with $\tau=1,\cdots,N_t$:

$$Z=Tr\left\{e^{h_0}e^v\cdots e^{h_0}e^v\right\}\ , \quad (95)$$

with

$$h_0=\hat{t}\sum_{\mathbf{R},\mu}\left(a^\dagger_{\mathbf{R}+\hat{\mu}\sigma}a_{\mathbf{R}\sigma}+h.c.\right)+\hat{\mu}\sum_{\mathbf{R}}a^\dagger_{\mathbf{R}\sigma}a_{\mathbf{R}\sigma},$$
$$v=-\hat{U}\sum_{\mathbf{R}}n_{\mathbf{R}+}n_{\mathbf{R}-} \quad (96)$$

Now it is time to utilize the second-quantization version to compute the traces. Note that in terms of creation and annihilation operators, the hopping term is quadratic (strictly speaking, it is bilinear) while the Coulomb interaction term is quartic. It is therefore crucial to transform it into a quadratic form. This is accomplished with the help of auxiliary fields. For the Hubbard model, there are two ways of doing this. The first one is the standard Hubbard-Stratonovich transformation, which introduces an continuous bosonic field $\xi_{\mathbf{R}}(\tau)$. The second one is to introduce a discrete Ising field variable $\sigma_{\mathbf{R}}(\tau)=\pm1$ instead of a continuous variable as proposed by J.E. Hirsch [9].

To perform the Hubbard-Stratonovich transformation, we first notice that for a fermionic number operator: $n^2_{\mathbf{R}\pm}=n_{\mathbf{R}\pm}$. It is then trivial to see that the following identities are satisfied:

$$n_{\mathbf{R}+}n_{\mathbf{R}-}=-\frac{1}{2}(n_{\mathbf{R}+}-n_{\mathbf{R}-})^2+\frac{1}{2}(n_{\mathbf{R}+}+n_{\mathbf{R}-})\ , \quad (97)$$
$$n_{\mathbf{R}+}n_{\mathbf{R}-}=+\frac{1}{2}(n_{\mathbf{R}+}+n_{\mathbf{R}-})^2-\frac{1}{2}(n_{\mathbf{R}+}+n_{\mathbf{R}-})\ . \quad (98)$$

These identities can transform the quantity $n_{\mathbf{R}+}n_{\mathbf{R}-}$ into a complete square (apart from the total particle number) with an either positive or negative coefficient. They are utilized in combination with the following Gaussian integral identities: [19]

$$\int_{-\infty}^{\infty}d\xi\exp\left[-\frac{1}{2}\xi^2+\sqrt{\hat{U}}\xi(n_{\mathbf{R}+}-n_{\mathbf{R}-})\right]=e^{\frac{\hat{U}}{2}(n_{\mathbf{R}+}-n_{\mathbf{R}-})^2}\ ,\hat{U}>0 \quad (99)$$
$$\int_{-\infty}^{\infty}d\xi\exp\left[-\frac{1}{2}\xi^2+\sqrt{|\hat{U}|}\xi(n_{\mathbf{R}+}+n_{\mathbf{R}-})\right]=e^{\frac{|\hat{U}|}{2}(n_{\mathbf{R}+}+n_{\mathbf{R}-})^2}\ ,\ \hat{U}<0, \quad (100)$$

Note that at this stage the positive-U Hubbard model and the negative-U Hubbard model yields a significant difference: Since on the right-hand-side of Eq. (99) and Eq. (100) *only positive squares* shows up (due to property of the Gaussian integral), the first and the second of these two integral identities are used for the positive-U and negative-U Hubbard model, respectively. Since we have to introduce an ξ variable for each $\mathbf{R}$ and for each given τ, we end up having an auxiliary field $\xi_{\mathbf{R}}(\tau)$. The big difference between the positive-U and negative-U Hubbard model is: the auxiliary field $\xi_{\mathbf{R}}(\tau)$ couples to the fermionic variable $(n_{\mathbf{R}+}-n_{\mathbf{R}-})$ in the positive-U case while it couples to $(n_{\mathbf{R}+}+n_{\mathbf{R}-})$ in the negative-U case instead. As we shall see in the following, this results in very different fermion matrix within the path integral representation. The conclusion is that, for the negative-U Hubbard model, the fermion matrix is identical for both up and down spins and the resulting fermionic determinant becomes positive-definite. For the positive-U case, however, since the auxiliary field couples to up and down spins differently, the resulting fermionic determinant is not necessarily positive-definite for all parameters. In fact, for $\mu\neq0$, it can have sign changes. This is the infamous sign-problem and complicates the numeri-

[19] We have dropped an irrelevant normalization factor for the Gaussian integral which is something like $1/\sqrt{\pi}$.

cal Monte Carlo. One can show, however, at half-filling (i.e. $\mu = 0$), the positive-U model has an extra symmetry (particle-hole symmetry) which then makes the determinant positive-definite again.

For either cases, we may re-write the partition function formally in terms of a path-integral:

$$Z = \int D\xi(\tau) e^{-\sum_{\tau,\mathbf{R}} \frac{\xi^2_{\mathbf{R}}(\tau)}{2}} Tr \prod_{\tau} \exp\left[-\left\{ H_0 + \sqrt{|\hat{U}|} \sum_{\mathbf{R}} \left[\xi_{\mathbf{R}}(\tau)(n_{\mathbf{R}+} \mp n_{\mathbf{R}-}) + \frac{\sqrt{|\hat{U}|}}{2}(n_{\mathbf{R}+} + n_{\mathbf{R}-}) \right] \right\} \right] , \quad (101)$$

where the upper and lower sign corresponds to the positive-U and negative-U case respectively. The free Hamiltonian in the above equation is given by: $H_0 = -\hat{t}\sum_{\mathbf{R},\mu}[a^\dagger_{\mathbf{R}+\hat{\mu}\sigma} a_{\mathbf{R}\sigma} + h.c.] - \hat{\mu}\sum_{\mathbf{R}} a^\dagger_{\mathbf{R}\sigma} a_{\mathbf{R}\sigma}$. Now the quantity in the exponential of the above path-integral becomes quadratic in the fermion creation and annihilation operators. So we may write it in a more compact form:

$$Z = \int D\xi(\tau) e^{-\sum_{\tau,\mathbf{R}} \frac{\xi^2_{\mathbf{R}}(\tau)}{2}} Tr \prod_{\tau} \exp\left[-\sum_{\mathbf{R},\mathbf{R}',\sigma,\sigma'} a^\dagger_{\mathbf{R},\sigma} T^{(\pm)}_{\mathbf{R},\sigma;\mathbf{R}'\sigma'}[\xi(\tau)] a_{\mathbf{R}',\sigma'} \right] , \quad (102)$$

where the trace is over the fermionic variables and the kernel $T^{(\pm)}_{\mathbf{R},\sigma;\mathbf{R}'\sigma'}[\xi(\tau)]$ (for the positive-U and negative-U case respectively) are given explicitly by:

$$T^{(+)}_{\mathbf{R},\sigma;\mathbf{R}'\sigma'}[\xi] = -\hat{t}\sum_{\mu}(\delta_{\mathbf{R},\mathbf{R}'+\mu} + \delta_{\mathbf{R},\mathbf{R}'-\mu})\,\delta_{\sigma\sigma'} + \left(\left[\frac{\hat{U}}{2} - \hat{\mu} \right] \delta_{\sigma\sigma'} + (\sigma_z)_{\sigma\sigma'} \sqrt{\hat{U}} \xi_{\mathbf{R}}(\tau) \right) \delta_{\mathbf{R},\mathbf{R}'} , \quad (103)$$

and similarly for $T^{(-)}$:

$$T^{(-)}_{\mathbf{R},\sigma;\mathbf{R}'\sigma'}[\xi] = \left\{ -\hat{t}\sum_{\mu}(\delta_{\mathbf{R},\mathbf{R}'+\mu} + \delta_{\mathbf{R},\mathbf{R}'-\mu}) + \left(\frac{|\hat{U}|}{2} - \hat{\mu} + \sqrt{\hat{U}} \xi_{\mathbf{R}}(\tau) \right) \delta_{\mathbf{R},\mathbf{R}'} \right\} \delta_{\sigma\sigma'} , \quad (104)$$

It is readily verified that this is a hermitian matrix. The trace over fermionic degrees of freedom can be evaluated exactly, basically using the fermionic coherent state formalism (mainly Eq. (89) and Eq. (92)). The derivation is contained in the next subsection. In terms of quantum field theory, this path-integral describes a fermion field interacting with a Gaussian scalar field $\xi_{\mathbf{R}}(\tau)$.

Instead of using a continuous real field $\xi_{\mathbf{R}}(\tau)$ as in the standard Hubbard-Stratonovich transformation, one could also transform the Hubbard model partition function using discrete Ising-like variables, as proposed by J.E. Hirsch [9]. To replace the Gaussian integral identities in Eq. (99) and Eq. (100), one can use the following identity:

$$e^{-\hat{U} n_{\mathbf{R}+} n_{\mathbf{R}-}} = \frac{1}{2} Tr_\sigma \exp\left[2a\sigma(n_{\mathbf{R}+} - n_{\mathbf{R}-}) - \frac{1}{2}\hat{U}(n_{\mathbf{R}+} + n_{\mathbf{R}-}) \right] , \quad \hat{U} > 0 \quad (105)$$

$$e^{|\hat{U}| n_{\mathbf{R}+} n_{\mathbf{R}-}} = \frac{1}{2} Tr_\sigma \exp\left[2a\sigma(n_{\mathbf{R}+} + n_{\mathbf{R}-} - 1) + \frac{1}{2}|\hat{U}|(n_{\mathbf{R}+} + n_{\mathbf{R}-} - 1) \right] , \hat{U} < 0 , \quad (106)$$

where the variable σ is an Ising variable that takes values of $+1$ and -1 and the parameter a is given by(in both the positive-U case and the negative-U case):

$$\cosh(2a) = e^{|\hat{U}|/2} . \quad (107)$$

It is easy to show these identities. Since the variable σ can take only two possible values, we simple write out the two terms in the r.h.s of Eq. (105) and Eq. (106) with the parameter a to be determined. Next, we notice that each of $n_{\mathbf{R}\pm}$ can only take two possible values: 0 and 1. This

gives four possibilities for the combination of $n_{\mathbf{R}+}$ and $n_{\mathbf{R}-}$. All we have to make sure is that the variable a has to be chosen such that for all these four cases the l.h.s and the r.h.s are equal. In fact, it is possible to derive other identities along this line, see Ref. [9] for more discussions.

Similar to the Gaussian case, we have to introduce the Ising field for each lattice site $\mathbf{R}$ and for each time slice τ. We will label the Ising field as $\sigma_{\mathbf{R}}(\tau)$. For the positive-$U$ and negative-U case, we will use either Eq. (105) or Eq. (106), respectively. With these transformations, the partition function will takes the same form as in Eq. (102) except that the kernel $\tilde{T}^{(\pm)}_{\mathbf{R},\sigma;\mathbf{R}'\sigma'}[\sigma(\tau)]$ (+ and − corresponds to the positive and negative-U case respectively) is different:

$$\tilde{T}^{(+)}_{\mathbf{R},\sigma;\mathbf{R}'\sigma'}[\sigma(\tau)] = -\hat{t}\sum_{\mu}\left(\delta_{\mathbf{R},\mathbf{R}'+\mu}+\delta_{\mathbf{R},\mathbf{R}'-\mu}\right)\delta_{\sigma\sigma'} + \left(\left[\frac{\hat{U}}{2}-\hat{\mu}\right]\delta_{\sigma\sigma'} + (\sigma_z)_{\sigma\sigma'}2a\sigma_{\mathbf{R}}(\tau)\right)\delta_{\mathbf{R},\mathbf{R}'}\ . \tag{108}$$

$$\tilde{T}^{(-)}_{\mathbf{R},\sigma;\mathbf{R}'\sigma'}[\sigma(\tau)] = \left\{-\hat{t}\sum_{\mu}\left(\delta_{\mathbf{R},\mathbf{R}'+\mu}+\delta_{\mathbf{R},\mathbf{R}'-\mu}\right) + \left(\frac{|\hat{U}|}{2}-\hat{\mu}+2a\sigma_{\mathbf{R}}(\tau)\right)\delta_{\mathbf{R},\mathbf{R}'}\right\}\delta_{\sigma\sigma'}\ . \tag{109}$$

This path-integral describes a fermion field interacting with an Ising field $\sigma_{\mathbf{R}}(\tau)$. This form is again quadratic in the fermionic variables and the trace can be evaluated using fermionic coherent state techniques.

No matter which of the transformation is used, one still has to deal with the integration (or the summation for the Ising field) of the auxiliary fields introduced, whether it be a continuous Gaussian field $\xi_{\mathbf{R}}(\tau)$ or an Ising field $\sigma_{\mathbf{R}}(\tau)$. Unfortunately, this step can not be done analytically in general. One usually has to rely on numerical methods like Monte Carlo simulations.

C. Evaluation of fermionic trace

Here we will use the coherent state techniques to compute the fermionic traces encountered in the last subsection (basically Eq. (102) for the Gaussian field situation and a similar formula for the Ising field situation). We start from the completeness relation Eq. (87) and the formula for the fermionic trace, Eq. (88), then Eq. (102) becomes:

$$Z = \int [D\xi D\bar{\eta}D\eta]\, e^{-\sum_{\tau,\mathbf{R}}\left[\frac{\xi^2_{\mathbf{R}}(\tau)}{2}+\bar{\eta}_{\mathbf{R},\tau}\eta_{\mathbf{R},\tau}\right]}\prod_{\tau=0}^{N_t-1}\left\langle\bar{\eta}_{\tau+1}\left|\exp\left[-\sum_{\mathbf{R},\mathbf{R}',\sigma,\sigma'}a^{\dagger}_{\mathbf{R},\sigma}T^{(\pm)}_{\mathbf{R},\sigma;\mathbf{R}'\sigma'}[\xi(\tau)]a_{\mathbf{R}',\sigma'}\right]\right|\eta_{\tau}\right\rangle\ , \tag{110}$$

where the so-called anti-periodic boundary condition for the fermion field $\bar{\eta}$ is understood: $-\bar{\eta}_0 = \bar{\eta}_{N_t}$. A typical factor in the above integrand can be computed using Eq. (92):

$$\left\langle\bar{\eta}_{\tau+1}\left|\exp\left[-a^{\dagger}\cdot\mathbb{T}[\xi(\tau)]\cdot a\right]\right|\eta_{\tau}\right\rangle = \exp\left[\bar{\eta}_{\tau+1}\cdot\left(e^{-\mathbb{T}}\right)\cdot\eta_{\tau}\right]\ ,$$

where we have used a compact (matrix and vector) notation for $T^{(\pm)}_{\mathbf{R},\sigma;\mathbf{R}'\sigma'}$, $a^{\dagger}_{\mathbf{R},\sigma}$, $a_{\mathbf{R},\sigma}$, $\bar{\eta}_{\mathbf{R},\tau+1,\sigma}$, $\eta_{\mathbf{R},\tau,\sigma}$. They are denotes as: $\mathbb{T}^{(\pm)}$, $a^{\dagger}$, a, $\bar{\eta}_{\tau+1}$ and η_{τ}, respectively. Since the matrix $\mathbb{T}^{(\pm)}$ is of at least of order $O(\sqrt{a_t})$ when the lattice spacing is small, we may simply keep the first two terms: $e^{-\mathbb{T}^{(\pm)}} \simeq \mathbb{1}-\mathbb{T}^{(\pm)}+\cdots$ in the exponential. Higher order terms involves next nearest-neighbor couplings of the fermion fields which will be neglected for the moment. In fact, we could use a better approximation:

$$e^{-\mathbb{T}^{(\pm)}} \simeq \mathbb{1}-\mathbb{T}^{(\pm)}+\frac{1}{2}\left[\mathbb{T}^{(\pm)}\right]^2+\cdots \tag{111}$$

This will give us an improved version of the path-integral. This point will be pursued later in subsection VIII A.

With this approximation, the partition function for the Hubbard model after the Hubbard-Stratonovich transfromation is obtained as:

$$Z = \int [D\xi D\bar{\eta} D\eta]\, e^{-\frac{\xi\cdot\xi}{2}} \exp\left(- \sum_{\tau=0}^{N_t-1} (\bar{\eta}_\tau - \bar{\eta}_{\tau+1}) \cdot \eta_\tau + \bar{\eta}_{\tau+1} \cdot \mathbb{T}^{(\pm)}[\xi(\tau)] \cdot \eta_\tau \right) , \tag{112}$$

In the above expression, the Grassmann variables to be integrated over are: $\eta_0, \eta_1, \cdots, \eta_{N_t-1}$ and $\bar{\eta}_0, \bar{\eta}_1, \cdots, \bar{\eta}_{N_t-1}$. Note that the integrand also explicitly contains $\bar{\eta}_{N_t}$ which is nothing but $(-\bar{\eta}_0)$ by anti-boundary condition. Recall that η and $\bar{\eta}$ are purely *independent* set of Grassmann variables. Therefore, one could redefine one set such that the hopping term in the above formula has the same temporal label τ:

$$\bar{\eta}_{\tau+1} = \bar{\zeta}_\tau, \quad \tau = 0, 1, \cdots, N_t - 1 . \tag{113}$$

After this substitution, one may re-write $\bar{\zeta}$ as $\bar{\eta}$ (since these are just dummy variables that are integrated over) and thus we arrive at

$$Z = \int [D\xi D\bar{\eta} D\eta]\, e^{-\frac{\xi\cdot\xi}{2}} \exp\left(- \sum_{\tau=0}^{N_t-1} \bar{\eta}_\tau \cdot (\eta_{\tau+1} - \eta_\tau) + \bar{\eta}_\tau \cdot \mathbb{T}^{(\pm)}[\xi(\tau)] \cdot \eta_\tau \right) , \tag{114}$$

In this form, since the integrand involves η_{N_t}, anti-periodic boundary condition is understood for it. This is the path integral representation for the Hubbard model using a Gaussian auxiliary field $\xi_{\mathbf{R}}(\tau)$ and the superscript $(\pm)$ in $\mathbb{T}^{(\pm)}$ stands for the positive-U and negative-U case respectively.

Quite analogously, one may express the partition function usind the Ising auxiliary field $\sigma_{\mathbf{R}}(\tau)$ as well. The result is the same except that the kernel $\mathbb{T}^{(\pm)}$ is replaced by $\tilde{\mathbb{T}}^{(\pm)}$. For example, Eq. (114) is replaced by:

$$Z = \sum_{\{\sigma_{\mathbf{R}}(\tau)\}} \int [D\bar{\eta} D\eta] \exp\left(- \sum_{\tau=0}^{N_t-1} \bar{\eta}_\tau \cdot (\eta_{\tau+1} - \eta_\tau) + \bar{\eta}_\tau \cdot \tilde{\mathbb{T}}^{(\pm)}[\sigma(\tau)] \cdot \eta_\tau \right) , \tag{115}$$

where the Gaussian integration is also replaced by the summation over all possible Ising field configurations.

The functions in the exponents of the path integral representation in both Eq. (114) and Eq. (115) are bilinear in the fermionic fields. Therefore, the integration of the fermion fields can be completed formally using Eq. (89), yielding the so-called fermion determinant. Normally, these fermion determinants cannot be computed analytically. Therefore, one usually relies on numerical methods, one of which being Monte Carlo. In such methods, the fermion determinant are further transformed back into normal bosonic Gaussian path integral using Eq. (90). For example, for the case of Ising auxiliary field, we denote the integrand in Eq. (115) as $\exp(-\bar{\eta} \cdot \tilde{\mathfrak{M}}^{(\pm)}[\sigma] \cdot \eta)$ with

$$\tilde{\mathfrak{M}}^{(\pm)}[\sigma] = \hat{\partial}_\tau + \tilde{\mathbb{T}}^{(\pm)}[\sigma] , \tag{116}$$

where $\hat{\partial}_\tau$ stands for the finite-difference operator in τ, i.e. $\hat{\partial}_\tau f(\tau) \equiv f(\tau+1) - f(\tau)$. Now we may transform the fermion determinant back into normal Gaussian integrals using Eq.(90):

$$Z = \sum_{\{\sigma_{\mathbf{R}}(\tau)\}} \det \tilde{\mathfrak{M}}^{(\pm)}[\sigma] \tag{117}$$

$$= \sum_{\{\sigma_{\mathbf{R}}(\tau)\}} \int \left[D\bar{\phi} D\phi\right] e^{-\bar{\phi}\cdot\left[\tilde{\mathfrak{M}}^{(\pm)}[\sigma]\right]^{-1}\cdot\phi} , \tag{118}$$

where $\bar{\phi} = \phi^*$ and ϕ are normal complex fields. Since these bosonic fields are utilized to treat the fermionic determinants, they are also called pseudo-fermion fields. Similarly, if we use the Gaussian auxiliary field, we would have

$$\mathfrak{M}^{(\pm)}[\xi] = \hat{\partial}_\tau + \mathbb{T}^{(\pm)}[\xi] , \tag{119}$$

and the partition function for the Hubbard model will look like

$$Z = \int \left[D\xi D\bar{\phi} D\phi\right] e^{-\frac{\xi\cdot\xi}{2}} e^{-\bar{\phi}\cdot\left[\tilde{\mathfrak{M}}^{(\pm)}[\xi]\right]^{-1}\cdot\phi} \,. \tag{120}$$

D. The sign problem

However, there might be a glitch in the above derivation. When expressing the fermion determinant in terms of integration over normal complex pseudo-fermion fields $\bar{\phi}$ and ϕ, we *must* impose a condition that the fermion determinant is positive definite: $\det(\tilde{\mathfrak{M}}^{(\pm)}[\sigma]) > 0$ (or $\det(\mathfrak{M}^{(\pm)}[\xi]) > 0$ for the Gaussian auxiliary field case). In fact, the whole Monte Carlo algorithm crucially depends on this assumption since it assumes that the fermion determinant is positively proportional to some probability distribution and, as a probability distribution, it has to be positive definite. Unfortunately, this is not guaranteed for the Hubbard model for all parameters. We shall see immediately that, for the negative-U Hubbard model, this is guaranteed; for the positive-U Hubbard model, this is only guaranteed for half-filling, i.e. at $\mu = 0$. If the fermion determinant is not positive definite, we say that the system being studied has a sign problem. Just because of this notorious sign problem, positive-U Hubbard model becomes extremely challenging for Monte Carlo simulations. The sign problem is not a rare problem only for Hubbard model. It is a widespread problem for all quantum fermionic systems. In fact, in the Monte Carlo study of finite temperature and finite density quantum chromodynamics (QCD for short, which is believed to be the fundamental theory for strong interations in nature), more severe problem shows up in which the fermionic determinant even becomes complex.

Now back to the Hubbard model. The negative-U case has no sign problem simply because the fermion matrix for it is trivial in spin space:

$$\mathfrak{M}^{(-)}[\xi]_{\mathbf{R}\tau\sigma;\mathbf{R}'\tau'\sigma'} = \left\{ \left[\delta_{\tau+1,\tau'} - \delta_{\tau\tau'}\right] \delta_{\mathbf{R},\mathbf{R}'} - \hat{t} \sum_{\mu} \left(\delta_{\mathbf{R},\mathbf{R}'+\mu} + \delta_{\mathbf{R},\mathbf{R}'-\mu}\right) \delta_{\tau\tau'} + \left(\frac{|\hat{U}|}{2} - \hat{\mu} + \sqrt{|\hat{U}|}\xi_{\mathbf{R}}(\tau) \right) \delta_{\mathbf{R},\mathbf{R}'}\delta_{\tau\tau'} \right\} \delta_{\sigma\sigma'} \,. \tag{121}$$

This implies that the fermion determinant in this case may be written as:

$$\det \mathfrak{M}^{(-)}[\xi] = \left[\det \mathbb{M}^{(-)}[\xi]\right]^2 \,, \tag{122}$$

where the reduced matrix $\mathbb{M}^{(-)}[\xi]$ is the matrix in curly brackets in Eq. (121) which has no spin indices. As a real matrix, it is readily seen that $(\det \mathbb{M}^{(-)}[\xi])^2 > 0$ and thus the negative-U Hubbard model has no sign problem for any set of parameters. This conclusion comes merely from the fact that the fermion matrix in Eq. (121) is trivial in spin space which is a direct consequence due to the coupling of the auxiliary field ξ with $(n_{\mathbf{R}+} + n_{\mathbf{R}-})$ in the negative-U case.

For the positive-U Hubbard model, however, the fermion matrix is *non-trivial* in spin space, though still diagonal:

$$\begin{aligned}\mathfrak{M}^{(+)}[\xi]_{\mathbf{R}\tau\sigma;\mathbf{R}'\tau'\sigma'} = & \left[\left[\delta_{\tau+1,\tau'} - \delta_{\tau\tau'}\right] \delta_{\mathbf{R},\mathbf{R}'} - \hat{t} \sum_{\mu} \left(\delta_{\mathbf{R},\mathbf{R}'+\mu} + \delta_{\mathbf{R},\mathbf{R}'-\mu}\right) \delta_{\tau\tau'} + \left(\frac{\hat{U}}{2} - \hat{\mu} \right) \delta_{\mathbf{R},\mathbf{R}'}\delta_{\tau\tau'} \right] \delta_{\sigma\sigma'} \\ & + \sqrt{\hat{U}}\xi_{\mathbf{R}}(\tau) \left(\sigma_z\right)_{\sigma\sigma'} \delta_{\mathbf{R},\mathbf{R}'}\delta_{\tau\tau'} \,.\end{aligned} \tag{123}$$

The fermion determinant in this case can be written as

$$\det \mathfrak{M}^{(+)}[\xi] = \det \mathbb{M}^{(+)}_{\uparrow}[\xi] \det \mathbb{M}^{(+)}_{\downarrow}[\xi] \,, \tag{124}$$

where the reduced matrices $\mathbb{M}^{(+)}_{\uparrow}[\xi]$ and $\mathbb{M}^{(+)}_{\downarrow}[\xi]$ are given by:

$$\mathbb{M}^{(+)}_{\uparrow,\downarrow}[\xi]_{\mathbf{R}\tau;\mathbf{R}'\tau'} = [\delta_{\tau+1,\tau'} - \delta_{\tau\tau'}]\,\delta_{\mathbf{R},\mathbf{R}'} - \hat{t}\sum_{\mu}\left(\delta_{\mathbf{R},\mathbf{R}'+\mu} + \delta_{\mathbf{R},\mathbf{R}'-\mu}\right)\delta_{\tau\tau'} + \left(\frac{\hat{U}}{2} - \hat{\mu} \pm \sqrt{\hat{U}}\xi_{\mathbf{R}}(\tau)\right)\delta_{\mathbf{R},\mathbf{R}'}\delta_{\tau\tau'}\ . \quad (125)$$

It is then not guaranteed that the total fermion determinant being positive definite. In fact, negative fermion determinant can happen which results in the infamous sign problem for the positive-U Hubbard model.

However, if we were exactly at half filling, namely $\mu = 0$, then using a symmetry described below, one can show that the model can be mapped into a negative-U Hubbard model and thus having no sign problem. This symmetry is the so-called "particle-hole symmetry". For a positive-U Hubbard model on a bi-partite lattice [20] with sublattices A and B, the Hamiltonian that enters the grand canonical partition function is

$$H' \equiv H - \mu N = -t\sum_{\mathbf{R},\mu}\left(a^{\dagger}_{\mathbf{R}+\hat{\mu}\sigma}a_{\mathbf{R}\sigma} + h.c.\right) - \mu\sum_{\mathbf{R}}(n_{\mathbf{R}+} + n_{\mathbf{R}-}) + U\sum_{\mathbf{R}} n_{\mathbf{R}+}n_{\mathbf{R}-}\ . \quad (126)$$

We now define the following transformation

$$a_{\mathbf{R}+} = \tilde{a}_{\mathbf{R}+}\ ;\ \ a_{\mathbf{R}-} = \begin{cases} +\tilde{a}^{\dagger}_{\mathbf{R}-}, & \text{for } \mathbf{R}\in A \\ -\tilde{a}^{\dagger}_{\mathbf{R}-}, & \text{for } \mathbf{R}\in B \end{cases} \quad (127)$$

together with the conjugate of the above equations. It is easy to verify that this transformation does not change the basic anti-commutation relations. Therefore, the new set of operators $\tilde{a}_{\mathbf{R}\pm}$ and $\tilde{a}^{\dagger}_{\mathbf{R}\pm}$ are also fermionic annihilation and creation operators. Furthermore, under this transformation, the hopping term in the Hubbard Hamiltonian is unchanged (the down spin part remains the same after anti-commuting the new creation and annihilation operators!). It is also seen that the repulsion part of the Hamiltonian changes a sign since: $n_{\mathbf{R}+} \to \tilde{n}_{\mathbf{R}+}$ while $n_{\mathbf{R}-} \to (1 - \tilde{n}_{\mathbf{R}-})$. Thus the Hamiltonian H' for the positive-U Hubbard model in Eq. (126)) changes to

$$H' = -t\sum_{\mathbf{R},\mu}\left(\tilde{a}^{\dagger}_{\mathbf{R}+\hat{\mu}\sigma}\tilde{a}_{\mathbf{R}\sigma} + h.c.\right) - \mu\sum_{\mathbf{R}}(\tilde{n}_{\mathbf{R}+} - \tilde{n}_{\mathbf{R}-}) - U\sum_{\mathbf{R}}\tilde{n}_{\mathbf{R}+}\tilde{n}_{\mathbf{R}-} + UN_{+} - \mu\mathcal{N}\ , \quad (128)$$

where $N_+ = \sum_{\mathbf{R}}\tilde{n}_{\mathbf{R}+}$ is the total number of spin-up electrons (which is a constant since the Hamiltonian contains no interaction that can flip spin) and $\mathcal{N}$ is the total number of lattice sites. Thus, at $\mu = 0$, the positive-U Hubbard Hamiltonian takes the same form (apart from an irrelevant constant term $UN_+ - \mu N$) after the particle-hole transformation except that the sign of the repulsion term is changed, namely it becomes a negative-U Hubbard model for which there is no sign problem in Monte Carlo simulations. For $\mu \neq 0$, however, since the original particle number operator $(n_{\mathbf{R}+} + n_{\mathbf{R}-})$ is mapped into the spin operator $(\tilde{n}_{\mathbf{R}+} - \tilde{n}_{\mathbf{R}-})$ (and also vice versa), [21] the term proportional to the chemical potential is not invariant. So if $\mu \neq 0$, the system does not have the particle-hole symmetry and the positive-U Hubbard model does have the sign problem.

E. A simple example: independent electron system

To illustrate the usefulness of the path-integral formalism introduced so far, let us look at a simple example: the independent electron system. Although we focused on the Hubbard model in previous sections, path-integral methods can be applied to any system, including the simple independent electron systems. In statistical physics, such a system is equivalent to ideal fermi gas system since the Hamiltonian is diagonal in reciprocal space and it is the sum of energies of individual single particle energies. The statistical properties for the system is well-known in standard statistical physics. Here, we will show that these familiar results arise naturally in the path-integral formalism.

Example V.1 *Consider the independent electron system whose Hamiltonian is given by:*

$$H = \sum_{\mathbf{k}\sigma}\epsilon_{\mathbf{k}}a^{\dagger}_{\mathbf{k}\sigma}a_{\mathbf{k}\sigma}\ , \quad (129)$$

where $\epsilon_{\mathbf{k}}$ is the band energy for a given reciprocal vector $\mathbf{k}$ and $a^{\dagger}_{\mathbf{k}\sigma}$, $a_{\mathbf{k}\sigma}$ being the creation and annihilation opera-

[20] A bi-partite lattice as a lattice formed by two identical sublattices A and B in which the sites of one sublattice being the nearest neighbors of the other set. Examples for this are the square lattices in two-dimensions, honeycomb lattice in two-dimensions, simple cubic lattice in three-dimensions, etc.

[21] This means that, under particle-hole transformation, the charge operator Q (proportional to $(n_{\mathbf{R}+}+n_{\mathbf{R}-})$) and the spin operator S_z (proportional to $(n_{\mathbf{R}+} - n_{\mathbf{R}-})$) are mapped into each other.

tors of the electron with spin σ, respectively. The electron number operator is also diagonal: $N = \sum_{\mathbf{k}\sigma} a^\dagger_{\mathbf{k}\sigma} a_{\mathbf{k}\sigma}$. In statistical physics, such a system is equivalent to the ideal Fermi gas system.

Let us first evaluate the grand partition function in "standard method". Since the number operator commute with the Hamiltonian, they can be diagonalized simultaneously. In fact, this basis is the particle number representation. We will use this basis to evaluate the grand partition function which is the trace of $e^{-\beta(H-\mu N)}$.

$$\begin{aligned} Z = Tr(e^{-\beta(H-\mu N)}) &= \sum_{\{n_{\mathbf{k}\sigma}\}} e^{-\beta\sum_{\mathbf{k}\sigma}(\epsilon_{\mathbf{k}}-\mu)n_{\mathbf{k}\sigma}} \\ &= \prod_{\mathbf{k}\sigma}\sum_{n_{\mathbf{k}\sigma}=0,1} e^{-\beta(\epsilon_{\mathbf{k}}-\mu)n_{\mathbf{k}\sigma}} \\ &= \prod_{\mathbf{k}\sigma}\left(1+e^{-\beta(\epsilon_{\mathbf{k}}-\mu)}\right) \equiv \prod_{\mathbf{k}\sigma} Z_{\mathbf{k}\sigma} \ , \end{aligned} \tag{130}$$

The average particle number $\langle n_{\mathbf{k}\sigma}\rangle$ on a given single particle quantum state labeled by $\mathbf{k}$ and σ is obtained by $-\partial \ln Z_{\mathbf{k}\sigma}/\partial\alpha$ with $\alpha = -\mu\beta$ and this gives:

$$\langle n_{\mathbf{k}\sigma}\rangle = \frac{1}{e^{\beta(\epsilon_{\mathbf{k}}-\mu)}+1} \ , \tag{131}$$

which is nothing but the standard Fermi distribution.

We now try to evaluate the partition function in the coherent state path-integral method. The steps are similar to what we did for the Hubbard model, but with great simplifications: Since the Hamiltonian is already bilinear in creation and annihilation operators, there is no need to use Hubbard-Stratonovich transformations, i.e. there is no need to introduce auxiliary fields. We could also start the calculation in reciprocal space such that the Hamiltonian is diagonal. So, quite similar to Eq. (114), after chopping the whole temporal length β into N_t slices with $a_t = \beta/N_t$, we get

$$Z = \int [D\bar\eta D\eta] \exp\left(-\sum_{\tau=0}^{N_t-1}\sum_{\mathbf{k}\sigma} \bar\eta_{\tau\mathbf{k}\sigma}\cdot(\eta_{\tau+1,\mathbf{k}\sigma}-\eta_{\tau\mathbf{k}\sigma}) + \bar\eta_{\tau\mathbf{k}\sigma} a_t(\epsilon_{\mathbf{k}}-\mu)\eta_{\tau\mathbf{k}\sigma}\right) \ . \tag{132}$$

Note that the bilinear expression in the exponential is already diagonal in both $\mathbf{k}$ and σ. Therefore, we may write:

$$Z = \prod_{\mathbf{k}\sigma}\int [d\bar\eta_\tau d\eta_\tau] \exp\left(-\sum_{\tau=0}^{N_t-1} \bar\eta_{\tau'} S^{(\mathbf{k}\sigma)}_{\tau'\tau}\eta_\tau\right) \ , \tag{133}$$

where the matrix $S^{(\mathbf{k}\sigma)}_{\tau'\tau}$ in τ-space is given explicitly by

$$S^{(\mathbf{k}\sigma)}_{\tau'\tau} = \begin{pmatrix} -a & 1 & 0 & \cdots & 0 \\ 0 & -a & 1 & \cdots & 0 \\ \vdots & & & & \vdots \\ -1 & \cdots & & 0 & -a \end{pmatrix} \ , \tag{134}$$

where the parameter a is given by

$$a \equiv 1 - a_t(\epsilon_{\mathbf{k}}-\mu) \ . \tag{135}$$

So the partition function becomes:

$$Z = \prod_{\mathbf{k}\sigma} \det\left(S^{(\mathbf{k}\sigma)}_{\tau'\tau}\right) \ . \tag{136}$$

The determinant of the matrix $S^{(\mathbf{k}\sigma)}_{\tau'\tau}$ can be evaluated explicitly:

$$\begin{aligned} \det\left(S^{(\mathbf{k}\sigma)}_{\tau'\tau}\right) &= (-a)^{N_t} + (-)^{N_t-1}(-1) \\ &= (-)^{N_t}\left[1+(1-a_t(\epsilon_{\mathbf{k}}-\mu))^{N_t}\right] \end{aligned} \tag{137}$$

The pre-factor $(-)^{N_t}$ is irrelevant (for example, we could always take N_t to be an even integer) and will be dropped. Therefore, the partition function of the system becomes

$$Z = \prod_{\mathbf{k}\sigma}\left[1+(1-a_t(\epsilon_{\mathbf{k}}-\mu))^{N_t}\right] \ . \tag{138}$$

This is somewhat different from the conventional result in Eq. (130) simply because we are using a discretized version in path-integral. We have chopped the temporal direction into finite number of slices while the result in Eq. (130) was obtained without slicing the temporal direction. It is easy to check that, in the limit of $N_t\to\infty$ but $N_t a_t = \beta$ hold fixed, we have

$$\lim_{N_t\to\infty}(1-a_t(\epsilon_{\mathbf{k}}-\mu))^{N_t} = e^{-\beta(\epsilon_{\mathbf{k}}-\mu)} \ , \tag{139}$$

and the result in Eq. (138) becomes identical with that in Eq. (130). Therefore, with this simple example, we have shown that the coherent path-integral method indeed yields the conventional result for an independent electron system.

Of course you might argue that, for such a simple system, the coherent path-integral formalism seems to be an overkill. This is indeed the case. But for more complicated systems like the Hubbard model, other methods will not work and only the path-integral sets up a foundation for possible numerical studies.

Example V.2 *In the previous example, we have evaluated the grand partition function using two methods: The first is the standard method in which we compute the trace in the energy and particle number eigenstates. The second is the path-integral method in which the fermionic determinant has to be evaluated. In the previous example, the determinant* $\det\left(S^{(\mathbf{k}\sigma)}_{\tau'\tau}\right)$ *was evaluated directly using the explicit expression of the matrix. This in fact can be computed in a different manner. We now look at Eq. (133) and notice that the matrix is not diagonal in* τ*-space. To evaluate the determinant, we try to make a transformation which brings the matrix* $S^{(\mathbf{k}\sigma)}_{\tau'\tau}$ *into diagonal form. It is easy to see that this transformation is nothing but the Fourier transform in* τ*-space. So, we expand*

$$\eta_\tau = \frac{1}{\sqrt{N_t}}\sum_n \tilde{\eta}_n e^{i\omega_n\tau}\ ,\quad \bar{\eta}_\tau = \frac{1}{\sqrt{N_t}}\sum_n \tilde{\bar{\eta}}_n e^{-i\omega_n\tau}\ . \tag{140}$$

Keep in mind that η_τ *has to satisfy the anti-periodic boundary condition, we have a restriction on the frequencies* ω_n *as*

$$\omega_n = \frac{(2n+1)\pi}{\beta}\ ,\quad n = 0, 1, \cdots, (N_t-1)\ . \tag{141}$$

Since τ *is a integer times* a_t*, so adding* N_t *to the index* n *will only change the phase by multiples of* 2π *and are therefore viewed as identical. So we may restrict the values of* n *from* 0 *to* N_t-1*. These frequencies are called Matsubara frequencies. For fermion fields that satisfy the anti-periodic boundary condition, the Matsubara frequencies are given by Eq. (141). For bosonic fields, however, they satisfy the periodic boundary conditions and the corresponding Matsubara frequencies are given by*

$$\omega_n = \frac{2n\pi}{\beta}\ ,\quad n = 0, 1, \cdots, (N_t-1)\ . \tag{142}$$

In frequency space, it is easy to see that the bilinear in the exponential of Eq. (??) becomes diagonal:

$$Z = \prod_{\mathbf{k}\sigma}\int\prod_n [d\tilde{\bar{\eta}}_n d\tilde{\eta}_n]\exp\left(-\sum_{n=0}^{N_t-1}\tilde{\bar{\eta}}_n(e^{i\omega_n}-a)\tilde{\eta}_n\right)\ , \tag{143}$$

where the parameter a *is the same as in Eq. (135). Therefore, the partition function is given by*

$$Z = \prod_{\mathbf{k}\sigma}\prod_n (e^{i\omega_n}-a)\ . \tag{144}$$

To evaluate $\prod_n(e^{i\omega_n}-a)$*, we notice that* $\zeta_n \equiv e^{i\omega_n}$ *are exactly the* N_t*-th roots of* (-1)*, i.e. they are the solutions of the following equation:*

$$F(\zeta) \equiv \zeta^{N_t} + 1 = 0\ . \tag{145}$$

We therefore have the following identity

$$F(\zeta) = \prod_n (\zeta - \zeta_n)\ . \tag{146}$$

So, by setting $\zeta = a$ *in the above identity, the desired product becomes*

$$\prod_n(\zeta_n - a) = (-)^{N_t}\left(1 + a^{N_t}\right)\ , \tag{147}$$

which is exactly the same result as in Eq. (137).

VI. MONTE CARLO SIMULATION OF HUBBARD MODEL

As discussed in the previous subsection, the positive-U Hubbard model cannot be studied using Monte Carlo directly when away from half-filling. At exactly half-filling, particle-hole symmetry makes it possible to map the model into a negative-U Hubbard model which can be simulated for any parameters without the sign problem. So, as far as the numerical simulation is concerned, we will only focus on the negative-U Hubbard model in this section. To simplify the notation then, we will denote the reduced fermion matrix $\mathbb{M}^{(-)}[\xi]$ in Eq. (122) by $\mathbb{M}[\xi]$:

$$\mathbb{M}[\xi]_{\mathbf{R}\tau;\mathbf{R}'\tau'} = [\delta_{\tau+1,\tau'} - \delta_{\tau\tau'}]\,\delta_{\mathbf{R},\mathbf{R}'} - \hat{t}\sum_\mu(\delta_{\mathbf{R},\mathbf{R}'+\mu} + \delta_{\mathbf{R},\mathbf{R}'-\mu})\,\delta_{\tau\tau'} + \left(\frac{|\hat{U}|}{2} - \hat{\mu} + \sqrt{|\hat{U}|}\xi_{\mathbf{R}}(\tau)\right)\delta_{\mathbf{R},\mathbf{R}'}\delta_{\tau\tau'}\ . \tag{148}$$

The path integral representation for the grand partition function of the model is

$$Z = \int [D\xi D\phi_1 D\phi_2]\, e^{-\frac{\xi\cdot\xi}{2}} e^{-\phi_\alpha^T\cdot\left[\mathbb{M}\mathbb{M}^T\right]^{-1}\cdot\phi_\alpha}\ , \tag{149}$$

where $\phi_{\alpha,\mathbf{R}\tau}$ with $\alpha = 1, 2$ are two *real* scalar fields (pseudo-fermion fields). In the above equation, it is

understood that the repeated index α in the exponent is summed over. The integrand in this path-integral representation then becomes purely positive definite and thus be viewed as some sort of probability distribution. Numerically, this can be simulated using standard Monte Carlo methods described in the following.

A. Markov process and Monte Carlo simulation

The numerical problem we are facing is the following: Suppose we have a collection of dynamical variables (fields) which are denoted by $\Phi(x)$ with $x \in X$ being the base space where these fields are defined. Although the set X could be a infinite set with continuous number of variables (like the real or complex numbers), here we will consider the case in which X is a finite set. For the fields defined on the lattice that we discussed so far, X is basically the set of all lattice points (plus possible internal labels like spin etc.). We want to generate a probability distribution for the fields $\Phi(x)$ of the form:

$$P[\Phi] = \frac{1}{Z} e^{-S[\Phi]} , \tag{150}$$

where $S[\Phi]$ is a known real functional of $\Phi(x)$ and is bounded below. We will call this distribution the Boltzmann distribution due to obvious reasons. The normalization condition indicates

$$Z = \int [D\Phi] e^{-S[\Phi]} . \tag{151}$$

Thermodynamical quantities are obtained as ensemble average

$$\langle \mathcal{O}[\Phi] \rangle = \frac{1}{Z} \int [D\Phi] \mathcal{O}[\Phi] e^{-S[\Phi]} . \tag{152}$$

For a finite set X, the total number of variable in the integration is finite, though very large. The number of integral is so large that any conventional numerical methods for the evaluation of the integral will not work. The only possibility is Monte Carlo which estimates the value of the multi-dimensional integral by stochastic methods.

To generate the desired Boltzmann distribution, one constructs a transition probability $W[\{\Phi\} \to \{\Phi'\}]$ which maps an old probability distribution to a new one as

$$P'[\Phi] = \int [D\Phi'] W[\{\Phi'\} \to \{\Phi\}] P[\Phi'] . \tag{153}$$

We call such a step an *update* of the field configuration $\{\Phi\}$. Suppose one starts with an arbitrary distribution $P^{(0)}[\Phi]$, one can update the configuration with the transition probability $W[\{\Phi\} \to \{\Phi'\}]$ iteratively

$$P^{(n+1)}[\Phi] = \int [D\Phi'] W[\{\Phi'\} \to \{\Phi\}] P^{(n)}[\Phi'] , \tag{154}$$

for $n = 0, 1, 2, \cdots$. This forms what we call a Markov chain. Our purpose is to find the suitable transition probability such that as $n \to \infty$, we end up with the desired Boltzmann distribution $P[\Phi] \propto e^{-S[\Phi]}$. It can be shown that this is guaranteed if the following two conditions are satisfied:

- Stability condition: If the probability distribution is already Boltzmann, then the update will not change it:

$$e^{-S[\Phi]} = \int [D\Phi'] W[\{\Phi'\} \to \{\Phi\}] e^{-S[\Phi']} . \tag{155}$$

- Ergodicity: For any configuration $\{\Phi\}$, the transition probability $W[\{\Phi'\} \to \{\Phi\}]$ is positive.

If the above conditions are satisfied, we than say that the probability distribution $W[\{\Phi'\} \to \{\Phi\}]$ implements an *exact algorithm* for the generation of Boltzmann distribution.

B. The hybrid Monte Carlo algorithm

One standard algorithm that deals with the pseudo-fermions is the so-called "hybrid Monte Carlo" algorithm which amounts to realize the probability distribution using a molecular dynamics evolutions in fictitious time t (also known as Monte Carlo time). To generate Boltzmann distribution, one introduces Gaussian distributed momenta $\pi(x)$ that is conjugate to $\Phi(x)$ and the Hamiltonian of this fictitious dynamical system is given by

$$H = \sum_x \frac{\pi(x)^2}{2} + S[\Phi(x)] . \tag{156}$$

The classical equation of motion for the system is then

$$\dot{\Phi}(x) \equiv \frac{d\Phi(x)}{dt} = \pi(x) , \quad \dot{\pi}(x) \equiv \frac{d\pi(x)}{dt} = -\frac{\partial S}{\partial \Phi(x)} . \tag{157}$$

Starting from some initial time, one first generate Gaussian distributed $\pi(x)$ as the initial momenta for the variable $\Phi(x)$. The the system is evolved in fictitious time t for some time t_0. We call this a trajectory and t_0 the trajectory length. At the end of one trajectory, the updated $\Phi(x)$ is recorded and another set of Gaussian distributed

momenta are generated. The system is evolved again to the second trajectory with the newly updated momenta. After enough iteration, the fields at the end of each trajectory then follow our desired Boltzmann distribution.

The idea behind this is to mimic the molecular dynamics in Nature. Imagine we have a system molecules forming an interacting system of gas. We denote the coordinate of the molecules by $\Phi(x)$ and assume that the potential energy of the system is $S[\Phi]$. It is known that, after enough collisions and evolution, the system then ends up in the Boltzmann distribution that is proportional to $e^{-S[\Phi]}$. The algorithm given above is trying to simulate this process: The generation of Gaussian distributed momenta is simulating the collision process between molecules while the Newtonian evolution is following the trajectory of each molecule in the system governed by classical mechanics.

One problem with this algorithm is that the functional $S[\Phi]$ might be quite complicated and the Newtonian equation of motion cannot be integrated analytically. Therefore, the integration of Newtonian equations of motion has to be accomplished numerically. This is done by making the fictitious time variable t discrete: $t_0 = N_{md}\Delta t$. However, this numerical integration procedure also creates a new problem. For exact integration of the Newtonian equation of motion, the Hamiltonian of the system is strictly conserved, i.e. $H_{\rm old} = H_{\rm new}$ with $H_{\rm old}$ and $H_{\rm new}$ being the Hamiltonian of the system at the beginning and end point of the trajectory, respectively. However, if the integration is done approximately using numerical methods, the Hamiltonian is not strictly conserved. The change in the Hamiltonian is usually proportional to some powers of the step size Δt. For example, for the leap-frog integration as described in subsection VI C, $\Delta H \propto \Delta t^3$. This error might be small and negligible for a few trajectories if Δt is small enough. However, as we iterate long enough, the final probability distribution will be distorted. Instead of arriving at the desired Boltzmann distribution, we end up with a new distribution of the form: $P[\Phi] \propto e^{-S[\Phi]+\Delta S[\Phi]}$ where $\Delta S[\Phi]$ is proportional to some (positive) powers of Δt. Not only the distribution is distorted, all physical observables are also distorted accordingly. To get the correct value of any physical quantity, one has to perform the simulation many times with different values of Δt and then finally extrapolate to a value at $\Delta t = 0$. In practice, this is rather unsatisfactory in the sense that the computation has to be repeated many times (for many values of Δt) and thus increase the computational cost considerably.

A clever solution has been found for this problem [10]. Kennedy et al showed that, one can make the algorithm exact by adding a Monte Carlo accept/reject step at the end of each molecular dynamics trajectory. That is say, if we denote the change in Hamiltonian before and after a trajectory as $\Delta H = H_{\rm new} - H_{\rm old}$, (which would be exactly zero if the Newtonian equations of motion were integrated exactly), we simply accept the new updated configurations of $\{\Phi(x)\}$ with the probability: $\min(1, e^{-\Delta H})$. This implies that, if $\Delta H \leq 0$, i.e. the Hamiltonian is *lowered*, we accept the new configuration; while if $\Delta H > 0$, we only accept the new configuration with probability $e^{-\Delta H}$. This is done by generating a uniformly distributed random number $r \in (0, 1)$ and compare r with $e^{-\Delta H}$. The updated configuration is accepted only when $e^{-\Delta H} > r$. If the updated configuration is rejected, the old configuration, namely the fields at the beginning of this trajectory is restored. Of course, one then re-generated Gaussian distributed momenta and start a new trajectory. This is the so-called hybrid Monte Carlo algorithm which we now summarize as follows:

1. For the given action $S[\Phi]$, assign a conjugate momenta $\pi(x)$ for each $\Phi(x)$ and form the Hamiltonian (156);

2. Generate Gaussian distributed momenta $\pi(x)$ for each x;

3. Integrate the Newtonian equation of motion (157) in fictitious time with step size Δt for some time t_0 and forms a trajectory;

4. Calculate the change in Hamiltonian at the end of the trajectory (relative to the start of the trajectory) ΔH;

5. Accept the updated configuration of $\{\Phi\}$ with probability $\min(1, e^{-\Delta H})$;

6. Go to step 2) and repeat the above steps forever.

After enough iteration, the distribution for the fields Φ will eventually follow the desired Boltzmann distribution. Once the probability distribution is correct, we say that the system has been thermalized. After the thermalization process, we can then measure physical quantities from this distribution. We can draw N samples from this distribution (this is accomplished by iterating the

HMC algorithm further), calculate some physical quantity $\mathcal{O}$ of interest, denoting the result for the i-th sample by $\mathcal{O}_i$, we then have:

$$\langle \mathcal{O} \rangle \simeq \frac{1}{N} \sum_{i=1}^{N} \mathcal{O}_i \ , \tag{158}$$

as an unbiased estimate for the ensemble average. The relative error between the two will be of order $1/\sqrt{N}$ according to probability theory. This is the basic idea of Monte Carlo simulation.

C. Some detailed issues concerning the hybrid Monte Carlo algorithm

In the previous subsection, we described the hybrid Monte Carlo algorithm, a generic algorithm for treating fermionic systems. In what follows, we will mention some issues that are crucial for the algorithms.

Leapfrog integration:
Within the hybrid Monte Carlo algorithm, one has to integrate the Newtonian equations of motion of the system. As is often the case, this set of equations are complicated enough such that numerical integration must be used. To do this, one normally uses a second-order integrator known as "leap-frog" integration. Suppose the step-size is given by Δt, the leap-frog integration is

1. Starting from the initial values of $\Phi(x, t = 0)$ and $\pi(x, t = 0)$, evolve the momenta forward by half a step:

$$\pi\left(x, \frac{\Delta t}{2}\right) = \pi(x, 0) - \frac{\partial S}{\partial \Phi}\left[\Phi(x, t = 0)\right]\left(\frac{\Delta t}{2}\right) \tag{159}$$

2. Evolve the fields $\Phi(x)$ by a full step using the momenta at the midpoint of the step:

$$\Phi(x, \Delta t) = \Phi(x, 0) + \pi\left(x, \frac{\Delta t}{2}\right)\Delta t \ . \tag{160}$$

3. Evolve the momenta $\pi(x)$ a full step, using the new fields at the midpoint of the step:

$$\pi\left(x, \frac{3\Delta t}{2}\right) = \pi\left(x, \frac{\Delta t}{2}\right) - \frac{\partial S}{\partial \Phi}\left[\Phi(x, \Delta t)\right]\Delta t \tag{161}$$

4. Repeat the above two steps iteratively and evolve the fields and the corresponding conjugate momenta by Δt for $(N_{md} - 1)$ steps. During each step, the quantity at the r.h.s of the Newtonian equation of motion is evaluated using the newly updated variables at the mid-point of the step. However, at the last evolving step for $\pi(x)$, evolve it only half a step with $(\Delta t/2)$. It is easily checked that in this process, both $\Phi(x)$ and $\pi(x)$ are evolved by a fictitious time interval $t_0 = N_{md}\Delta t$.

The trick in the leap-frog integration is that the fields and momenta are updated at interleaved time points using each other's value at the mid-point of the step. The naïve integration methods (known as the Euler method in numerical analysis) will evolve both the fields and momenta simultaneously, using their old values that are one full step before. The naïve method is called first-order in the sense that it is only accurate to first order in Δt, i.e. the error in the integration is of $O(\Delta t^2)$. The leap-frog method, however, is second order as can be shown explicitly. That is to say, by sandwiching the updates for the fields and momenta in between each other, the error in the integration is $O(\Delta t^3)$. This integration sometimes is also known as the second-order Runge-Kutta method.

Fermionic force term:
When updating the momenta in HMC, the force term $-\partial S[\Phi]/\partial \Phi(x)$ has to be evaluated which is usually the most complicated and time-consuming part in the calculation. The explicit formula of the force of course depends on the form of the action of the system. For our concern, we will now focus on the Hubbard model. To simplify the notation, we will introduce the three-dimensional lattice label $x = (\mathbf{R}, \tau)$ so that the fields $\xi_{\mathbf{R}\tau}$ will be labeled as ξ_x and similarly for other fields. For the Hubbard model this action is given by (see Eq. (149))

$$S[\xi, \phi_1, \phi_2] = \frac{1}{2}\xi_x \xi_x + (\phi_\alpha)_x \left[\mathbb{M}\mathbb{M}^T\right]^{-1}_{x;y} (\phi_\alpha)_y \ , \tag{162}$$

where all repeated indices (including α which runs from 1 to 2) are summed over and the matrix $\mathbb{M}[\xi]$ is given explicitly by Eq. (148). Our task is to update these fields using the hybrid Monte Carlo algorithm.

The pseudo-fermion fields ϕ_α need not to be updated during the molecular dynamics trajectory. They are generated (or updated) only *at the beginning of each trajectory*. In fact, at the beginning of each trajectory, they can be generated as

$$\phi_\alpha = \mathbb{M}[\xi] \cdot \eta_\alpha \ , \ \ \eta_\alpha \in P[\eta_\alpha] \propto e^{-\eta_\alpha^T \eta_\alpha} \ . \tag{163}$$

It is then seen that, due to $\eta_\alpha = \mathbb{M}^{-1} \cdot \phi_\alpha$, the distribution for ϕ_α is proportional to $\exp(-\eta_\alpha^T \eta_\alpha) = \exp(-\phi_\alpha^T \mathbb{M}^{T,-1}\mathbb{M}^{-1}\phi_\alpha) = \exp(-\phi_\alpha^T [\mathbb{M}\mathbb{M}^T]^{-1}\phi_\alpha)$ which

is exactly what we want. Therefore, the molecular dynamics process (i.e. the integration of Newtonian equations of motion) only deals with the bosonic fields ξ_x. The hybrid Monte Carlo Hamiltonian for the system is then

$$H = \frac{1}{2}\pi_x\pi_x + S[\xi, \phi_1, \phi_2] \ , \tag{164}$$

where $\pi_x \equiv \pi_{\mathbf{R}\tau}$ is conjugate to $\xi_x \equiv \xi_{\mathbf{R}\tau}$. To calculate the force for field ξ_x, we would need to take variation of the action with respect to the fields ξ_x (with ϕ_α being fixed). Under an infinitesimal change, the change in the action can be written as

$$\delta S[\xi, \phi_1, \phi_2] \equiv -F_x \delta\xi_x \tag{165}$$

The coefficients $F_x = F_{\mathbf{R}\tau}$ are then the force terms entering the Newtonian equations of motion for the system. Using the explicit expression in Eq. (148), we get

$$\delta S = \left(\xi_x - 2\sqrt{|\hat{U}|}X_{\alpha y}\mathbb{M}_{y;x}X_{\alpha x}\right)\delta\xi_x \ , \tag{166}$$

where the field $X_{\alpha x} \equiv X_{\alpha\mathbf{R}\tau}$ is the solution of the following linear equation

$$\left[\mathbb{M}\mathbb{M}^T\right]_{x,y} X_{\alpha y} = \phi_{\alpha x} \ . \tag{167}$$

Therefore, it is seen that at each molecular dynamics step within a trajectory, whenever one has to update the momenta π_x, one has to solve a large sparse linear system with a give ϕ_α. Once the solution vector $X_{\alpha x}$ is obtained, the force term needed to update the momenta π_x is given by

$$F_x = -\xi_x + 2\sqrt{|\hat{U}|}X_{\alpha y}\mathbb{M}_{y;x}X_{\alpha x} \ . \tag{168}$$

The first term in this formula is simple and the second term is rather complicated. Since the second term comes from the pseudo-fermion fields (which originates from the fermionic determinants), we call the second term the fermionic force. The calculation of the fermionic force requires the numerical solution of a large sparse linear system and is by far the most time-consuming part in most fermionic Monte Carlo simulations.

Krylov solvers:

We have seen that, in order to perform the updates for the conjugate momenta in a molecular dynamics step, one has to solve a large, sparse linear system given by Eq. (167). This is accomplished numerically using iterative methods.

Suppose we have a symmetric, positive-definite, real sparse matrix $\mathbb{A}$ and we want to solve the linear system: $\mathbb{A}\cdot X = \phi$ with some known vector ϕ. In our previous example, the matrix corresponds to $\mathbb{A} = \mathbb{M}\mathbb{M}^T$. We first start with some arbitrary trial $X^{(0)}$ and form the residual vector

$$r^{(0)} = \phi - \mathbb{A}\cdot X^{(0)} \ , \tag{169}$$

Of course, we assume that $r^{(0)}$ is not a null vector otherwise our trial $X^{(0)}$ is already a solution. For simplicity, one can pick $X^{(0)} = 0$ (the null vector) which then results in $r^{(0)} = \phi$. We then form the vector space spanned by:

$$\mathcal{K}^n = \text{span}(r^{(0)}, \mathbb{A}r^{(0)}, , \cdots, \mathbb{A}^{n-1}r^{(0)}) \tag{170}$$

This subspace is called the Krylov subspace of the system. The dimensionality of the subspace is usually n, assuming no exceptional case occurs. Note also that, to get from $\mathcal{K}^{n-1}$ to $\mathcal{K}^n$, one only has to perform a matrix times a vector operation. Since the $\mathcal{N}\times\mathcal{N}$ matrix $\mathbb{A}$ is sparse, this operation will cost $O(\mathcal{N})$ operations instead of $O(\mathcal{N}^2)$ operations. This is the main reason why large sparse linear systems favors the iterative solvers. Iterative algorithms for large, sparse, linear systems relies on finding the approximate solution vector X within the Krylov subspaces. There exist many such algorithms. Here we will only mention two of them: one being the minimal residue algorithm (MR) and the other being the conjugate gradient algorithm (CG).

The Minimal Residual (MR) algorithm change the solution vector by a suitable amount that is proportional to the previous residual vector $r^{(n)}$. The proportionality coefficient is obtained by demanding the norm of the new residual vector $r^{(n+1)}\cdot r^{(n+1)}$ to be minimized. Assuming

$$X^{(n+1)} = X^{(n)} + \alpha_n r^{(n)} \ , \tag{171}$$

it is then verified that

$$r^{(n+1)} = \phi - \mathbb{A}(X^{(n)} + \alpha_n r^{(n)}) = r^{(n)} - \alpha_n \mathbb{A}\cdot r^{(n)} \ . \tag{172}$$

The minimization condition gives:

$$\alpha_n = \frac{r^{(n)T}\mathbb{A}^T r^{(n)}}{r^{(n)T}\mathbb{A}^T\cdot\mathbb{A}r^{(n)}} \ . \tag{173}$$

One can iterate the above cycle until the residual is small enough such that an approximate solution is found. This is the Minimal Residual (MR) algorithm. Within each iteration of the MR algorithm, one has to compute a matrix vector multiplication (in $\mathbb{A}\cdot r^{(n)}$), some inner products (in α_n) and some linear operations of known vectors. The MR algorithm is quite simple and also quite

general in the sense that the matrix $\mathbb{A}$ can be any real (or even complex) matrix [22].

The Conjugate Gradient (CG) algorithm is a modified (improved) version of the MR algorithm in the case of symmetric, positive-definite real matrix $\mathbb{A}$ [23]. In addition to the residual vector, one further introduces a search vector $p^{(n)}$ with $p^{(0)} = r^{(0)}$. The algorithm reads:

$$X^{(n+1)} = X^{(n)} + \alpha_n p^{(n)} \, , \alpha_n = \frac{r^{(n)T} r^{(n)}}{p^{(n)T} \mathbb{A} p^{(n)}} \, , \quad (174)$$

$$r^{(n+1)} = r^{(n)} - \alpha_n \mathbb{A} \cdot p^{(n)} \, , \quad (175)$$

$$p^{(n+1)} = r^{(n+1)} + \beta_n p^{(n)} \, , \beta_n = \frac{r^{(n+1)T} r^{(n+1)}}{r^{(n)T} r^{(n)}} \, (176)$$

Note that within each iteration, the operations that are needed include: one matrix vector multiplication (in $\mathbb{A} \cdot p^{(n)}$), some vector inner products (in the evaluation of the coefficients α_n and β_n) and some vector linear operations (adding vectors or multiply a vector with a number). Among these operations, usually the matrix vector multiplication takes the most computer time. But, as we addressed earlier, the total number of operation in each iteration is of $O(\mathcal{N})$ since $\mathbb{A}$ is sparse. Again, the iteration is stopped once the norm of the residual vector is small enough.

VII. GREEN'S FUNCTIONS AND PHYSICAL OBSERVABLES[24]

In the previous section, we have only discussed how to generate the correct probability distribution of the Hubbard model (plus related algorithmic issues). We have not touched our goal yet, namely to compute physical observables using Monte Carlo methods. In this section, we will list some of the important physical observables that can be measured in Monte Carlo simulations. The building block in the measurement of physical quantities is the so-called "correlation functions" or "Green's functions" of operators in the Heisenberg picture. These functions have an intimate relation with the spectrum of the quantum many-body system and can be utilized to study various properties of the system.

For the Hubbard model, since the original dynamical degrees of freedom are all fermionic in nature, interesting physical observables are all described using fermionic creation and annihilation operators. We first define the imaginary-time Heisenberg picture operator as:

$$\mathcal{O}_H(\tau) = e^{\tau(H-\mu N)} \mathcal{O} e^{-\tau(H-\mu N)} \, , \quad (177)$$

where $\mathcal{O}$ is the operator in the Schrödinger picture. To simplify the notation, we usually drop the subscript "H" with the understanding that any field operator with an explicit imaginary time label denotes a Heisenberg operator. Almost all physical quantities of interests can be expressed as ensemble average of product of several Heisenberg operators.

A. Two-point functions

One basic observable is the so-called two-point correlation function, or Green's function, for the electron. In real space, it is define by the following ensemble average:

$$\mathcal{G}^{(2)}_{\mathbf{R}'\tau'\sigma';\mathbf{R}\tau\sigma} \equiv \left\langle T \left[a_{\mathbf{R}'\tau'\sigma'} a^\dagger_{\mathbf{R}\tau\sigma} \right] \right\rangle \, , \quad (178)$$

where both $a^\dagger_{\mathbf{R}\tau\sigma}$ and $a_{\mathbf{R}'\tau'\sigma'}$ are the imaginary-time Heisenberg operators defined as

$$\begin{cases} a^\dagger_{\mathbf{R}\tau\sigma} \equiv e^{\tau(H-\mu N)} a^\dagger_{\mathbf{R}\sigma} e^{-\tau(H-\mu N)}, \\ a_{\mathbf{R}\tau\sigma} \equiv e^{\tau(H-\mu N)} a_{\mathbf{R}\sigma} e^{-\tau(H-\mu N)}, \end{cases} \quad (179)$$

Note that, by this definition, $a^\dagger_{\mathbf{R}\tau\sigma} \neq [a_{\mathbf{R}\tau\sigma}]^\dagger$ although $a^\dagger_{\mathbf{R}\sigma} = [a_{\mathbf{R}\sigma}]^\dagger$. The symbol $T[\cdot]$ in Eq. (178) stands for "time-ordering" of the product of operators inside the bracket. It merely shuffles the Heisenberg operators with the latest time to the far left, plus possible minus signs for interchanging fermion operators. For example, for the two-point function of fermions we have

$$T \left[a_{\mathbf{R}'\tau'\sigma'} a^\dagger_{\mathbf{R}\tau\sigma} \right] = \begin{cases} +a_{\mathbf{R}'\tau'\sigma'} a^\dagger_{\mathbf{R}\tau\sigma} & \text{if } \tau' > \tau, \\ -a^\dagger_{\mathbf{R}\tau\sigma} a_{\mathbf{R}'\tau'\sigma'} & \text{if } \tau' < \tau, \end{cases} \quad (180)$$

Or equivalently, one may define the two-point Green's function as

$$\mathcal{G}^{(2)}_{\mathbf{R}'\tau'\sigma';\mathbf{R}\tau\sigma} \equiv \theta(\tau' - \tau) \left\langle a_{\mathbf{R}'\tau'\sigma'} a^\dagger_{\mathbf{R}\tau\sigma} \right\rangle - \theta(\tau - \tau') \left\langle a^\dagger_{\mathbf{R}\tau\sigma} a_{\mathbf{R}'\tau'\sigma'} \right\rangle \, . \quad (181)$$

---

[22] In this case, the transpose operations in the formulae are replaced by Hermitian conjugate operations.

[23] In fact, one can also generalize to complex matrices. Then the condition of using CG algorithm is that the matrix must be Hermitian and positive-definite.

[25] Okay, here comes a bit more on field theory. If the reader is sick of it, simply skip it. A good reference is chapter 2 in Negele's book [8].

One can also define the Heisenberg operators associated with the reciprocal space creation and annihilation operators:

$$\begin{cases} a^\dagger_{\mathbf{k}\tau\sigma} \equiv e^{\tau(H-\mu N)} a^\dagger_{\mathbf{k}\sigma} e^{-\tau(H-\mu N)}, \\ a_{\mathbf{k}\tau\sigma} \equiv e^{\tau(H-\mu N)} a_{\mathbf{k}\sigma} e^{-\tau(H-\mu N)}. \end{cases} \tag{182}$$

With these operators, one can define the corresponding two-point correlation function (or Green's function) in reciprocal space:

$$\mathcal{G}^{(2)}_{\mathbf{k}'\tau'\sigma';\mathbf{k}\tau\sigma} \equiv \left\langle T\left[a_{\mathbf{k}'\tau'\sigma'} a^\dagger_{\mathbf{k}\tau\sigma}\right]\right\rangle . \tag{183}$$

Example VII.1 The two point function for independent electron systems: *The definition in reciprocal space (**k**-space) is more commonly used since for the independent electron systems, both the Hamiltonian and the particle number operators are diagonal:*

$$H = \sum_{\mathbf{k}\sigma} \epsilon_{\mathbf{k}} a^\dagger_{\mathbf{k}\sigma} a_{\mathbf{k}\sigma},\ N = \sum_{\mathbf{k}\sigma} a^\dagger_{\mathbf{k}\sigma} a_{\mathbf{k}\sigma} , \tag{184}$$

which results in: $H - \mu N = \sum_{\mathbf{k}\sigma} (\epsilon_{\mathbf{k}} - \mu) a^\dagger_{\mathbf{k}\sigma} a_{\mathbf{k}\sigma}$. *Statistically speaking, the independent electron systems are identical to ideal gas systems since different modes are statistically independent and the energy and particle number can be expressed as summation over different modes. For an independent electron system, it is easy to show that*

$$a^\dagger_{\mathbf{k}\tau\sigma} = e^{+\tau(\epsilon_{\mathbf{k}}-\mu)} a^\dagger_{\mathbf{k}\sigma},\ a_{\mathbf{k}\tau\sigma} = e^{-\tau(\epsilon_{\mathbf{k}}-\mu)} a_{\mathbf{k}\sigma}. \tag{185}$$

Therefore, in the independent electron systems, we have

$$\mathcal{G}^{(2)}_{\mathbf{k}'\tau'\sigma';\mathbf{k}\tau\sigma} = \delta_{\mathbf{k}\mathbf{k}'}\delta_{\sigma\sigma'} e^{-(\tau'-\tau)(\epsilon_{\mathbf{k}}-\mu)} \times \\ \times \left[\frac{\theta(\tau'-\tau)}{1+e^{-\beta(\epsilon_{\mathbf{k}}-\mu)}} - \frac{\theta(\tau-\tau')}{1+e^{\beta(\epsilon_{\mathbf{k}}-\mu)}}\right] \tag{186}$$

where we have used the fact that

$$\langle a_{\mathbf{k}\sigma} a^\dagger_{\mathbf{k}\sigma}\rangle = 1 - \langle a^\dagger_{\mathbf{k}\sigma} a_{\mathbf{k}\sigma}\rangle = \frac{1}{1+e^{-\beta(\epsilon_{\mathbf{k}}-\mu)}} . \tag{187}$$

¶ The physical significance of the two-point correlation function defined above is quite clear, particularly for an independent electron system (an ideal gas system). Assuming $\tau' > \tau$, the two-point function describes the following process: One first creates an extra electron with definite **k**, σ at imaginary time τ, then let the system evolve in imaginary time for a time interval of $(\tau' - \tau)$ (which then gives the typical time-dependence $\exp(-(\tau'-\tau)(\epsilon_{\mathbf{k}}-\mu))$), and finally annihilates the electron at a later imaginary time τ'. This gives the expression:

$$\mathcal{G}^{(2)}_{\mathbf{k}'\tau'\sigma';\mathbf{k}\tau\sigma} = \delta_{\mathbf{k}\mathbf{k}'}\delta_{\sigma\sigma'} \frac{e^{-(\tau'-\tau)(\epsilon_{\mathbf{k}}-\mu)}}{1+e^{-\beta(\epsilon_{\mathbf{k}}-\mu)}} \tag{188}$$

Assuming that the temperature is low so that β is very large, then the Fermi distribution tells us that the average number of electron on a state $\mathbf{k}\sigma$ is very much like a step function: all states above the Fermi surface μ are almost empty while all states below the Fermi surface are all filled. This means that the factor $1/[1+e^{-\beta(\epsilon_{\mathbf{k}}-\mu)}] \sim 1$ for $\epsilon_{\mathbf{k}} > \mu$ while $1/[1+e^{-\beta(\epsilon_{\mathbf{k}}-\mu)}] \sim e^{-\beta|\epsilon_{\mathbf{k}}-\mu|}$ for $\epsilon_{\mathbf{k}} < \mu$. Therefore, the two-point function shows the following temporal dependence (assuming $\tau' > \tau$):

$$\mathcal{G}^{(2)}_{\mathbf{k}'\tau'\sigma';\mathbf{k}\tau\sigma} \simeq \delta_{\mathbf{k}\mathbf{k}'}\delta_{\sigma\sigma'} \begin{cases} e^{-(\tau'-\tau)(\epsilon_{\mathbf{k}}-\mu)}, & \epsilon_{\mathbf{k}} > \mu \\ e^{-[\beta-(\tau'-\tau)]|\epsilon_{\mathbf{k}}-\mu|}, & \epsilon_{\mathbf{k}} < \mu \end{cases} \tag{189}$$

The two-point function thus exhibits a unique $(\tau' - \tau)$ dependence: with increasing $(\tau' - \tau)$, it is either exponentially decaying or exponentially increasing. In the former case, we know that $\epsilon_{\mathbf{k}} > \mu$ and the difference $(\epsilon_{\mathbf{k}} - \mu)$ controls the decaying rate; in the latter case, we know that $\epsilon_{\mathbf{k}} < \mu$ and the exponential increasing rate also gives $(\epsilon_{\mathbf{k}} - \mu)$. In other words, the exponential decay (or increase) rate with respect to the time separation depends only on $(\epsilon_{\mathbf{k}} - \mu)$ which is the single-particle spectrum of the system. This is in fact a general feature which is valid beyond the independent electron approximation. The property can be turned around: Suppose we have a many-particle system which is not necessarily an independent electron system. It could be a strongly correlated electron system like the Hubbard model or something else. Then, in general, we will not be able to compute the two-point functions analytically. However, if we could manage to measure the two-point functions numerically (for example, in Monte Carlo simulations), then from its temporal dependence on $(\tau' - \tau)$, we could still infer the spectral parameter $(\epsilon_{\mathbf{k}} - \mu)$ of the system. It is exactly due to this reason that makes the Green's functions so important: almost all thermodynamic properties of the system at equilibrium can be derived from various appropriate Green's functions.

Finally, let me point out why the two-point correlation functions are also called "Green's functions". For the independent electron system whose two-point function is given by Eq. (186), it is easily verified that it satisfies the following differential equation:

$$(\partial_{\tau'} + \epsilon_{\mathbf{k}} - \mu)\mathcal{G}^{(2)}_{\mathbf{k}'\tau'\sigma';\mathbf{k}\tau\sigma} = \delta(\tau' - \tau) , \tag{190}$$

which is the typical equation for a Green's function.

B. Two-point functions in path-integral

In the previous subsection, we defined the two-point correlation function in terms of Heisenberg operators. In fact, the two-point function of a system is most conveniently obtained within the path-integral formalism as discussed in section V. To see this, assuming that $\tau' > \tau$ and denoting $H' \equiv H - \mu N$, we find that

$$\mathcal{G}^{(2)}_{\mathbf{k}'\tau'\sigma';\mathbf{k}\tau\sigma} = \frac{1}{Z} Tr\left(e^{-(\beta-\tau')H'} a_{\mathbf{k}'\sigma'} e^{-(\tau'-\tau)H'} a^{\dagger}_{\mathbf{k}\sigma} e^{-\tau H'}\right) , \tag{191}$$

while the partition function is $Z = Tr(e^{-\beta H'})$. Within the path-integral formalism for Z, one first chops the exponential evolution operator $e^{-\beta H'}$ into N_t slices: $e^{-\beta H'} = e^{-a_t H'} \cdots e^{-a_t H'}$ with $N_t a_t = \beta$. Then the completeness relation for Grassmann coherent states are inserted in between the N_t factors. Finally, the creation and annihilation operators in H' are replaced by their corresponding Grassman eigenvalues. We can now do the same for the two-point function. Everything will be the same except that at temporal point τ, we have an extra operator $a^{\dagger}_{\mathbf{k}\sigma}$ while at a later temporal point τ', we have another extra operator $a_{\mathbf{k}'\sigma'}$. Since both of these extra operators may be replaced by their Grassmann eigenvalues, we can obtain a path-integral representation for the two-point function. For example, for the Hubbard model, following Eq. (114), we have

$$\mathcal{G}^{(2)}_{\mathbf{k}'\tau'\sigma';\mathbf{k}\tau\sigma} = \frac{1}{Z}\int [D\xi D\bar{\eta} D\eta]\, e^{-\frac{\xi\cdot\xi}{2}} \left(\eta_{\mathbf{k}\tau'\sigma'}\bar{\eta}_{\mathbf{k}\tau\sigma}\right) \exp\left(-\sum_{\tau=0}^{N_t-1} \bar{\eta}_\tau \cdot (\eta_{\tau+1} - \eta_\tau) + \bar{\eta}_\tau \cdot \mathbb{T}^{(\pm)}[\xi(\tau)] \cdot \eta_\tau\right) , \tag{192}$$

while the partition function Z is given by a similar expression with the factor of $(\eta_{\mathbf{k}\tau'\sigma'}\bar{\eta}_{\mathbf{k}\tau\sigma})$ being omitted in the integrad (which is nothing but Eq. (114) back again). The Grassmannian path-integral can be completed formally using the identity introduced in Eq. (91):

$$\mathcal{G}^{(2)}_{\mathbf{k}'\tau'\sigma';\mathbf{k}\tau\sigma} = \frac{1}{Z}\int [D\xi]\, e^{-\frac{\xi\cdot\xi}{2}} \det \mathfrak{M}^{(\pm)}[\xi] \left[\mathfrak{M}^{(\pm)}[\xi]\right]^{-1}_{\mathbf{k}'\tau'\sigma';\mathbf{k}\tau\sigma} , \tag{193}$$

where the matrix $\mathfrak{M}^{(\pm)}[\xi]$ is introduced in Eq. (119). Since the partition function Z itself is nothing but $Z = \int [D\xi]\, e^{-\frac{\xi\cdot\xi}{2}} \det \mathfrak{M}^{(\pm)}[\xi]$, we could write the two-point function in Hubbard model as:

$$\mathcal{G}^{(2)}_{\mathbf{k}'\tau'\sigma';\mathbf{k}\tau\sigma} = \left\langle \left[\mathfrak{M}^{(\pm)}[\xi]\right]^{-1}_{\mathbf{k}'\tau'\sigma';\mathbf{k}\tau\sigma} \right\rangle_{\xi} , \tag{194}$$

where the symbol $\langle\cdot\rangle_\xi$ stands for the expectation value of a quantity within the corresponding probability distribution $P[\xi]$ given by

$$P[\xi] = \frac{1}{Z} e^{-\frac{\xi\cdot\xi}{2}} \det \mathfrak{M}^{(\pm)}[\xi] . \tag{195}$$

Note that, this probability distribution is exactly the distribution that we generate in a Monte Carlo simulation. So, to compute a two-point function, we first simply generate the right probability distribution using some exact algorithm. Then, we take many samples from the right probability distribution and compute the inverse matrix element $\left[\mathfrak{M}^{(\pm)}[\xi]\right]^{-1}_{\mathbf{k}'\tau'\sigma';\mathbf{k}\tau\sigma}$ for each sample. We then take the sample average of this quantity which then gives an unbiased estimate for the two-point function of the Hubbard model.

For an independent electron system, the path-integral representation is simpler in the sense that no auxiliary fields are needed. We have shown in subsection V E how to express the partition function of the system using path-integrals, see Example V.1 and Example V.2. In the next example, we would like to evaluate the two-point function using path-integral method. The result is already obtained in the previous subsection in Example VII.1.

Example VII.2 The two point function for independent electron systems using path-integral: *Here we would like to evaluate the two-point function for an independent electron system (an ideal fermi gas system) using the path-integral method. Since the Hamiltonian and total particle number operators are both diagonal*

in $\mathbf{k}$-space, the corresponding fermion matrix is also block-diagonal in the index $\mathbf{k}$ and σ. So, we have (see Eq. (133) in subsection V E)

$$Z = \prod_{\mathbf{k}\sigma} \int [d\bar{\eta}_\tau d\eta_\tau] \exp\left(- \sum_{\tau=0}^{N_t-1} \bar{\eta}_{\tau'} S^{(\mathbf{k}\sigma)}_{\tau'\tau} \eta_\tau \right) , \quad (196)$$

Therefore, the two-point function is nothing but the matrix element for the inverse matrix $[S^{(\mathbf{k}\sigma)}]^{-1}$. The explicit expression for the matrix $S^{(\mathbf{k}\sigma)}$ is shown in Eq. (134). Assuming for the moment $\tau' > \tau$, we obtain the two-point function as:

$$\begin{aligned} \mathcal{G}^{(2)}_{\mathbf{k}'\tau'\sigma';\mathbf{k}\tau\sigma} &= \delta_{\mathbf{k}\mathbf{k}'}\delta_{\sigma\sigma'} \left[S^{(\mathbf{k}\sigma)} \right]^{-1}_{\tau'\tau} \\ &= \delta_{\mathbf{k}\mathbf{k}'}\delta_{\sigma\sigma'} \frac{a^{(\tau'-\tau)}}{1+a^{N_t}} \end{aligned} \quad (197)$$

with $a = 1 - a_t(\epsilon_{\mathbf{k}} - \mu)$. Obviously, in the limit $N_t \to \infty$ but $\beta = N_t a_t$ fixed, the above expression exactly reduces to the first term in Eq. (186).

Another way of obtaining the two-point correlation function for the independent electron system is to diagonalize the fermion matrix $S^{(\mathbf{k}\sigma)}$ using Fourier transform into Matsubara frequencies. Just like what we did in subsection V E Example V.2, we could use the Fourier transform in Eq. (140) to bring the fermion matrix into diagonal form. Then, the two-point correlation function, which is nothing but the inverse of the fermion matrix is easily obtained in frequency-space. Transforming back to τ-space then gives the result (assuming $\tau' > \tau$ for definiteness):

$$\mathcal{G}^{(2)}_{\mathbf{k}'\tau'\sigma';\mathbf{k}\tau\sigma} = \frac{1}{N_t} \sum_n \frac{(\zeta_n)^{\tau'-\tau}}{\zeta_n - a} , \quad (198)$$

where $\zeta_n \equiv e^{i\omega_n}$ and ω_n are the Matsubara frequencies and $a = 1 - a_t(\epsilon_{\mathbf{k}} - \mu)$.

C. More complicated physical quantities: Wick's theorem

As we have mentioned, all physical quantities can be expressed in terms of fermionic creation and annihilation operators. Therefore, without loss of generality, we are led to compute the following ensemble average:

$$\langle \mathcal{O} \rangle = \frac{1}{Z} \int [D\bar{\eta} D\eta] \, \mathcal{O}[\eta, \bar{\eta}] e^{-\bar{\eta}\cdot\mathfrak{M}\cdot\eta} , \quad (199)$$

where for simplicity we have not shown the integral for the auxiliary fields if there are any. The physical quantity $\mathcal{O}[\eta, \bar{\eta}]$, originally expressed in terms of creation and annihilation operators but now replaced by their eigenvalues, usually contains equal number of η and $\bar{\eta}$ fields such that it contains even number of Grassmann variables (and therefore looks like an ordinary number). The simplest quantity is the two-point correlation function discussed in the previous subsections. Of course, more complicated quantities can contain more numbers of fields. The most general form to be computed is the $2n$-point function defined as

$$\mathcal{G}^{(n)}_{i_1,\cdots,i_n;j_1,\cdots,j_n} = \frac{1}{Z} \int [D\bar{\eta} D\eta] \, \eta_{i_n} \cdots \eta_{i_1} \bar{\eta}_{j_1} \cdots \bar{\eta}_{j_n} e^{-\bar{\eta}\cdot\mathfrak{M}\cdot\eta} , \quad (200)$$

where we have used the collective index $i_1, \cdots, i_n$ and $j_1, \cdots, j_n$ to label *all possible indices*, e.g. $\mathbf{k}$, τ, spin, or any other labels that are necessary. In the case of $n = 1$, we recover the two-point function that has been discussed already. The fermionic $2n$-point correlation function can be computed using the famous Wick's theorem:

$$\frac{1}{Z} \int [D\bar{\eta} D\eta] \, \eta_{i_n} \cdots \eta_{i_1} \bar{\eta}_{j_1} \cdots \bar{\eta}_{j_n} e^{-\bar{\eta}\cdot\mathfrak{M}\cdot\eta} = \sum_P (-)^P \mathfrak{M}^{-1}_{i_1 j_{P1}} \cdots \mathfrak{M}^{-1}_{i_n j_{Pn}} . \quad (201)$$

This theorem says that the $2n$-function contains basically $n!$ terms, each term is simply a product of n matrix elements of the inverse fermion matrix. We will call each factor of the inverse matrix element a contraction of the

corresponding two fermion fields. Therefore, each term is a product of n possible contractions. There is also a possible minus sign associated with each term, depending on how many times one has to shuffle the fields next to each other to form the n contractions. The final result is the summation of all possible contractions, each multiplied by a possible sign. The expression on the right-hand-side of Eq. (201) can be written in yet another form. It is nothing but the determinant of a $n \times n$ sub-matrix formed by the inverse matrix elements $\mathfrak{M}^{-1}_{ij}$ whose rows and columns are indexed by $i_1, \cdots, i_n$ and $j_1, \cdots, j_n$, respectively. As an example, if we have $n = 2$, then Wick's theorem is simply:

$$\langle \eta_1 \eta_2 \bar{\eta}_3 \bar{\eta}_4 \rangle = \mathfrak{M}^{-1}_{23} \mathfrak{M}^{-1}_{14} - \mathfrak{M}^{-1}_{24} \mathfrak{M}^{-1}_{13} = \begin{vmatrix} \mathfrak{M}^{-1}_{23} & \mathfrak{M}^{-1}_{24} \\ \mathfrak{M}^{-1}_{13} & \mathfrak{M}^{-1}_{14} \end{vmatrix} . \tag{202}$$

Thus, Wick's theorem in principle enables us to compute all physical quantities built from fermionic creation and annihilation operators. The crucial quantity to be computed is the inverse of the fermion matrix. In practice, unless in a few exceptional cases, the inverse of the fermion matrix cannot be obtained analytically. One usually has to rely on numerical methods. Here, the algorithms described in subsection VI C (e.g. the minimal residue algorithm and the conjugate gradient algorithm) will be useful. For the Hubbard model, the fermion matrix itself still depends on the auxiliary fields (the Gaussian fields ξ or the Ising fields σ). Therefore, one has to average over these fields with appropriate probability weights to get the final result for the physical quantity.

¶ As an example, we can compute the electron number correlation function within path-integral formalism. The electron number at a given site $\mathbf{R}$ is $n_{\mathbf{R}} = a^{\dagger}_{\mathbf{R}\sigma} a_{\mathbf{R}\sigma}$. So the correlation function is defined by

$$C(\mathbf{R}, \mathbf{R}') = \langle (n_{\mathbf{R}} - \langle n_{\mathbf{R}} \rangle)(n_{\mathbf{R}'} - \langle n_{\mathbf{R}'} \rangle) \rangle , \tag{203}$$

where the spin indices σ and σ' are summed over. Due to translational invariance on the lattice, this function only depends on $(\mathbf{R}' - \mathbf{R})$. The Fourier transform of the function is known as the structure function $S(\mathbf{k})$, a quantity useful for many purposes. With the help of the standard anti-commutation relation for the creation and annihilation operators, the electron number correlation function reduces to something like

$$C(\mathbf{R}, \mathbf{R}') = \langle a_{\mathbf{R}\sigma} a^{\dagger}_{\mathbf{R}\sigma} a_{\mathbf{R}'\sigma'} a^{\dagger}_{\mathbf{R}'\sigma'} \rangle - \langle a_{\mathbf{R}\sigma} a^{\dagger}_{\mathbf{R}\sigma} \rangle \langle a_{\mathbf{R}'\sigma'} a^{\dagger}_{\mathbf{R}'\sigma'} \rangle \tag{204}$$

Using path-integral, the second term is related to the average electron number which requires only the two-point correlation functions. The first term in the above equation involves four fermion fields (with two η's and two $\bar{\eta}$'s) at the same temporal slice: [26]

$$\langle a_{\mathbf{R}\sigma} a_{\mathbf{R}'\sigma'} a^{\dagger}_{\mathbf{R}\sigma} a^{\dagger}_{\mathbf{R}'\sigma'} \rangle = \langle \eta_{\mathbf{R}(\tau+1)\sigma} \eta_{\mathbf{R}'(\tau+1)\sigma} \bar{\eta}_{\mathbf{R}\tau\sigma} \bar{\eta}_{\mathbf{R}'\tau\sigma'} \rangle \tag{205}$$

The average over fermion fields in the equation above can then be accomplished using Wick's theorem, cf. Eq. (202). Similarly, one can also investigate the spin correlation function which also involves four fermion fields.

To summarize, within the path-integral formalism, with the help of Wick's theorem, almost all physical quantities can be expressed in terms of fermionic field contractions which are appropriate matrix elements of the inverse fermion matrix. This sets up the foundation for the numerical computation of physical quantities.

¶ Not only properties at equilibrium can be computed within path-integral formalism, transport properties (i.e. various susceptibility coefficients, a somewhat familiar example is the electric conductivity) close to equilibrium can also be obtained using the famous Kubo's formula in linear response theory. Since this goes too far away from our focus, I will not continue further along this line. Interested readers can consult Chapter 5 of Ref. [8], for example.

VIII. HALF-FILLED HUBBARD MODEL ON GRAPHENE

In this section, we will get back to graphene and study the half-filled Hubbard model on graphene structure. Our starting point is the tight-binding model (an independent electron model) discussed in Sec. III. Graphene lattice structure is a bipartite lattice made up of two sets of triangular lattices, which will be called sublattice A and B, respectively. The Hamiltonian for the system is

[26] Note that this quantity does not depend on the temporal label τ. Therefore, the correlation can be computed for any τ. In practical numerical studies, in order to achieve better statistics, one usually computes the quantity at various time slices and average the results obtained from them.

given by (c.f. Eq. (43) in Sec. III):

$$H = H_0 + H_{\rm int} \ , \tag{206}$$

$$H_0 = -t \sum_{\mathbf{R}\in\Lambda_A,i,\sigma} \left[a^\dagger_{\mathbf{R}\sigma} b_{\mathbf{R}+\boldsymbol{\delta}_i\sigma} + h.c. \right] \ , \tag{207}$$

$$H_{\rm int} = U \sum_{\mathbf{R}\in\Lambda_A} \left[\left(n^A_{\mathbf{R},\uparrow} - \frac{1}{2} \right) \left(n^A_{\mathbf{R},\downarrow} - \frac{1}{2} \right) + \left(n^B_{\mathbf{R},\uparrow} - \frac{1}{2} \right) \left(n^B_{\mathbf{R},\downarrow} - \frac{1}{2} \right) \right] \ , \tag{208}$$

where we have written the repulsive interaction term in the particle-hole symmetric form. We will use $\sigma = \uparrow, \downarrow$ to designate the spin index. The number operators are given in terms of creation and annihilation operators: $n^A_{\mathbf{R},\sigma} = a^\dagger_{\mathbf{R},\sigma} a_{\mathbf{R},\sigma}$ and $n^B_{\mathbf{R},\sigma} = b^\dagger_{\mathbf{R},\sigma} b_{\mathbf{R},\sigma}$ with $\mathbf{R}$ running over all sites on sublattice A. Although strictly speaking the operators associated with sublattice B are defined at site $\mathbf{R} + \boldsymbol{\delta}_1$ physically, as indicated previously, to simplify the notation, we will simply use $b_{\mathbf{R}}$. Here we assume that the interaction is repulsive, i.e. $U > 0$.

Using the more compact notation introduced in Sec. I-II, we have

$$H_0 = -t \sum_{\mathbf{R},\mathbf{R}',\sigma,\alpha,\beta} \psi^\dagger_{\mathbf{R},\sigma,\alpha} \mathcal{M}_{\mathbf{R},\alpha;\mathbf{R}',\beta} \psi_{\mathbf{R}',\sigma,\beta} \ , \tag{209}$$

where the matrix $\mathcal{M}$ is given by Eq. (47) in Sec. III. The number operators can also be expressed in terms of the operators $\psi^\dagger$ and ψ:

$$n^{A/B}_{\mathbf{R},\sigma} = \psi^\dagger_{\mathbf{R},\sigma} \left(\frac{1 \pm \sigma_3}{2} \right) \psi_{\mathbf{R},\sigma} \ . \tag{210}$$

So the interaction Hamiltonian $H_{\rm int}$ can also be expressed in terms of the $\psi^\dagger$ and ψ.

To study the thermodynamical properties using grand canonical ensemble, we need the operator $H' = H - \mu N$ where μ being the chemical potential of the system. Due to the sign problem, we will only study the case $\mu = 0$, namely the half-filled case. [27] As we pointed out in subsection V D, we could carry out the particle-hole transformation for the model (c.f. Eq. (127) in subsection V D):

$$\begin{aligned} a_{\mathbf{R},\uparrow} &= \tilde{a}_{\mathbf{R},\uparrow}; \ \ a_{\mathbf{R},\downarrow} = +\tilde{a}^\dagger_{\mathbf{R},\downarrow}, \\ b_{\mathbf{R},\uparrow} &= \tilde{b}_{\mathbf{R},\uparrow}; \ \ b_{\mathbf{R},\downarrow} = -\tilde{b}^\dagger_{\mathbf{R},\downarrow}. \end{aligned} \tag{211}$$

With this transformation, the tight-binding Hamiltonian H_0 is invariant while the Hubbard interaction term gets an extra minus sign. The new operator $H' = H - \mu N$, focusing on the particular case of $\mu = 0$, looks like that of a negative-U Hubbard model:

$$H' = H_0 - U \sum_{\mathbf{R}\in\Lambda_A} \left[\left(n^A_{\mathbf{R},\uparrow} - \frac{1}{2} \right) \left(n^A_{\mathbf{R},\downarrow} - \frac{1}{2} \right) + \left(n^B_{\mathbf{R},\uparrow} - \frac{1}{2} \right) \left(n^B_{\mathbf{R},\downarrow} - \frac{1}{2} \right) \right] \ , \tag{212}$$

One can then use the Hubbard-Stratonovich transformation and express the grand partition function into the following form:

$$Z = \int D\xi(\tau) e^{-\frac{1}{2\tilde{U}} \sum_{\tau,\mathbf{R}} (\xi^L_{\mathbf{R}\tau})^2 + (\xi^R_{\mathbf{R}\tau})^2} Tr \prod_\tau \exp \left[- \sum_{\mathbf{R},\mathbf{R}',\alpha,\beta,\sigma,\sigma'} \psi^\dagger_{\mathbf{R}\alpha\sigma} \mathcal{T}_{\mathbf{R}\alpha\sigma;\mathbf{R}'\beta\sigma'}[\xi(\tau)] \psi_{\mathbf{R}'\beta\sigma'} \right] \ , \tag{213}$$

where the kernel matrix $\mathcal{T}[\xi]$ is given by

$$\mathcal{T}_{\mathbf{R}\alpha\sigma;\mathbf{R}'\beta\sigma'} = \left\{ -\hat{t} \mathcal{M}_{\mathbf{R}\alpha;\mathbf{R}'\beta} + \left[\hat{U} \delta_{\alpha\beta} + \xi^L_{\mathbf{R}\tau} \left(\frac{1+\sigma_3}{2} \right)_{\alpha\beta} + \xi^R_{\mathbf{R}\tau} \left(\frac{1-\sigma_3}{2} \right)_{\alpha\beta} \right] \delta_{\mathbf{R}\mathbf{R}'} \right\} \delta_{\sigma\sigma'} \ . \tag{214}$$

Here the matrix $\mathcal{M}$ is given by Eq. (47) in Sec. III. We can now apply the coherent state path-integral technique again. Since the fermion matrix is trivial in spin space,

[27] Written in the form of Eq. (212), the half-filled case corresponds exactly to $\mu = 0$.

the fermion determinant is simply the square of the determinant for the reduced matrix (which makes it positive-definite):

$$Z = \int D\xi(\tau) e^{-\frac{1}{2\hat{U}} \sum_{\tau,\mathbf{R}} (\xi^L_{\mathbf{R}\tau})^2 + (\xi^R_{\mathbf{R}\tau})^2} \left[\det \mathbb{M}[\xi]\right]^2 , \quad (215)$$

with the reduced fermion matrix $\mathbb{M}[\xi]$ given by $\mathbb{M}[\xi] = \hat{\partial}_\tau + \tilde{\mathcal{T}}[\xi]$ where $\tilde{\mathcal{T}}[\xi]$ is obtained from the matrix $\mathcal{T}$ in Eq. (214) by omitting the unit matrix in spin space (i.e. dropping the $\delta_{\sigma\sigma'}$ factor). To simplify the notation for the fermion matrix, we now introduce the $2+1$ dimensional notation for lattice coordinates. For example:

$$x = (\tau, \mathbf{R}), y = (\tau', \mathbf{R}') , \quad (216)$$

are called 3-vectors. We will also call τ the temporal, or zeroth component of the coordinate x, namely $x_0 = \tau$. We will also use notations like $x+\hat{0}$, $x+\hat{i}$ to represent the neighboring site of x that is arrived by moving one lattice spacing to the positive temporal and the i-th spatial direction (i.e. along lattice base vector $\mathbf{a}_i$), respectively. Similarly, the lattice point $x - \hat{\mu}$ with $\mu = 0, 1, 2$ designates the neighboring point of x obtained by moving one lattice spacing to the corresponding negative directions. With these notations, the fermion matrix for the model may be expressed as:

$$\mathbb{M}[\xi] = (\delta_{x+\hat{0},y} - \delta_{xy}) - \hat{t}\left[\left(\delta_{xy} + \frac{1}{2}\sum_{i=1}^{2}[\delta_{x+\hat{i},y} + \delta_{x-\hat{i},y}]\right)\sigma_1 - \frac{i}{2}\left(\delta_{x+\hat{i},y} - \delta_{x-\hat{i},y}\right)\sigma_2\right] + \hat{U}\delta_{xy} + \sqrt{\hat{U}}\left[\xi^L_x P_L + \xi^R_x P_R\right]\delta_{xy} \quad (217)$$

where we have suppressed the chiral indices (into Pauli matrices) and re-scaled the fields ξ by a factor $\sqrt{\hat{U}}$ for the convenience of perturbation theory (see next section).

This form now looks similar to the form we have already discussed in Sec. V. In particular, the matrix $\mathbb{M}[\xi]$ is a real matrix and the square of its determinant is positive-definite. Therefore there exists no sign problem in this case and the standard Monte Carlo algorithms (like hybrid Monte Carlo that we briefly discussed in subsection VI B) can be readily applied. To be specific, the Hybrid Monte Carlo Hamiltonian is introduced:

$$H = \frac{1}{2}\sum_x \pi_x^2 + S[\xi, \phi_1, \phi_2] , \quad (218)$$

$$S[\xi, \phi_1, \phi_2] = \frac{1}{2}\sum_x \left[(\xi^L_x)^2 + (\xi^R_x)^2\right] + \sum_{\alpha=1,2} \phi^T_\alpha \left[\mathbb{M}\mathbb{M}^T[\xi]\right]^{-1} \phi_\alpha \quad (219)$$

The infinitesimal change in the action is written as

$$\delta S[\xi, \phi_1, \phi_2] = -\sum_x \left(F^L_x \delta\xi^L_x + F^R_x \delta\xi^R_x\right) . \quad (220)$$

The force terms $F^{L/R}_x$ can be found by taking the variation of the action with respect to the $\xi^{L/R}_x$ fields. With the fermion matrix given explicitly by Eq. (217), after some trivial manipulations, the following expressions for the fermionic force are obtained:

$$F^{L/R}_x = -\xi^{L/R}_x + 2\sqrt{\hat{U}}\sum_\alpha tr\left[\left(Y_{\alpha x} \otimes X^T_{\alpha x}\right) P_{L/R}\right] , \quad (221)$$

where the vectors $X_{\alpha x}$ and $Y_{\alpha x}$ are given by the solutions of the linear system:

$$\left[\mathbb{M}\mathbb{M}^T[\xi]\right] \cdot X_\alpha = \phi_\alpha , \; Y_{\alpha x} = \mathbb{M}[\xi] \cdot X_\alpha . \quad (222)$$

The trace in the fermionic force is taken within the chiral space. With these formulae, it is then straightforward to set up a hybrid Monte Carlo algorithm that generates the correct Boltzmann distribution for the effective action.

A. An improved formula for the path integral

As mentioned in subsection V C, we could use a better approximation for the matrix $e^{-\mathbb{T}}$ which amounts to the

following fermion matrix:

$$\mathbb{M}[\xi] = \hat{\partial}_0 + \mathbb{T} - \frac{1}{2}\mathbb{T}^2 + \cdots \tag{223}$$

where the matrix $\mathbb{T}$ is given explicitly by

$$\mathbb{T} = \hat{f}_1\sigma_1 + \hat{f}_2\sigma_2 + [\hat{U} + \sqrt{\hat{U}}(\xi_x^L P_L + \xi_x^R P_R)]\delta_{xy} \tag{224}$$

with the matrix $\hat{f}_1$ and $\hat{f}_2$ given by

$$\begin{cases} \left[\hat{f}_2\right]_{xy} = (-\hat{t})\left[\delta_{xy} + \frac{1}{2}\sum_{i=1}^{2}\left(\delta_{x+\hat{i},y} + \delta_{x-\hat{i},y}\right)\right] \\ \left[\hat{f}_2\right]_{xy} = \frac{i\hat{t}}{2}\sum_{i=1}^{2}\left(\delta_{x+\hat{i},y} - \delta_{x-\hat{i},y}\right) \end{cases} \tag{225}$$

Although it is straightforward to derive an explicit formula for the new fermion matrix $\mathbb{M}[\xi] = \hat{\partial}_0 + \mathbb{T} - \frac{1}{2}\mathbb{T}^2$, on the numerical side, it is easier to simply call the matrix multiplication function, say $\mathbb{T}$, twice. The relevant formula for the fermionic force is also changed and the result looks like

$$F_x^{L/R} = -\xi_x^{L/R} + \frac{\sqrt{\hat{U}}}{2}\sum_\alpha tr\left[\left(\tilde{Y}_{\alpha x}\otimes X_{\alpha x}^T + \tilde{X}_{\alpha x}\otimes Y_{\alpha x}^T + Y_{\alpha x}\otimes \tilde{X}_{\alpha x}^T + X_{\alpha x}\otimes \tilde{X}_{\alpha x}^T\right)P_{L/R}\right] , \tag{226}$$

where X_α and Y_α are obtained from the linear system in Eq. (222) with

$$\tilde{X}_\alpha = (\mathbb{1} - \mathbb{T})\cdot X_\alpha \, , \tilde{Y}_\alpha = (\mathbb{1} - \mathbb{T})Y_\alpha \, . \tag{227}$$

Therefore, if $\mathbb{T} \ll \mathbb{1}$, we recover the old result. This new result will be more accurate if the matrix $\mathbb{T}$ is not small (e.g. when the parameter U/t is large).

B. Possible acceleration of the program

Let us briefly discuss the rate of convergence of the algorithm. Not surprisingly, a big portion of the computer time will be spent on the solution of the sparse linear system given in Eq. (222). The linear system is solved using iterative methods, like the Conjugate Gradient Algorithm, as described in subsection VI C. It is known that the rate of convergence for these iterative solvers is mainly determined by the so-called condition number of the matrix being solved. For our example here, the condition number of the positive-definite matrix $\mathbb{M}\mathbb{M}^T[\xi]$ is defined to be the ratio of its largest eigenvalue $\lambda_{\max}$ to the smallest eigenvalue $\lambda_{\min}$ (both are positive numbers):

$$cond\left(\mathbb{M}\mathbb{M}^T[\xi]\right) = \frac{\lambda_{\max}}{\lambda_{\min}} \, . \tag{228}$$

The larger the condition number is, the slower the convergence of the iteration will become. Normally, the largest eigenvalue does not change appreciably for difference field configurations of $\xi(x)$ and different parameters in the matrix. However, it can happen that for some set of parameters, or for some field configuration $\xi(x)$, the matrix develops a very small eigenvalue $\lambda_{\min}$. In other words, the matrix being solved is almost singular and the condition number of the matrix is very large. It is exact in this case that the iteration of the conjugate gradient algorithm can become enormously long.

Although the exact eigenvalues for the general fermion matrix (217), which depends on the fluctuating fields $\xi^{L/R}(x)$, cannot be found analytically, one still can get some feeling of it from perturbation theory (which is discussed in some detail in the next section). For example, around the mean-field (uniformly distributed) configuration $\sqrt{\hat{U}}S_x = \check{S}$, $P_x = 0$ with $\check{S}$ determined by the gap equation (272), the eigenvalues for the fermion matrix is found to be

$$\lambda_{\alpha,k} = 1 + \left[1 - \hat{U} - \check{S} + \hat{E}_\alpha(\mathbf{k})\right]^2 - 2\cos(k_0)\left[1 - \hat{U} - \check{S} + \hat{E}_\alpha(\mathbf{k})\right] \, , \tag{229}$$

where $\check{S}$ is the solution from the gap equation (272) while $\alpha = +, -$ stands for the two eigenvalues in the chiral space. In the limit of $N_t \to \infty$, $a_t \to 0$ but $N_t a_t = \beta$ being fixed, the largest eigenvalue occurs when $\cos(k_0) \simeq (-1)$ so that $\lambda_{\max} \simeq 4 + O(a_t)$. The smallest eigenvalue happens when $\cos(k_0) \simeq +1$. This is when $k_0 = \pi/N_t$:

$$\frac{\lambda_{\max}}{\lambda_{\min}} \simeq \frac{1}{(\hat{U} + \check{S} - \hat{E}_\alpha(\mathbf{k}))^2 + \sin^2 \frac{\pi}{2N_t}} , \tag{230}$$

Both terms in the denominator of this equation will become small in the limit of $N_t \to \infty$, $a_t \to 0$. The first term, if the parameter $\hat{U}+\check{S}$ lies within the band of $\pm E_+(\mathbf{k})$, will vanish for some values of $\mathbf{k}$ in the first Brillouin zone. [28] We therefore expect a rather large condition number in this limit:

$$\frac{\lambda_{\max}}{\lambda_{\min}} \sim \frac{4N_t^2}{\pi^2} . \tag{231}$$

Normally, in order to keep discretization errors under control, the parameter a_t cannot be too large. That means when β is large (low temperature), one has to increase the number of time slices N_t. Hence the condition number diverges as N_t^2 when $N_t \to \infty$. Therefore, at low temperatures, simulation of the system becomes more and more difficult.

To overcome this difficulty, one could utilize the preconditioning methods. Instead of evaluating the fermion matrix $\mathbb{M}[\xi]$, one could use another matrix $\tilde{\mathbb{M}}[\xi]$:

$$\tilde{\mathbb{M}}[\xi] = \mathbb{P}\mathbb{M}[\xi] , \tag{232}$$

where the matrix $\mathbb{P}$ is another matrix, called preconditioning matrix, whose determinant is easily computable. One possibility would be to take $\mathbb{P} = [\mathbb{M}_0]^{-1}$ where $\mathbb{M}_0$ may be taken as the free fermion matrix given in the next section, see Eq. (248). One could also use the fermion matrix in the mean-field approximation with the value of $\check{S}$ obtained from the gap equation (272). In all these cases, the determinant of $\mathbb{P}$ is field-independent and can be dropped completely. The inverse of the matrix is also computable analytically by Fourier transformation. To put it more explicitly, we simulate the following partition function

$$H = \frac{1}{2}\sum_x \pi_x^2 + S[\xi, \phi_1, \phi_2] , \tag{233}$$

$$S[\xi, \phi_1, \phi_2] = \frac{1}{2}\sum_x \left[(\xi_x^L)^2 + (\xi_x^R)^2\right] + \sum_{\alpha=1,2} \phi_\alpha^T \left[\tilde{\mathbb{M}}\tilde{\mathbb{M}}^T[\xi]\right]^{-1} \phi_\alpha , \tag{234}$$

with $\tilde{\mathbb{M}} = \mathbb{M}_0^{-1} \cdot \mathbb{M}[\xi]$:

$$\tilde{\mathbb{M}} = \mathbb{1} - \check{S}\mathbb{M}_0^{-1} + \sqrt{\hat{U}}\mathbb{M}_0^{-1}(\xi_x^L P_L + \xi_x^R P_R) . \tag{235}$$

In order to make this feasible for numerical calculation, we would need to compute the new fermion matrix $\tilde{\mathbb{M}}$ times a (field) vector: $\tilde{\mathbb{M}} \cdot \phi_x$:

$$\begin{aligned} \tilde{\mathbb{M}}_{xy}\phi_y &= \phi_x + [\mathbb{M}_0^{-1}]_{xy}\Phi_y , \\ \Phi_{\alpha x} &= \left(\sqrt{\hat{U}}\xi_x - \check{S}\right)_{\alpha\beta} \phi_{\beta x} \end{aligned} \tag{236}$$

where the chiral indices are suppressed in the first equation while they are explicitly shown in the second. How do we compute something like $[\mathbb{M}_0^{-1}]_{xy}\Phi_y$? We could use Fast Fourier Transformation (FFT) technique:

$$\begin{aligned} [\mathbb{M}_0^{-1}]_{xy}\Phi_y &= \frac{1}{\sqrt{\Omega}}\sum_k \tilde{\mathbb{M}}_0^{-1}(k)\tilde{\Phi}(k)e^{-ik\cdot x} , \\ \tilde{\Phi}(k) &= \frac{1}{\sqrt{\Omega}}\sum_y \Phi_y e^{ik\cdot y} , \end{aligned} \tag{237}$$

where $\tilde{\mathbb{M}}_0^{-1}(k) = \tilde{G}_0(k)$ is given by Eq. (257) in the next section. Therefore, to obtain the result of $[\mathbb{M}_0^{-1}]_{xy}\Phi_y$, we need only $O(\Omega \ln \Omega)$ number of computations due to the advantage of FFT. This is moderately larger than the original cost of $O(\Omega)$ without the preconditioning.

The force formula in this case is also modified:

$$F_x^{L/R} = -\xi_x^{L/R} + 2\sqrt{\hat{U}}\sum_\alpha tr\left(Y_{\alpha x} \otimes \left[\mathbb{M}_0^{-1} \cdot X_\alpha\right]_x^T P_{L/R}\right) , \tag{238}$$

where the field vectors $X_{\alpha x}$ and $Y_{\alpha x}$ are obtained from

[28] For infinitely large lattice, the energy band is continuous and this term will vanish for some $\mathbf{k}_0$ in the first Brillouin zone if the parameter $\hat{U} + \check{S}$ lies in the band. For finite lattice, the band is quasi-continuous and this term will almost vanish.

the linear systems for $\tilde{\mathbb{M}}$ as in Eq. (222), with the matrix $\mathbb{M}$ substituted by $\tilde{\mathbb{M}}$.

C. Spin correlation functions

Here we would like to construct the spin-spin correlation function of the system. We first would like to write out the spin operator in the second-quantized form: [29]

$$\mathbf{S}_{\mathbf{R}}^{A,a} = a_{\mathbf{R},\sigma}^{\dagger} \left(\tau^a\right)_{\sigma\sigma'} a_{\mathbf{R},\sigma'} \ . \tag{239}$$

where τ^a with $a = 1, 2, 3$ indicates the Pauli matrices in spin space while the summation over repeated indices σ and σ' is understood. The superscript A indicates that this is the spin operator on sublattice A. A similar expression (with A replaced by B and all the creation and annihilation operators $a_{\mathbf{R}}$'s replaced by $b_{\mathbf{R}+\boldsymbol{\delta}_1}$'s) gives the spin operator at site $\mathbf{R}+\boldsymbol{\delta}_1$ on sublattice B.

Sometimes, for convenience, one could also introduce another basis for the Pauli matrices, namely $a = +, -, 3$ with $\mathbf{S}_{\mathbf{R}}^{A,\pm} = (\mathbf{S}_{\mathbf{R}}^{A,1} \pm i\mathbf{S}_{\mathbf{R}}^{A,2})/2$. To be more explicit, we have,

$$\begin{cases} \mathbf{S}_{\mathbf{R}}^{A,3} = a_{\mathbf{R},\uparrow}^{\dagger} a_{\mathbf{R},\uparrow} - a_{\mathbf{R},\downarrow}^{\dagger} a_{\mathbf{R},\downarrow} \ , \\ \mathbf{S}_{\mathbf{R}}^{A,+} = a_{\mathbf{R},\uparrow}^{\dagger} a_{\mathbf{R},\downarrow}, \ \mathbf{S}_{\mathbf{R}}^{A,-} = a_{\mathbf{R},\downarrow}^{\dagger} a_{\mathbf{R},\uparrow}, \end{cases} \tag{240}$$

One should also keep in mind that these are the forms *before* the particle-hole transformation that we have to perform in Eq. (211). After the transformation, the spin-up operators do not change while all the spin-down creation and annihilation operators are swapped (apart from a possible minus sign). Therefore, the form of the operators are modified. For example, the third component (z-component) of the spin operator $\mathbf{S}_{\mathbf{R}}^{A,3}$ on sublattice A before the transformation is modified to

$$\mathbf{S}_{\mathbf{R}}^{A,3} = \tilde{a}_{\mathbf{R},\uparrow}^{\dagger} \tilde{a}_{\mathbf{R},\uparrow} + \tilde{a}_{\mathbf{R},\downarrow}^{\dagger} \tilde{a}_{\mathbf{R},\downarrow} - 1 \ , \tag{241}$$

after the particle-hole transformation in Eq. (211).

We can then define various spin correlation functions as usual. For example, the correlation functions among the spins on sublattice A will look like:

$$\begin{cases} C_{zz}^{AA}(\mathbf{R}) = \left\langle \mathbf{S}_{\mathbf{R}}^{A,3} \mathbf{S}_{\mathbf{0}}^{A,3} \right\rangle \ , \\ C_{-+}^{AA}(\mathbf{R}) = \left\langle \mathbf{S}_{\mathbf{R}}^{A,-} \mathbf{S}_{\mathbf{0}}^{A,+} \right\rangle \ , \\ C_{+-}^{AA}(\mathbf{R}) = \left\langle \mathbf{S}_{\mathbf{R}}^{A,+} \mathbf{S}_{\mathbf{0}}^{A,-} \right\rangle \ , \end{cases} \tag{242}$$

where $\langle\cdot\rangle$ stands for ensemble average.

It is also possible to express the operators in terms of the composite operator $\psi_{\mathbf{R},\sigma}$ defined previously. Note that $a_{\mathbf{R},\sigma} = P_L \psi_{\mathbf{R},\sigma}$, $b_{\mathbf{R}+\boldsymbol{\delta}_1,\sigma} = P_R \psi_{\mathbf{R},\sigma}$, thus the spin operators can be written as

$$\mathbf{S}_{\mathbf{R}}^{A/B,a} = \psi_{\mathbf{R}}^{\dagger} P_{L/R} \tau^a \psi_{\mathbf{R}} \ , \tag{243}$$

where $P_{L/R} = (1 \pm \sigma_3)/2$ acts in chiral space (also known as pseudo-spin space) while τ^a acts in spin space. Both spin and chiral indices are suppressed in this equation for convenience.

After the particle-hole transformation, the form of these operators become

$$\begin{cases} \mathbf{S}_{\mathbf{R}}^{A/B,3} = \psi_{\mathbf{R}}^{\dagger} P_{L/R} \psi_{\mathbf{R}} - 1 \ , \\ \mathbf{S}_{\mathbf{R}}^{A/B,+} = \pm \psi_{\mathbf{R}}^{\dagger} P_{L/R} \left(\dfrac{\tau^1 + i\tau^2}{2} \right) (\psi_{\mathbf{R}}^{\dagger})^T \ , \\ \mathbf{S}_{\mathbf{R}}^{A/B,-} = \pm (\psi_{\mathbf{R}})^T P_{L/R} \left(\dfrac{\tau^1 - i\tau^2}{2} \right) \psi_{\mathbf{R}} \ , \end{cases} \tag{244}$$

It is more straightforward to write out the spin indices explicitly in the fields: [30]

$$\begin{cases} \mathbf{S}_{\mathbf{R}}^{A/B,3} = \psi_{\mathbf{R},\uparrow}^{\dagger} P_{L/R} \psi_{\mathbf{R},\uparrow} + \psi_{\mathbf{R},\downarrow}^{\dagger} P_{L/R} \psi_{\mathbf{R},\downarrow} - 1 \ , \\ \mathbf{S}_{\mathbf{R}}^{A/B,+} = \pm \psi_{\mathbf{R},\uparrow}^{\dagger} P_{L/R} (\psi_{\mathbf{R},\downarrow}^{\dagger})^T \ , \\ \mathbf{S}_{\mathbf{R}}^{A/B,-} = \pm (\psi_{\mathbf{R},\downarrow})^T P_{L/R} \psi_{\mathbf{R},\uparrow} \ , \end{cases} \tag{245}$$

Within path integral, the relevant operators are inserted at a particular time-slice τ while the creation and annihilation operators $\psi_{\mathbf{R},\alpha,\sigma}$ and $\psi_{\mathbf{R},\alpha,\sigma}^{\dagger}$, with $\alpha = +, -$ the chiral index and $\sigma = \uparrow, \downarrow$ the spin index, are replaced by their corresponding Grassmanian eigenvalues $\eta_{\mathbf{R},\tau+1,\alpha,\sigma}$ and $\bar{\eta}_{\mathbf{R},\tau,\alpha,\sigma}$. This insertion can be done at any τ, meaning that the spin correlation function will eventually become independent of τ. In practice, one could utilize this to average over results at different time-slices. Since the fermion matrix is trivial in spin space which means that only contraction between the same spin indices are possible. This greatly simplifies that matter when applying Wick's theorem. For example, the correlation function $C_{+-}^{AA}(\mathbf{R})$ is given by

$$\begin{aligned} C_{-+}^{AA}(\mathbf{R}) &= \langle \eta_{\mathbf{R},\tau+1,+,\downarrow} \eta_{\mathbf{R},\tau+1,+,\uparrow} \bar{\eta}_{\mathbf{0},\tau,+,\uparrow} \bar{\eta}_{\mathbf{0},\tau,+,\downarrow} \rangle \\ &= \langle \mathbb{M}^{-1}_{\mathbf{R},\tau+1,+;\mathbf{0},\tau,+} \mathbb{M}^{-1}_{\mathbf{R},\tau+1,+;\mathbf{0},\tau,+} \rangle \ , \end{aligned} \tag{246}$$

[29] Apart from an irrelevant factor $(\hbar/2)$.

[30] With spin indices are written out explicitly while chiral indices are suppressed.

In the first line of the above equation, we have written out all indices explicitly: $\pm$ for chiral indices and $\uparrow\downarrow$ for spin indices. Contraction only occurs between fields with the *same* spin indices which leads to the second line of the above equation.

One could also compute the correlation between the spin at sublattice A and sublattice B, for example,

$$\begin{aligned} C^{AB}_{-+}(\mathbf{R}) &= \langle \mathbf{S}^{A,-}_{\mathbf{R}} \mathbf{S}^{B,+}_{\mathbf{0}} \rangle \ , \\ &= \langle \eta_{\mathbf{R},\tau+1,+,\downarrow} \eta_{\mathbf{R},\tau+1,+,\uparrow} \bar{\eta}_{\mathbf{0},\tau,-,\uparrow} \bar{\eta}_{\mathbf{0},\tau,-,\downarrow} \rangle, \\ &= \langle \mathbb{M}^{-1}_{\mathbf{R},\tau+1,+;\mathbf{0},\tau,-} \mathbb{M}^{-1}_{\mathbf{R},\tau+1,+;\mathbf{0},\tau,-} \rangle \ . \end{aligned} \tag{247}$$

IX. THE PERTURBATIVE CALCULATION AT SMALL $\hat{U}$

For small U/t, a perturbative calculation can be formulated as usual. To do this, we split the fermion matrix into a free part $\mathbb{M}_0$, which is independent of the bosonic fields, and a perturbative part that depends on the bosonic fields. Thus, we may write the fermion matrix $\mathbb{M}[\xi]$ as

$$\begin{aligned} \mathbb{M}[\xi] &= \mathbb{M}_0 + \delta\mathbb{M}[\xi] \ , \\ [\mathbb{M}_0]_{x;y} &= (\delta_{x+\hat{0},y} - \delta_{xy}) - \hat{t} \left[\left(\delta_{xy} + \frac{1}{2} \sum_{i=1}^{2} [\delta_{x+\hat{i},y} + \delta_{x-\hat{i},y}] \right) \sigma_1 - \frac{i}{2} \left(\delta_{x+\hat{i},y} - \delta_{x-\hat{i},y} \right) \sigma_2 \right] + \hat{U} \delta_{xy} \\ \delta\mathbb{M}[\xi]_{xy} &= \sqrt{\hat{U}} \left[\xi^L_x P_L + \xi^R_x P_R \right] \delta_{xy} \equiv \sqrt{\hat{U}} \left[S_x + P_x \sigma_3 \right] \delta_{xy} \end{aligned} \tag{248}$$

Note that for simplicity, we have put a diagonal term $U\delta_{xy}$ into the free-part of the fermion matrix. The perturbation theory amounts to compute the partition function and physical observables by expanding into power series of $\delta\mathbb{M}[\xi]$ which is treated as a small perturbation. The left-handed and right-handed auxiliary bosonic fields ξ^L_x and ξ^R_x are introduced via the standard Hubbard-Stratonovich transformation. For later convenience we also introduced the notation for the scalar field $S_x = (\xi^L_x + \xi^R)/2$ and the pseudo-scalar field $P_x = (\xi^L_x - \xi^R)/2$.

The partition function of the theory is given by

$$Z = \int D\xi e^{-\frac{1}{2}\sum_x (\xi^L_x)^2 + (\xi^R_x)^2} \left[\det \mathbb{M}_0\right]^2 e^{-S_{\text{eff}}[\xi]} \ , \tag{249}$$

where the effective action arising from the fermion determinant is:

$$S_{\text{eff}}[\xi] = -2Tr \ln(1 + \mathbb{M}_0^{-1} \delta\mathbb{M}[\xi]) \ . \tag{250}$$

Perturbation in terms of $\delta\mathbb{M}[\xi]$ then gives

$$S_{\text{eff}}[\xi] = -2Tr \left[\mathbb{M}_0^{-1} \delta\mathbb{M} \right] + Tr \left[\mathbb{M}_0^{-1} \delta\mathbb{M} \mathbb{M}_0^{-1} \delta\mathbb{M} \right] + \cdots \ . \tag{251}$$

Diagrammatically, each term in the above expansion corresponds to a closed fermion loop with n external bosonic field lines for $n = 1, 2, \cdots$. We will now compute the first two terms below. But before the computation, we will first need the free fermion propagator, i.e. $G_0 \equiv \mathbb{M}_0^{-1}$.

A. The free electron propagator

We will call the inverse free fermion matrix the free fermion propagator

$$(G_0)_{xy} \equiv \left(\mathbb{M}_0^{-1} \right)_{xy} \ . \tag{252}$$

where we have note written out the chiral indices explicitly, i.e. they are written in a compact notation. The expression for the free fermion propagator in real-space may be obtained by standard Fourier transform. For example, the fermion matrix itself can be written as

$$(\mathbb{M}_0)_{xy} = \frac{1}{\Omega} \sum_k \tilde{\mathbb{M}}_0(k) e^{-ik\cdot(x-y)} \ . \tag{253}$$

Here $\Omega = N_t \times N_1 \times N_2$ is the three-volume (the area of the graphene system times the extension in the imaginary time direction) of the system. The summation over three-vector k implies to sum over both k_0 (the Matrubara frequencies) and $\mathbf{k}$ which runs over the first Brillouin zone. The product in the exponential represents

the inner product of the two three-vectors: $k = (k_0, \mathbf{k})$ and $(x - y) = (x_0 - y_0, \mathbf{x} - \mathbf{y})$, with the definition: $k \cdot (x - y) = k_0(x_0 - y_0) - \mathbf{k} \cdot (\mathbf{x} - \mathbf{y})$. The Fourier transformed fermion matrix is given by

$$\tilde{\mathbb{M}}_0(k) = g_0(k) - g_1(k)\sigma_1 - g_2(k)\sigma_2 = g_0 - \mathbf{g} \cdot \boldsymbol{\sigma} \ . \quad (254)$$

The two-vector inner product in the above equation is defined via $\mathbf{g} \cdot \boldsymbol{\sigma} = g_1\sigma_1 + g_2\sigma_2$ and the components g_μ (with $\mu = 0, 1, 2$) are given by

$$g_0(k) = e^{-ik_0} - 1 + \hat{U}, \ g_1(k) = \hat{t} f_1(k), \ g_2(k) = \hat{t} f_2(k) \ . \quad (255)$$

The functions $f_1(k) = f_1(\mathbf{k})$ and $f_2(k) = f_2(\mathbf{k})$ are exactly the same function that we defined in Eq. (51) in subsection III B. Note the fact that $f_0(k)$ *only* depends on $k_0 = \omega_n$ while $f_1(k)$ and $f_2(k)$ *only* depend on $\mathbf{k}$. This will become important in the following calculation.

With the notations introduced above, we easily obtain the free fermion propagator as

$$(G_0)_{xy} = \frac{1}{\Omega} \sum_k \left(\frac{1}{g_0 - \mathbf{g} \cdot \boldsymbol{\sigma}} \right) e^{-ik\cdot(x-y)} \ . \quad (256)$$

In this form, the free fermion propagator is not diagonal in chiral indices. That is to say, the momentum-space propagator

$$\tilde{G}_0(k) = \frac{1}{g_0 - \mathbf{g} \cdot \boldsymbol{\sigma}} = \frac{g_0 + \mathbf{g} \cdot \boldsymbol{\sigma}}{g_0^2 - \mathbf{g} \cdot \mathbf{g}} \ , \quad (257)$$

is still a matrix in chiral space. This can be diagonalized with the same 2×2 unitary matrix V that we used (see Eq. (55) there) in subsection III B. This unitary matrix brings the combination $\mathbf{g} \cdot \boldsymbol{\sigma}$ into diagonal and therefore will also diagonalize $(g_0 - \mathbf{g} \cdot \boldsymbol{\sigma})$. So we have

$$(V^\dagger G_0 V)_{xy} = \frac{1}{\Omega} \sum_k \begin{pmatrix} \frac{e^{-ik\cdot(x-y)}}{g_0 + \hat{E}_+(\mathbf{k})} & 0 \\ 0 & \frac{e^{-ik\cdot(x-y)}}{g_0 + \hat{E}_-(\mathbf{k})} \end{pmatrix} \ , \quad (258)$$

where $\hat{E}_\alpha(\mathbf{k}) = a_t E_\alpha(\mathbf{k})$ for $\alpha = +, -$.

In real Monte Carlo simulations, one usually measures the propagator that is partially Fourier transformed only in two spatial dimensions. In the free case, this is the quantity (we call it a correlation matrix)

$$G_0(x_0 - y_0; \mathbf{k}) = \frac{1}{N_t} \sum_{k_0} \frac{e^{-ik_0(x_0 - y_0)}}{g_0 - \mathbf{g}(\mathbf{k}) \cdot \boldsymbol{\sigma}} \ . \quad (259)$$

Similar, by using the unitary matrix V, one can diagonalize this correlation matrix with two eigenvalues given by

$$\left[V^\dagger G_0(x_0 - y_0; \mathbf{k}) V \right]_\alpha = \frac{1}{N_t} \sum_{k_0} \frac{e^{-ik_0(x_0 - y_0)}}{g_0 + \hat{E}_\alpha(\mathbf{k})} \ , \quad (260)$$

with $\alpha = +, -$ for two different eigenvalues.

B. Effective action to first order

Using the setup established previously, the first order contribution to the effective action, $S^{(1)}_{\text{eff}}[\xi]$ may be expressed as

$$S^{(1)}_{\text{eff}}[\xi] = (-2) Tr \left[\mathbb{M}_0^{-1} \delta\mathbb{M} \right] = (-2) \sum_{x,y} tr \left[(G_0)_{xy} (\delta\mathbb{M})_{yx} \right] \ , \quad (261)$$

where $tr(\cdot)$ represents the trace over chiral indices. Substitute the expression for G_0 we obtain

$$S^{(1)}_{\text{eff}}[\xi] = (-2)\sqrt{\hat{U}} \sum_k tr \left[\tilde{G}_0(k)(\bar{S} + \bar{P}\sigma_3) \right] \ , \quad (262)$$

where $\bar{S} = (1/\Omega)\sum_x S_x$ and $\bar{P} = (1/\Omega)\sum_x P_x$. The pseudo-scalar part contains a σ_3 and will not contribute after the trace. So we are left with only the scalar part:

$$\begin{aligned} S^{(1)}_{\text{eff}}[\xi] &= (-2)\sqrt{\hat{U}}\bar{S} \sum_k tr \left(\tilde{G}_0(k) \right) \ , \\ &= (-2)\sqrt{\hat{U}} \left[\sum_x S_x \right] \left[\frac{1}{\Omega} \sum_{k,\alpha} \frac{1}{g_0 + \hat{E}_\alpha(\mathbf{k})} \right] \end{aligned} \quad (263)$$

The summation over k_0 in the above formula can be completed exactly. We utilize the identity: [31]

$$\frac{1}{N_t} \sum_{k_0} \frac{1}{e^{-ik_0} - \zeta} = -\frac{\zeta^{N_t - 1}}{1 + \zeta^{N_t}} \ . \quad (264)$$

We thus obtain the following for the effective action:

$$\begin{aligned} S^{(1)}_{\text{eff}}[\xi] &= 2\sqrt{\hat{U}} F(U) \sum_x S_x \\ F(U) &= \frac{1}{N} \sum_{\mathbf{k},\alpha} \frac{(1 - \hat{U} + \hat{E}_\alpha(\mathbf{k}))^{N_t - 1}}{1 + (1 - \hat{U} + \hat{E}_\alpha(\mathbf{k}))^{N_t}} \ . \end{aligned} \quad (265)$$

Here $N = N_1 \times N_2$ is the total number of lattice points for sublattice A of the graphene system. The function $F(U)$ [32] does not have a simple analytic form but can be computed numerically with ease. In the limit $N_t \to \infty$, $a_t \to 0$, but $\beta = N_t a_t$ being fixed (we call this the continuum limit), the function $F(U)$ reduces to

$$\lim_{a_t \to 0} F(U) = \frac{1}{N} \sum_{\mathbf{k}} \frac{e^{-\beta U} + \cosh[\beta E_+(\mathbf{k})]}{\cosh(\beta U) + \cosh[\beta E_+(\mathbf{k})]} \ . \quad (266)$$

---

[31] We assume here that k_0 runs over all fermionic Matsubara frequencies. For bosonic fields, the corresonding formula is: $(1/N_t)\sum_{q_0}[1/(e^{-iq_0} - \zeta)] = -\zeta^{N_t - 1}/[1 - \zeta^{N_t}]$ where q_0 runs over all bosonic Matsubara frequencies.

[32] The function $F(U)$ also depends on a_t and N_t implicitly. But to simplify the notation, we will simply denote it as $F(U)$.

It is also noticed that in the continuum limit we have $\lim_{a_t\to 0} F(U=0)=1$.

This basically concludes our calculation of the effective action to the first order. Note that, to this order, a term linear in the bosonic field S_x is obtained via the fermionic loop (also known as the tadpole diagram in field theory). This then generates a non-vanishing expectation value for the field S_x. One easily verifies that

$$\langle S_x\rangle \simeq -\sqrt{\hat{U}}F(U)\ . \tag{267}$$

This result can be checked explicitly in a Monte Carlo simulation. One picks a small enough parameter U and estimate the ensemble average $\langle S_x\rangle$ using Monte Carlo. The numerical result can be cross-checked against the perturbative result given above.

C. The gap equation

The treatment in the previous subsection relies on the perturbative expansion in $\delta\mathbb{M}[\xi]$. In fact, we could do a bit more than that. Note that the fermion determinant contributes an effective action to the bosonic feilds ξ. Therefore, the total action for the bosonic fields becomes

$$S_{\rm eff}[\xi]=\frac{1}{2}\sum_x\left[(\xi_x^L)^2+(\xi_x^R)^2\right]-2Tr\ln(\mathbb{M}[\xi])\ . \tag{268}$$

We have seen that, to first order in $\delta\mathbb{M}[\xi]$, the action will contain a term that is linear in ξ, meaning that the original $\xi\to(-\xi)$ symmetry is broken by the fermion determinant. Instead, we could try to search for the minimum of the effective bosonic action given above. In particular, we are looking for mininum of the action with uniform (i.e. x independent) field configurations: $S_x=\bar{S}$ and $P_x=\bar{P}$. Requiring that

$$S_x=\bar{S}\ ,\ \ P_x=\bar{P}\ , \tag{269}$$

indeed minimize the effective action, we obtain the equation satisfied by $\bar{S}$ and $\bar{P}$. These equations are also known as gap equations. We find that

$$\bar{S}=-\frac{\sqrt{\hat{U}}}{N}\sum_{\mathbf{k},\alpha=\pm}\left\{\frac{\left[1-\hat{U}-\sqrt{\hat{U}}\bar{S}+\alpha\sqrt{E_+(\mathbf{k})^2+\hat{U}\bar{P}^2}\right]^{N_t-1}}{1+\left[1-\hat{U}-\sqrt{\hat{U}}\bar{S}+\alpha\sqrt{E_+(\mathbf{k})^2+\hat{U}\bar{P}^2}\right]^{N_t}}\right\} \tag{270}$$

$$\bar{P}=\frac{\sqrt{\hat{U}}}{N}\sum_{\mathbf{k},\alpha=\pm}\frac{\alpha\hat{U}\bar{P}}{2\sqrt{E_+(\mathbf{k})^2+\hat{U}\bar{P}^2}}\left\{\frac{\left[1-\hat{U}-\sqrt{\hat{U}}\bar{S}+\alpha\sqrt{E_+(\mathbf{k})^2+\hat{U}\bar{P}^2}\right]^{N_t-1}}{1+\left[1-\hat{U}-\sqrt{\hat{U}}\bar{S}+\alpha\sqrt{E_+(\mathbf{k})^2+\hat{U}\bar{P}^2}\right]^{N_t}}\right\} \tag{271}$$

Note that $\bar{P}=0$ is always a solution for the second gap equation. We therefore focus on the solution of the type $\bar{S}\neq 0$ while $\bar{P}=0$. Setting $\check{S}=\sqrt{\hat{U}}\bar{S}$ we get the equation as follows:

$$\check{S}=-\frac{\hat{U}}{N}\sum_{\mathbf{k},\alpha=\pm}\frac{\left[1-\hat{U}-\check{S}+\hat{E}_\alpha(\mathbf{k})\right]^{N_t-1}}{1+\left[1-\hat{U}-\check{S}+\hat{E}_\alpha(\mathbf{k})\right]^{N_t}}\ . \tag{272}$$

This equation is in agreement with the results in the previous subsection when $\bar{S}$ is small, as can be easily checked, c.f. Eq. (267) and Eq. (265). But this gap equation will give more accurate result than the naive perturbative result in the previous subsection. Note that, one may expand the fields around the mean-field configuration given by the gap equation as: $S_x=\bar{S}+s_x$ and $P_x=\bar{P}+p_x=p_x$, this results in an effective action in terms of the fields s_x and p_x. The only difference is that the free propagator is somewhat modified. The form of the free propagator is still given by Eq. (257) except that the function $g_0(k)$ in Eq. (255) is replaced by a similar expression with $\hat{U}$ substituted for $\hat{U}+\check{S}$ with $\check{S}$ being the solution of the gap equation (272).

The solution $\check{S}$ for the gap equation (272) cannot be obtained analytically. Numerical methods has to be utilized to find the value for $\check{S}$. A simple and direct way of doing this is by iteration. To be more explicit, one first sets $\check{S}=0$ on the r.h.s of Eq. (272) and compute the summation over $\mathbf{k}$. This gives a first estimate for the value $\check{S}$. It is easy to see that this is nothing but the perturbative result obtained in the previous subsection, i.e.

Eq. (267). In the second step, the calculated value of $\check{S}$ from the previous step is substituted into the r.h.s of the gap equation to compute a new value of $\check{S}$. This will be in general somewhat different from the first trial. One can perform this iteration a number of times until the values of $\check{S}$ do not change appreciably within the desired numerical accuracy.

D. Effective action to second order

To second order in $\delta\mathbb{M}[\xi]$, which is the deviation of the fermion matrix from the mean-field value predicted by the gap equation, the effective action takes the form:

$$S^{(2)}_{\rm eff}[\xi] = \frac{\hat{U}}{\Omega}\sum_{k,p} tr\left[\tilde{G}_0(k)\tilde{\xi}(k-p)\tilde{G}_0(p)\tilde{\xi}(p-k)\right] . \tag{273}$$

The free propagators in the equation is given by Eq. (257) in which the parameter $\hat{U}$ in the function $g_0(k)$ is substituted by $\hat{U}+\check{S}$. We have also used the matrix-valued field notation:

$$\xi_x = s_x + p_x\sigma_3 \ , \ \ \tilde{\xi}(q) = \frac{1}{\sqrt{\Omega}}\sum_x \xi_x e^{iq\cdot x} . \tag{274}$$

Note that, the three-momentum for the bosonic fields is $(k-p)$ or $(p-k)$. Since k_0 and p_0 are the fermionic Matsubara frequencies, their difference is automatically a bosonic Matsubara frequency as it should be the case for bosonic fields. So the effective action reads

$$S^{(2)}_{\rm eff}[\xi] = \sum_q \frac{\hat{U}}{\Omega}\sum_k tr\left[\tilde{G}_0(k)\tilde{\xi}(-q)\tilde{G}_0(k+q)\tilde{\xi}(q)\right] , \tag{275}$$

where the momentum k is fermionic while q is bosonic. After the summation over k is performed, this yields an effective action that is quadratic in ξ fields. Since $\tilde{\xi}(q) = \tilde{s}(q) + \sigma_3\tilde{p}(q)$, We now parameterize this contribution as

$$S^{(2)}_{\rm eff} = \sum_q \left[\tilde{s}(-q)\Sigma^{SS}(q)\tilde{s}(q) + \tilde{s}(-q)\Sigma^{SP}(q)\tilde{p}(q) + \tilde{p}(-q)\Sigma^{PS}(q)\tilde{s}(q) + \tilde{p}(-q)\Sigma^{PP}(q)\tilde{p}(q)\right] \tag{276}$$

Note that the free part of the action for the bosonic fields may be written as

$$S^{(0)} = \Omega(\bar{S}^2 + \bar{P}^2) + \sum_{q\neq 0}[\tilde{s}(-q)\tilde{s}(q) + \tilde{p}(-q)\tilde{p}(q)] \tag{277}$$

Therefore, the contribution $S^{(2)}_{\rm eff}$ will modify the coefficients for $\tilde{S}(-q)\tilde{S}(q)$ and $\tilde{P}(-q)\tilde{P}(q)$ in the whole action from unity to $1+\Sigma^{SS}(q)$ and $1+\Sigma^{PP}(q)$, respectively. We now proceed to evaluate the functions (they will be called self-energy functions) $\Sigma^{SS}(q)$, $\Sigma^{SP}(q)$, $\Sigma^{PS}(q)$ and $\Sigma^{PP}(q)$.

¶ Let us first look at contribution $\Sigma^{SS}(q)$. After tracing over the chiral indices, we get

$$\Sigma^{SS}(q) = \frac{2\hat{U}}{\Omega}\sum_k \frac{g_0(k)g_0(k+q) + \mathbf{g}(k)\cdot\mathbf{g}(k+q)}{[g_0^2(k) - E_+^2(k)][g_0^2(k+q) - E_+^2(k+q)]} \tag{278}$$

Our objective here is to complete the summation over k_0 exactly while leaving the summation over $\mathbf{k}$ to computers. The summation over k_0 is a bit more complicated than the one we treated before. Denoting the denominator as $\mathcal{D}$, the first term in the numerator may be factorized as

$$\frac{g_0(k)g_0(k+q)}{\mathcal{D}} = \frac{1}{4}\left(\frac{1}{g_0(k)-E_+(k)} + \frac{1}{g_0(k)+E_+(k)}\right)\left(\frac{1}{g_0(k+q)-E_+(k+q)} + \frac{1}{g_0(k+q)+E_+(k+q)}\right) \tag{279}$$

So we would need to sum over k_0 of the terms like $1/[(g_0(k)\pm E_+(q))(g_0(k+q)\pm E_+(k+q))]$. These terms can be treated similarly. For example, taking one of the four terms, we have

$$\frac{1}{g_0(k)-E_+(k)}\frac{1}{g_0(k+q)-E_+(k+q)} = \frac{e^{iq_0}}{[e^{-ik_0} - 1 + \hat{U} - \hat{E}_+(k)][e^{-ik_0} - e^{iq_0}(1-\hat{U}+\hat{E}_+(k+q))]} \tag{280}$$

We can now split the right-hand-side of the above equation into two single fractions and the summation over k_0 may now be completed using the identity (264). The contribution $\Sigma^{PP}(q)$ is quite similar. In fact it merely changes the sign of $\mathbf{g}(\mathbf{k})$ due to anti-commuting σ_3 through. After some algebra, the following somewhat lengthy expression emerges

$$\Sigma^{SS/PP}(q) = -\frac{\hat{U}}{2N}\sum_{\mathbf{k},\alpha,\beta}\left[1 \pm \frac{\mathbf{g}(\mathbf{k})\cdot\mathbf{g}(\mathbf{k}+\mathbf{q})}{E_\alpha(\mathbf{k})E_\beta(\mathbf{k}+\mathbf{q})}\right]\left[\frac{[1-\hat{U}-\check{S}+\hat{E}_\alpha(\mathbf{k})]^{N_t-1}e^{iq_0}}{1+[1-\hat{U}-\check{S}+\hat{E}_\alpha(\mathbf{k})]^{N_t}} - \frac{[1-\hat{U}-\check{S}+\hat{E}_\beta(\mathbf{k}+\mathbf{q})]^{N_t-1}}{1+[1-\hat{U}-\check{S}+\hat{E}_\beta(\mathbf{k}+\mathbf{q})]^{N_t}}\right]\times$$
$$\times\left(\frac{1}{1-\hat{U}-\check{S}+\hat{E}_\alpha(\mathbf{k})-e^{iq_0}[1-\hat{U}-\check{S}+\hat{E}_\beta(\mathbf{k}+\mathbf{q})]}\right) . \tag{281}$$

In this formula, the + and − sign corresponds to the case SS and PP, respectively. We have also utilized the fact that $e^{iN_tq_0} \equiv 1$ since q_0 is a bosonic Matsubara frequency. The value of $\check{S}$ is obtained from the gap equation. Similarly, we obtain the expression for the self-energy function $\Sigma^{SP}(q)$ as

$$\Sigma^{SP/PS}(q) = \mp i\frac{\hat{U}}{N}\sum_{\mathbf{k},\alpha,\beta}\frac{[\mathbf{g}(\mathbf{k})\times\mathbf{g}(\mathbf{k}+\mathbf{q})]_3}{E_\alpha(\mathbf{k})E_\beta(\mathbf{k}+\mathbf{q})}\left[\frac{[1-\hat{U}-\check{S}+\hat{E}_\alpha(\mathbf{k})]^{N_t-1}e^{iq_0}}{1+[1-\hat{U}-\check{S}+\hat{E}_\alpha(\mathbf{k})]^{N_t}} - \frac{[1-\hat{U}-\check{S}+\hat{E}_\beta(\mathbf{k}+\mathbf{q})]^{N_t-1}}{1+[1-\hat{U}-\check{S}+\hat{E}_\beta(\mathbf{k}+\mathbf{q})]^{N_t}}\right]\times$$
$$\times\left(\frac{1}{1-\hat{U}-\check{S}+\hat{E}_\alpha(\mathbf{k})-e^{iq_0}[1-\hat{U}-\check{S}+\hat{E}_\beta(\mathbf{k}+\mathbf{q})]}\right) . \tag{282}$$

Here the − and + sign corresponds to the case Σ^{SP} and Σ^{PS}, respectively. They differ only by a sign. This implies that the cross terms in the effective action may be expressed as:

$$\sum_q \Sigma^{SP}\left[\tilde{s}(-q)\tilde{p}(q) - \tilde{p}(-q)\tilde{s}(q)\right] , \tag{283}$$

which is real.

Finally we note that the whole loop expansion only makes sense when the effective mass matrix

$$M^2_{\text{eff}}(q) \equiv \begin{pmatrix} 1+\Sigma^{SS}(q) & \Sigma^{SP}(q) \\ \Sigma^{PS}(q) & 1+\Sigma^{PP}(q)\end{pmatrix} , \tag{284}$$

is positive definite. This is equivalent to the fact that the solution from the gap equation is indeed a minimum of the action. When the interaction is weak, i.e. $U/t \ll 1$, this is always guaranteed.

¶ The results obtained for the self-energy can be checked in physical observables in Monte Carlo simulations. For example, when we measure the correlation functions for the bosonic fields, we have

$$\langle S_x S_y\rangle = \bar{S}^2 + \langle s_x s_y\rangle . \tag{285}$$

We can also expand in Fourier space and obtain

$$\langle S_x S_y\rangle = \frac{1}{\Omega}\sum_q \langle\tilde{S}(q)\tilde{S}(-q)\rangle e^{-iq\cdot(x-y)} . \tag{286}$$

The value of $\langle\tilde{S}(q)\tilde{S}(-q)\rangle$ is obtained from the corresponding matrix element of the inverse matrix for $M^2_{\text{eff}}(q)$ in Eq. (284):

$$\langle\tilde{S}(q)\tilde{S}(-q)\rangle = \frac{1+\Sigma^{PP}(q)}{[1+\Sigma^{SS}(q)][1+\Sigma^{PP}(q)]+[\Sigma^{SP}(q)]^2} , \tag{287}$$

which can be verified directly in a Monte Carlo simulation.

E. The electron self-energy

It is also straightforward to compute the fermion self-energy in perturbation theory. For this purpose, we notice that the full fermion propagator is nothing but the inverse of the fermion matrix $\mathbb{M}^{-1}$ which is given by (c.f. Eq. (248) in the beginning of this section)

$$\mathbb{M}[\xi] = \mathbb{M}_0 + \delta\mathbb{M}[\xi] \ ,$$
$$[\mathbb{M}_0]_{x;y} = (\delta_{x+\hat{0},y} - \delta_{xy}) - \hat{t}\left[\left(\delta_{xy} + \frac{1}{2}\sum_{i=1}^{2}[\delta_{x+\hat{i},y} + \delta_{x-\hat{i},y}]\right)\sigma_1 - \frac{i}{2}\left(\delta_{x+\hat{i},y} - \delta_{x-\hat{i},y}\right)\sigma_2\right] + (\hat{U} + \check{S})\delta_{xy}$$
$$\delta\mathbb{M}[\xi]_{xy} = \sqrt{\hat{U}}\,[s_x + p_x\sigma_3]\,\delta_{xy} \tag{288}$$

In this expression, the mean-field value $\check{S}$ is obtained from the gap equation (272).

We may now expand schematically

$$G \equiv \mathbb{M}^{-1} = G_0 - G_0\delta\mathbb{M}G_0 + G_0\delta\mathbb{M}G_0\delta\mathbb{M}G_0 + \cdots \tag{289}$$

with $G_0 \equiv \mathbb{M}_0^{-1}$. This expression has to be integrated over s_x and p_x to obtain the fermion propagator. Since $\delta\mathbb{M}$ is proportional to s_x and p_x and the integration measure is even in these fields, we see that terms with odd powers of $\delta\mathbb{M}$ vanish. Furthermore, the matrix $\delta\mathbb{M}$ is diagonal in coordinate space, therefore the first correction to the free fermion propagator is given by:

$$(\delta G)_{xy} = \sum_{z,w}(G_0)_{xz}\delta\mathbb{M}_{zz}(G_0)_{zw}\delta\mathbb{M}_{ww}(G_0)_{wy} \tag{290}$$

We can now substitute in the explicit form of $(G_0)_{xy}$ given in Eq.(256) and obtain

$$(\delta G)_{xy} = \frac{\hat{U}}{\Omega^3}\sum_{w,z}\sum_{k,k',k''}\left\langle \tilde{G}_0(k)(s_z + p_z\sigma_3)\tilde{G}_0(k')(s_w + p_w\sigma_3)\tilde{G}_0(k'')\right\rangle_{s,p} e^{-ik\cdot(x-z)}e^{-ik'\cdot(z-w)}e^{-ik''\cdot(w-y)} \ , \tag{291}$$

where the symbol $\langle\cdot\rangle$ stands for taking average (integration) with respect to the field s_x and p_x which is nothing but average in the Gaussian distribution that is proportional to $\exp(-\sum_x[s_x^2 + p_x^2])$. This means that we have:

$$\langle s_x s_y\rangle = \frac{1}{2}\delta_{xy}, \ \ \langle p_x p_y\rangle = \frac{1}{2}\delta_{xy}, \tag{292}$$

while all the cross terms vanish (in the first approximation, of course). Using this fact, the above equation for δG then simplifies to

$$\delta G = \frac{\hat{U}}{2\Omega^2}\sum_{k,k'}\tilde{G}_0(k)\left[\tilde{G}_0(k') + \sigma_3\tilde{G}_0(k')\sigma_3\right]\tilde{G}_0(k)e^{-ik\cdot(x-y)} \tag{293}$$

This can also be written in terms of the propagator in momentum space

$$\delta\tilde{G}(k) = \tilde{G}_0(k)\left[\frac{\hat{U}}{2\Omega}\sum_{k'}\left[\tilde{G}_0(k') + \sigma_3\tilde{G}_0(k')\sigma_3\right]\right]\tilde{G}_0(k) \tag{294}$$

If we define the self-energy function as:

$$\tilde{G}(k) = g_0(k) - \mathbf{g}(\mathbf{k})\cdot\boldsymbol{\sigma} + \Sigma(k) \ , \tag{295}$$

then to first order in perturbation theory, we have

$$\Sigma(k) = \frac{\hat{U}}{2\Omega}\sum_{k'}\left[\tilde{G}_0(k') + \sigma_3\tilde{G}_0(k')\sigma_3\right] \ , \tag{296}$$

which is a constant (matrix in chiral space!) independent of k. The matrix $(1/\Omega)\sum_{k'}\tilde{G}_0(k')$ can be computed easily following similar steps as in previous subsections. The following result is obtained:

$$\frac{1}{\Omega}\sum_{k'}\tilde{G}_0(k') = -\frac{1}{2N}\sum_{\mathbf{k},\alpha}\left[1 + \frac{\mathbf{g}(\mathbf{k})\cdot\boldsymbol{\sigma}}{\hat{E}_\alpha(\mathbf{k})}\right]\frac{[1 - \hat{U} - \check{S} + \hat{E}_\alpha(\mathbf{k})]^{N_t - 1}}{1 + [1 - \hat{U} - \check{S} + \hat{E}_\alpha(\mathbf{k})^{N_t}} \tag{297}$$

Since we have to add this with the result sandwiched between two σ_3, it is seen that the term proportional to $\boldsymbol{\sigma}$ will cancel exactly. We thus have:

$$\Sigma(k) = -\hat{U}F(U) \ , \tag{298}$$

where $F(U)$ is introduced before in Eq.(265). To summarize, perturbative self-energy merely adds a constant to *all* the energy levels. This will globally shift the energy bands but at the Dirac point, the energy band remains gapless.

---

* Work supported in part by NSFC under grant No.10835002 and No.10721063.

[1] N.W. Ashcroft and N.D. Mermin. *Solid state physics*. Brooks Cole, 1976.

[2] C. Kittel. *Introduction to solid state physics, 8th ed.* Wiley, 2004.

[3] Kun Huang and Ru-Qi Han. *Solid State Physics*. Higher Education Press, 1988.

[4] L.D. Landan and E.M. Lifshitz. *Quantum Mechanics, 3rd ed.* Pergamon Press, Oxford, UK, 1977.

[5] Chuan Liu. *Equillibrium Statistical Physics*. Lecture notes of Peking University, 2008.

[6] L. D. Landau and E. M. Lifschitz. *Statistical Physics*. Pergamon Press, 1994.

[7] M. Plischke and B. Bergerson. *Equilibrium Statistical Physics*. Prentice Hall, 1989.

[8] J. W. Negele and H. Orland. *Quantum Many-Particle Systems*. Adidison-Wesley, 1988.

[9] J.E. Hirsch. Discrete hubbard-stratonovich transformation for fermion lattice models. *Phys. Rev.*, B28:4059, 1983.

[10] S. Duane, A. D. Kennedy, B. J. Pendleton, and D. Roweth. Hybrid Monte Carlo. *Phys. Lett.*, B195: 216–222, 1987. doi:10.1016/0370-2693(87)91197-X.